

2010-01-01

# Automated Fluid Handling And Leveling System For Multiple Material Stereolithography

Yinko I. Grajeda

University of Texas at El Paso, [yinko.grajeda@bwigroup.com](mailto:yinko.grajeda@bwigroup.com)

Follow this and additional works at: [https://digitalcommons.utep.edu/open\\_etd](https://digitalcommons.utep.edu/open_etd)



Part of the [Mechanical Engineering Commons](#)

---

## Recommended Citation

Grajeda, Yinko I., "Automated Fluid Handling And Leveling System For Multiple Material Stereolithography" (2010). *Open Access Theses & Dissertations*. 2693.

[https://digitalcommons.utep.edu/open\\_etd/2693](https://digitalcommons.utep.edu/open_etd/2693)

This is brought to you for free and open access by DigitalCommons@UTEP. It has been accepted for inclusion in Open Access Theses & Dissertations by an authorized administrator of DigitalCommons@UTEP. For more information, please contact [lweber@utep.edu](mailto:lweber@utep.edu).

AUTOMATED FLUID HANDLING AND LEVELING SYSTEM FOR MULTIPLE  
MATERIAL STEREOLITHOGRAPHY

YINKO IBSAIN GRAJEDA GAMBOA

Department of Mechanical and Industrial Engineering

APPROVED:

---

Ryan B. Wicker, Ph.D., Chair

---

Jae-Won Choi, Ph.D.

---

Eric MacDonald, Ph.D.

---

Patricia D. Witherspoon, Ph.D.  
Dean of the Graduate School

AUTOMATED FLUID HANDLING AND LEVELING SYSTEM FOR MULTIPLE  
MATERIAL STEREOLITHOGRAPHY

D{

YINKO IBSAIN GRAJEDA GAMBOA

THESIS

Presented to the Faculty of the Graduate School of

The University of Texas at El Paso

in Partial Fulfillment

of the Requirements

for the Degree of:

MASTER OF SCIENCE

Department of Mechanical and Industrial Engineering

THE UNIVERSITY OF TEXAS AT EL PASO

May 2010

## **ACKNOWLEDGEMENTS**

My sincere gratitude to; my parents Jose Luis and Marina, my wife Veronica, and my beautiful daughters Ileana and Tania who have shown me love and support that enabled me to meet my goals.

A special recognition goes to Doctor Ryan Wicker for the confidence he had in me (even from the first interview), through the completion of this project. His confidence granted me access to the W.M. Keck Center for 3D Innovation under a, “Research Assistantship” and finally lead to the completion of this work. I would also like to thank Doctor Jack Dowdy for the opportunity to learn and grow as one of his “Teaching Assistants” which provided me with experience and an excellent sense of fulfillment.

I would like to acknowledge and gratefully thank the support provided by the, “Gobierno del Estado de Chihuahua Scholarship” that made my education and degree possible.

Finally, thanks to my colleagues in the W.M. Keck Center for 3D Innovation for all of their suggestions and support.

This thesis was submitted to the Supervising Committee in May, 2010.

## EXECUTIVE SUMMARY

The work presented in this document addresses the development of an automated fluid leveling system for application in a Multiple-Material Stereolithography (MMSL) apparatus. Information regarding fluid handling systems, fluid level measuring systems and control theory is presented in an effort to demonstrate the development and implementation of an accurate and reliable multiple material fluid handling and leveling system.

A patent filed by Wicker et al. (US Patent 7,556,490) disclosing a MMSL apparatus served as the basis for the development of this work. The system described in this work was developed to have sufficient robustness and flexibility for adequate performance when installed in a variety of MMSL apparatus configurations. The majority of the development and experimental setup was carried out as a standalone sub-system separate from the main MMSL apparatus. Some of the key elements included resin vats, a peristaltic pump drive with a peristaltic pump head and a non- contact level sensor.

The resin vats' design was driven by the mounting, or special restrictions posed by the particular MMSL system where they were going to be used. An effort was made to maintain uniform, constant and simple cross-sectional area geometries with the knowledge that this cross-sectional area would play a key role in the leveling system algorithm, system accuracy and resolution. Due to its modeling flexibility, Stereolithography (SL) materials were frequently used to create custom vat models. Stainless steel and glass containers frequently served as experimental vats.

A key element of the leveling system is the fluid handling unit, or in this the case, the pump. The MMSL patent recommended the use of a peristaltic pump due to the fluid isolation

from the pump mechanical elements and the bi-directional flow capabilities. Particular attention was paid to the pump's accuracy. Factors such as flow rates and pressure capacity were considered. Strategies such as: using a combination of high-flow and high-accuracy pumps, including a combination of normally open and normally closed valves and using a combination of a peristaltic pump with a syringe pump were considered. An assessment of the desirable system outputs against the commercially available peristaltic pumps performance was made. A MasterFlex® L/S® 7550-50 peristaltic pump with a computer-compatible console drive in combination with an EasyLoad® peristaltic pump head was ultimately selected.

One of the main objectives of this leveling system was to maintain a specific fluid level, which in some cases would be subject to disturbances and possible level changes. As with the fluid handling system, fluid isolation was greatly desired leading towards a non-contact sensor choice. In order to support the SL “build-by-layers” approach, accuracies of at least 10 microns were required. Serving as the feedback for the control system, the ability to communicate directly to a central computer was an essential feature for the level sensor. A review of various sensing units' performance led to the selection of a non-contact Microtrak 7000™ laser displacement sensor processing unit with a MT 600 laser head.

In addition, to the existing commercial communication software for the digital pump drive and the level sensor, LabVIEW® routines were developed to establish communication between the central control computer and the digital pump drive and level sensor. Simple LabVIEW® sub-routines were created to operate the individual pump drive and level sensor features while supporting system implementation flexibility.

The “classical control theory” addresses items related to the system time response such as: overshoot, rise and settling times. Part of this work included modeling of the control system

using mathematical equations to represent the individual system physical elements. A transfer function was formulated to represent the input to output relationship of the mathematical model. Among the several control techniques designed to meet particular control requirements, the PID controller is one of the most common and simple feedback control techniques, which in this case was applied as the control strategy. The desired system output was then obtained by tuning the KP, KI and KD control parameters. Due to the nature of this system, a PD approach was identified as the best control approach.

The individual hardware, software and control elements of the leveling system were then integrated as a standalone system. Satisfactory system performance was demonstrated through several trials under diverse system conditions. Finally, the leveling system was successfully incorporated as a sub-system into an automated MMSL machine which was able to produce simple multiple material parts.

## TABLE OF CONTENTS

ACKNOWLEDGEMENTS .....	iii
EXECUTIVE SUMMARY.....	iv
TABLE OF CONTENTS .....	vii
LIST OF TABLES .....	xii
LIST OF EQUATIONS .....	xiii
LIST OF FIGURES.....	xiv
1.0 INTRODUCTION.....	1
1.1 RESEARCH MOTIVATION .....	1
1.2 W.M. KECK CENTER FOR 3D INNOVATION.....	2
1.3 PROBLEM STATEMENT.....	2
1.4 PROJECT OBJECTIVES AND SCOPE.....	4
1.5 THESIS OUTLINE .....	5
2.0 LITERATURE REVIEW .....	6
2.1 PUMPS .....	6
2.1.1 Peristaltic Pump .....	6
2.1.2 Flow Dynamics .....	7
2.1.3 Applications .....	9
2.1.4 Variations .....	9
2.1.5 Syringe Pumps .....	10
2.2 LEVEL MEASUREMENT TECHNOLOGIES.....	10
2.2.1 Introduction.....	10



2.2.2 Various level sensing techniques .....	11
2.3 LASER TRIANGULATION LEVEL SENSOR.....	12
2.3.1 Introduction.....	12
2.3.2 Operating Principle .....	14
2.3.3 Accuracy, Resolution and Repeatability.....	16
2.4 SERIAL COMMUNICATION .....	17
2.5 PROCESS CONTROL .....	19
2.5.1 Classical Control Theory .....	19
2.5.2 Model Philosophies.....	20
2.5.3 Modeling of Processes .....	20
2.5.4 Closed Loop Control Systems .....	21
2.5.5 On-Off Controllers.....	23
2.5.6 Proportional Part.....	23
2.5.7 Integral part.....	24
2.5.8 Proportional Plus Integral Control.....	25
2.5.9 Derivative Part .....	25
2.5.10 PID Controller.....	26
2.5.11 Typical Responses of feedback control systems.....	27
2.5.12 Effect of controller gain .....	28
2.5.13 Laplace Transform .....	28
2.5.14 The Transfer Function .....	29
2.5.15 Control Tuning.....	29
2.6 RAPID PROTOTYPING.....	30

2.6.1 The SL Process .....	30
2.6.2 RP influence to other disciplines .....	32
3.0 EXPERIMENTAL SETUP .....	34
3.1 PERISTALTIC PUMP .....	34
3.1.1 Operation Curves .....	36
3.1.2 Drive communication specification .....	41
3.2 LASER TRIANGULATION LEVEL SENSOR .....	43
3.3 SENSOR CALIBRATION, SETUP AND HEAD ALIGNMENT .....	44
3.4 EXISTING LEVELING SYSTEM .....	49
3.5 FLUID VAT .....	49
3.6 RESINS .....	50
4.0 SYSTEM OPERATION .....	52
4.1 INTRODUCTION .....	52
4.2 PERISTALTIC PUMP .....	54
4.2.1 Start Up Sequence .....	57
4.2.2 Command Format .....	59
4.2.3 Pump Drive Communication Configuration .....	60
4.2.4 Pump Drive Direction and Speed VI .....	62
4.2.5 Pump Drive Volume Conversion VI .....	63
4.2.6 Pump Drive Stop VI .....	64
4.2.7 Pump Drive Control Front Panel .....	64
4.2.8 Operation Tests .....	66
4.3 LASER TRIANGULATION SENSOR .....	69

4.3.1	Triangulation Sensor Communication Configuration.....	69
4.3.2	Triangulation Sensor Front Panel .....	72
4.3.3	Level Data Collection .....	73
4.4	OPERATION TESTS .....	73
4.4.1	Laser Beam Surface Penetration.....	77
4.4.2	Float and Guide.....	77
4.4.3	Float Calibration .....	79
4.4.4	Surface reflective properties .....	81
4.5	LABVIEW CONTROL .....	81
4.5.1	PID Control Front Panel .....	82
5.0	SYSTEM DEMONSTRATION.....	84
5.1	SEMI-AUTOMATED LEVELING SYSTEM STRATEGY.....	84
5.2	SYSTEM DEMONSTRATION .....	85
5.3	SYSTEM IMPLEMENTATION.....	87
6.0	RESULTS OF STUDY .....	90
6.1	INTRODUCTION .....	90
6.2	SYSTEM DESCRIPTION AND MODELING.....	90
6.3	TUNING .....	94
7.0	CONCLUSIONS AND RECOMMENDATIONS .....	97
7.1	SUMMARY OF DESIGN .....	97
7.2	SUMMARY OF OPERATION .....	98
7.3	SUMMARY OF RESULTS .....	99
7.4	RECOMMENDATIONS FOR FUTURE RESEARCH .....	100

REFERENCES.....	102
Apendix A – DSM SOMOS® NANOFORM™ DATA SHEET.....	110
Apendix B – MICROTRACK 7000™ LASER DISPLACEMENT SENSOR SPECIFICATIONS .....	111
Apendix C – MASTERFLEX® L/S® 7550-50 peristaltic pump SPECIFICATIONS .....	116
Apendix D LABVIEW CONTROL STRUCTURE.....	123
Apendix E - MICRO-EPSILON® OPTONCDT 1800® LASER DISPLACEMENT SENSOR SPECIFICATIONS.....	133
8.0 CURRICULUM VITAE .....	135

## LIST OF TABLES

Table 4.1 Pump satellite commands (Cole Palmer® MasterFlex® L/S® Operating Manual: Pump Drives 13) .....	55
Table 4.2 Table 4.3 Sample pump commands and responses (Cole Palmer® MasterFlex® L/S® Operating Manual: Pump Drives 14) .....	56
Table 4.4 ASCII Control characters used (Cole Palmer® MasterFlex® L/S® Operating Manual: Pump Drives 14) .....	57
Table 4.5 Flow rates for MasterFlex® L/S® Drive (Cole-Palmer®, “Peristaltic Pumps Offer Economical Multichannel Pumping”).....	63
Table 4.6 Triangulation Sensor RS-232 Communication Format (MTI Instruments, Inc. Microtrak 7000™ – User Manual 22) .....	70
Table 4.7 Microtrak 7000 Displacement Sensor RS-232 Control Codes (MTI Instruments, Inc. Microtrak 7000™ – User Manual) .....	71
Table 6.1 Ziegler-Nichols tuning using the oscillation method.....	95

## LIST OF EQUATIONS

Equation 2.1. Fundamental Law of Mass Conservation .....	21
Equation 2.2. Fundamental Law of Energy Conservation .....	21
Equation 2.3. Output of an ideal On-Off controller .....	23
Equation 2.4. Proportional controller transfer function .....	24
Equation 2.5. Integral controller transfer function .....	25
Equation 2.6. Transfer function for a derivative controller .....	26
Equation 2.7. Transfer function for an ideal PID controller .....	26
Equation 2.8. PID physical approximation to an ideal controller .....	27
Equation 6.1. Mass Balance .....	91
Equation 6.2. Pump linear characteristic equation for a 500 cps fluid above 250RPM .....	92
Equation 6.3. Pump equation for small changes in speed .....	92
Equation 6.4. Mass – Flow balance between vat and pump .....	92
Equation 6.5. Transfer function for the pump – vat .....	93
Equation 6.6. Transfer function of the level sensor .....	93
Equation 6.7. Sensor gain .....	93
Equation 6.8. Transfer function for a PID controller .....	93
Equation 6.9. Step function .....	94
Equation 6.10. Closed loop transfer function .....	94

## LIST OF FIGURES

Figure 2.1 Peristaltic Pumping Principle .....	8
Figure 2.2 Laser Triangulation Sensor Head .....	13
Figure 2.3 Triangulation sensor operating principle (Haus 70).....	15
Figure 2.4 Typical feedback control system responses .....	27
Figure 2.5 Effect of controller gain in process response .....	28
Figure 2.6 “Sketch of the stereolithography process” (Beal 40). ....	31
Figure 3.1 MasterFlex® L/S® 7550 Console Drive (Cole Palmer® MasterFlex® L/S® Operating Manual: Pump Drives 1).....	35
Figure 3.2 MasterFlex® L/S® Easy-Load Peristaltic Pump Head (Cole Palmer® MasterFlex® L/S® Operating Manual: Easy-Load® Pump Heads) .....	35
Figure 3.3 MasterFlex® Peristaltic Pump Tubing Selection Guide (Cole-Palmer®. MasterFlex® Tubing Application Guide) .....	36
Figure 3.4 Vat - Reservoir to Peristaltic Pump Setup.....	37
Figure 3.5 Peristaltic pump flow rate vs. speed for different viscosities (Cole-Palmer® “Pumping Viscous Fluids Figures”).....	38
Figure 3.6 Peristaltic pump viscosity vs. flow rate for different tubing sizes at 100rpm (Cole- Palmer® “Pumping Viscous Fluids Figures”) .....	38
Figure 3.7 Peristaltic pump flow rate vs. speed for different tubing sizes at 50cps (Cole-Palmer® “Pumping Viscous Fluids Figures”) .....	39
Figure 3.8 Peristaltic pump flow rate vs. speed for different tubing sizes at 100cps (Cole- Palmer® “Pumping Viscous Fluids Figures”) .....	39

Figure 3.9 Peristaltic pump flow rate vs. speed for different tubing sizes at 500cps (Cole-Palmer® “Pumping Viscous Fluids Figures”)	40
Figure 3.10 Peristaltic pump flow rate vs. speed for different tubing sizes at 1500cps (Cole-Palmer® “Pumping Viscous Fluids Figures”)	40
Figure 3.11 Laser Sensor Processing Unit and Head by Microtrak (MTI Instruments, Inc. Microtrak 7000TM – User Manual)	44
Figure 3.12 Displacement Sensor Head and Vat Experimental Setup	48
Figure 3.13 Vat model used for Experiments	50
Figure 4.1 Leveling System Experimental Setup	53
Figure 4.2 Pump Drive LabVIEW™ VISA Configure Serial Port Block Diagram	60
Figure 4.3 Pump Enquire VI front panel.	61
Figure 4.4 Direct Code Write SubVI front panel	61
Figure 4.5 Pump RPM and Direction VI front panel	62
Figure 4.6 Pump Stop Sub-VI front panel	64
Figure 4.7 Pump Drive Control Front Panel	65
Figure 4.8 Pump measured vs. pre-programmed volume up to 200mL	66
Figure 4.9 Pump measured vs. pre-programmed volume up to 10mL	67
Figure 4.10 Pump Dispense Accuracy (% error) for different RPM	67
Figure 4.11 Pump Dispense Precision at different RPM (coefficient of variation %)	68
Figure 4.12 Sensor LabVIEW™ VISA Configure Serial Port Block Diagram	70
Figure 4.13 Direct Code Write SubVI front panel	71
Figure 4.14 Control-Sensor Front Panel	72
Figure 4.15 Displacement Sensor Head to Linear Stage Setup	75



Figure 4.16 Sensor measured vs. pre-programmed displacement up to 50mm .....	76
Figure 4.17 Sensor measured vs. pre-programmed displacement up to 5mm. ....	76
Figure 4.18 Sensor Read Accuracy (% error) on different surfaces .....	77
Figure 4.19 Vat model with Float-Guide Element.....	79
Figure 4.20 Control Interface front panel .....	83
Figure 5.1 Control and Level output using Water and DSM Somos® NanoForm® 15120 with PID values of P=1, I=0.001, D=0.3 .....	86
Figure 5.2 Control and Level output using Water and DSM Somos® NanoForm® 15120 with PID values of P=9, I=0.001, D=0.3 .....	87
Figure 6.1 Fluid handling experimental Setup.....	91
Figure 6.2 Block diagram of the system .....	93
Figure 6.3 System step response .....	96

# **1.0 INTRODUCTION**

## **1.1 RESEARCH MOTIVATION**

Rapid Prototyping (RP) techniques also known as, “Solid Freeform Fabrication Layered Manufacturing”, or “Additive Manufacturing” are Computer-Aided Manufacturing (CAM) techniques based on an additive process where part of a model is sliced in thin layers defining the parts’ cross sections. In stereolithography, during the RP process, a photosensitive polymer material is solidified from the bottom up for each of the different cross sectional slices. Individual layers are stacked up and adhered until the final part is complete. This approach allows the creation of highly complex models, even with embedded components within a single run which otherwise would require the assembly of multiple components.

One of the main differences of RP technologies over classic manufacturing, is the reduced virtual to physical model creation, or manufacturing time. RP techniques provide a quick and economical means to make customized physical models. Stereolithography is one of the most widely used RP technologies. In general, SL technologies include: a liquid level sensing system, a vertically movable platform, a single resin vat or receptacle, a recoating device, a laser, a mirror system and laser beam optics.

In May 2004, inventors Dr. Ryan B. Wicker, Francisco Medina and Dr. Christopher Elkins formally started the development of a Multi-Material SL (MMSL) system or a system able to SL manufacture with multiple materials (“Multiple Material Micro-Fabrication...” 754-764). Many fields of study would benefit from this technology. A vast range of possibilities was envisioned

particularly in the fields of tissue engineering, functional device manufacturing and micro fabrication.

## **1.2 W.M. KECK CENTER FOR 3D INNOVATION**

Housed at the UTEP College of Engineering and under the direction of Dr. Ryan B. Wicker, the W.M. Keck Center for 3D Innovation is home to several specialized laboratories. The Keck Center facilities include; cardiovascular hemodynamics, tissue engineering and anatomical modeling laboratories, and contain equipment for rapid prototyping, microfabrication, and advanced materials research. In addition to university research, design and fabrication services are provided to local medical and manufacturing industries within the Juarez - El Paso- Las Cruces region.

## **1.3 PROBLEM STATEMENT**

A filling and leveling system must be developed capable to accurately control multiple fluid resin materials level and provide functional customization flexibility to complement a Multiple Material Stereolithography (MMSL) apparatus. An existing 3D Systems Stereolithography (SL) apparatus can be modified to accommodate multiple material fabrication for building multi-material, multi-functional and multi-colored prototypes, models and devices.

The system has four vats arranged in a rotary carousel. This is the preferred array compatible with the existing SL machine. The main vat chamber must be configured so that a build platform will fit inside. . Each vat was designed to actively maintain a uniform, desired

level of material. Particular applications may require an interface with other SL machines, or additive and subtractive manufacturing technologies as well as quality control and inspection technologies.

Peristaltic pumps were sought to handle the multiple vat material fill and removal as well as fluid level control in each vat. Peristaltic pumps allow material to be isolated from the moving parts of the pump while providing a method for accurately adding and removing fluid to and from the vat, or bi-directional supply. Fluid is manipulated at different rates and times; allowing the flow to be controlled by a separate pump, or an individual pump with multiple heads and channels. The fluids are delivered through sterile, yet disposable components.

In addition to building by moving the platform this system must be capable of building by controlling layer thickness of  $13\text{ }\mu\text{m}$  (0.5-mil) or better using the pump system alone (i.e. without moving the platform). For micro-fabrication, resolutions of  $0.1\text{ }\mu\text{m} \pm 1.0\text{ }\mu\text{m}$  must be achieved (i.e. linear stage resolution).

Various level sensing contact or non-contact displacement measurement systems such as eddy current displacement systems, confocal chromatic displacement measurement systems, linear variable displacement transducers, and proximity switches can be utilized individually, or in combination to provide accurate displacement measurements of the liquid level. Laser level sensing systems may be utilized. Such level systems must increase build tolerances.

The pump system must be integrated with the level system to precisely control the liquid level. Several alternative approaches may be combined for a particular application, or for use in a customized system.

## 1.4 PROJECT OBJECTIVES AND SCOPE

The goal of this project is to develop a leveling system able to effectively manipulate the distribution of multiple fluid materials into a multi-material stereolithography (MMSL) apparatus. The system must maintain a specific fluid level regardless of the volume changes placed upon it, and hold level accuracies of at least five microns to match the existing SL systems layer thickness. A system control should account for variable operational conditions, process variation over time and various kinds of perturbations and disturbances. A strategy needs to be developed to effectively handle multiple material vats considering a variety of vat arrays aimed to achieve material loss reduction, low contamination and improvement in overall build times. An individual, or a combination of level sensing strategies can be incorporated to improve control accuracy and build tolerances

Inherent design process issues, definitions and solutions can be tackled by retrofitting a system onto an existing single material SL apparatus. An acceptable system operation must be demonstrated by incorporating the leveling system into a multi-material apparatus, build samples and account for the resulting samples.

The scope of this project includes identifying appropriate flow measurement techniques for very low flow rates. Identifying suitable and high accuracy level measurement techniques. Carrying out experimental laboratory based investigations of multi-pump systems on the effects of relevant interventions and variables upon individual material agents and fluid behavior as delivered to the apparatus by a multi-pump system. Finally, to produce a system design, or re-design for key hardware components which would result in consistent system performance.

## 1.5 THESIS OUTLINE

A “Literature Review” including Peristaltic Pumping, Fluid Level Measuring Techniques, Laser Triangulation Leveling Principles, along with a brief review of Classical Control Theory, Process Control Techniques and Rapid Prototyping is presented. “Experimental Setup” provides a detailed description of the Peristaltic Pump and the Laser Triangulation Sensor setup and configuration. A general description of the Stereolithography (SL) System’s operation with focus on the existing leveling systems is also provided. The “System Operation” describes the vat design and the different LabVIEW® communication and control Virtual-Instruments (VI) created for the Pump and Sensor operation. Integration of the various VI’s integration into an automated control system and a description of the problems encountered during the system operation is mentioned. “System Demonstration” presents the system demonstration as a standalone unit and as a sub-system incorporated into an Automated Multi-Material Stereolithography (MMSL) machine. “Results of Study”, presents a basic mathematical model of the system and its elements. A simple tuning approach is included. Finally,” Conclusions and Recommendations”, presents a summary of the work conclusions along with general recommendations for future study.

## **2.0 LITERATURE REVIEW**

### **2.1 PUMPS**

“A pump is a device that expends energy in to raise, transport, or compress fluids” (Girdhar 1). A pump moves fluids from a lower pressure to a higher pressure, and it overcomes the difference by adding energy to the system. Pumps can be classified according to the principle in which they impart energy to the fluid. The two basic methods are by an addition of kinetic energy and by volumetric, or positive displacement. Kinetic pumps continuously add energy to the fluid by increasing its velocity. Positive displacement pumps add energy in periods by applying a force directly to movable volumes of fluid (Volk 5-7).

In kinetic or rotodynamic pumps, a mass of fluid is rotated inside a casing, creating a centrifugal head which develops a pressure head. This pressure head can move the fluid from a lower to a higher head (Sahu 35).

Positive displacement pumps have a reciprocating or rotary action. Reciprocating pumps have an inherent pulsation associated with the periodic fluid passage. Rotary pumps can have a smoother output depending on their design. Flow control in positive displacement pumps must be done by speed control or fluid recirculation (Mulley 122-124).

#### **2.1.1 Peristaltic Pump**

Peristaltic pumps are also called, “flexible tube pumps” or simply “hose pumps”. Peristaltic pumps have a flexible tube, usually made of rubber placed within a circular housing.

Rollers or cams affixed to a rotor pass over and squeeze the tube drawing liquid through the pump (Volk 26). The most significant advantage of the peristaltic pump is the use of flexible tubing as the pump chamber. The fluid being pumped remains inside the tubing at all times. The tubing is the only wetted part of the pump. This feature greatly reduces the risk of contamination (Cole-Palmer® “Peristaltic Pumps Offer Economical Multichannel Pumping”). Other advantages include its seal-less nature, compatibility with corrosive fluids, dry self-priming and their relative low cost (Volk 26). Additional significant advantages include orientation insensitive and reversible pumping, and that a wide range of flow rates can be achieved with the diverse drive motor, pump head and tube combinations.

### **2.1.2 Flow Dynamics**

As the rollers are driven by the turning motion of the rotor, the flexible tube is occluded or compressed forcing the fluid in front of the roller through the tube. As the tube behind the rollers opens and returns to its natural state, it creates a vacuum drawing fluid behind it. As the rollers’ speed increases the flow rate is increased (Cole-Palmer® “Peristaltic Pumps Offer Custom Fluid Solutions”; Seibel 16). Figure 2.1 displays an EasyLoad® peristaltic pump head diagram. This diagram highlights the head rollers compressing or occluding the tubing and rotating clockwise driving the fluid from left to right inside the tubing.



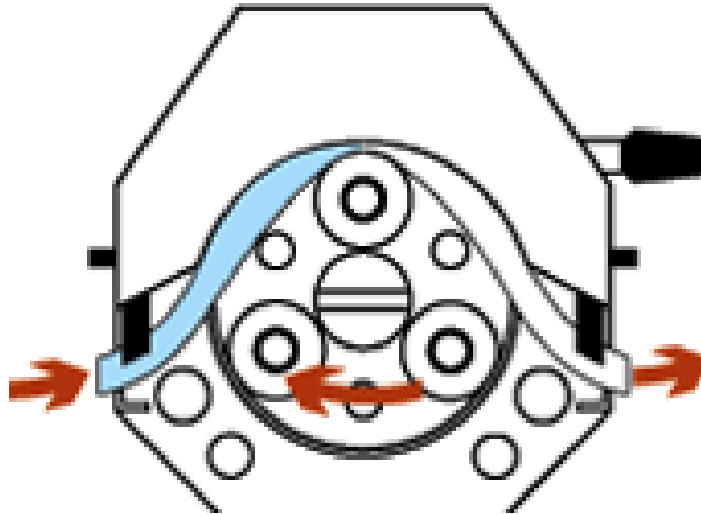


**Figure 2.1 Peristaltic Pumping Principle**

**(Cole Palmer® MasterFlex® L/S® Operating Manual: Easy-Load® Pump Heads)**

Peristaltic pumping flow dynamics are a function of the tubing dimensions and pump head characteristics. Tubing inside the diameter is directly proportional to the flow rate. The pumped volume increases as the pump head rotor diameter increases. This volume stays constant except with highly viscous fluids. The combination of tubing and pump head displays a characteristic set of flow per revolution performance. High tolerance tubing is manufactured with a tighter control of the internal diameter and wall thickness intended to improve and ensure pumping accuracy. Additional factors such as tubing squeeze or occlusion, motor speed and run time, need to be properly adjusted to improve repeatability and reduce variation. A greater degree of pulsation exists with larger volumes and higher flow rates pumps. Pumps with smaller volumes per revolution develop a rapid motion succession creating an apparent smoother flow, similar to that seen in gear pumps.

### **2.1.3 Applications**

Due to its inherent ability to isolate the pumped fluid preventing cross contamination, and the capacity of some pumps' tubing to undergo traditional sterilization routines such as autoclave or gamma radiation, peristaltic pumps are frequently used to pump sterile, aggressive or corrosive fluids. Common applications are relevant where isolation of the product-from-the-environment and the environment-from-the product is critical. Applications include medical, biomedical, industrial, chemical, agricultural, food, pharmaceutical, engineering and scientific industries (Seibel 16-29; Mohamed 875-878).

### **2.1.4 Variations**

Lower pressure peristaltic pumps, typically have dry casings, rotors with rollers and use non-reinforced tubing. Higher pressure peristaltic pumps, often called "hose pumps" are designed to employ a single oversized roller on an eccentric shaft that compresses a low friction hose through 360 degrees of rotation. This design provides more flow per revolution and only requires one compression and expansion per cycle. It operates at lower speeds at equal performance points resulting in longer hose life than pumps with multiple shoes or rollers. Larger industrial peristaltic pumps operate with lubricated and supported, or braided tube. Lubricants prevent abrasion of the tube exterior wall and assist with heat dissipation. An increased operating pressure range can be achieved; from approximately 2-3 bar (40-45 psi) for a common unsupported tubing, to 15-20 bar (300 psi) for supported and lubricated tubing.

### **2.1.5 Syringe Pumps**

Syringe pumps contain a small-angle stepping motor that drives a lead screw to progressively compress the syringe plunger, achieving in this way a smooth delivery of a precise volume per unit of time (Mohamed 875-878). Syringe pumps are generally used for “fed-batch” applications rather than continuous medium feed. Some advantages include: high precision and accuracy, non-pulsating flow, very low flow rates, ability to pump viscous fluid and against backpressure (El-Mansi 428). A significant disadvantage of syringe pumps is its low volume capacity. In order to deliver large fluid volumes, several pumps need to be used simultaneously or regular refill-replace routines need to be implemented.

## **2.2 LEVEL MEASUREMENT TECHNOLOGIES**

### **2.2.1 Introduction**

“The most significant part of level determination is its measuring technique. In practice, level is either measured directly, or inferred by some indirect action. The direct method uses an actual physical change. The inferential method uses an outside variable such as pressure to indicate a change in level” (Fardo 190).

The physical property most commonly used to sense the level surface is specific gravity. A simple float having a specific gravity will float at the surface accurately following its level. When more complex physical principles are involved, often computers are needed to perform the level calculations. (Hambrice 1)

### 2.2.2 Various level sensing techniques

Floats work on the simple principle of placing a buoyant object into the fluid. The float rides the fluids' surface revealing the fluids' surface position or level. While the float solves the basic problem of locating the fluids surface, the actual reading of the float's position still remains a challenge (Hambrice 2). A sensing device is added to track the float's position. This device can range from a mechanical, magnetic, electric, or optical element.

The displacer level sensors respond to a force equal to the weight of the liquid being displaced by the displacing element (Fardo 192). A probe of solid material is submerged into the fluid. As the fluid's level increases the probe displaces a volume equal to the probe's cross-sectional area times the fluid's level (Hambrice 3). The buoyant force increases while the weight of the displacer is reduced. A transducer converts the change in force to a level change.

Another significant indirect method of determining level is the use of load cells. Load cells can be employed to detect fluid level changes by associating a force reading change to working fluid mass changes when the fluid's specific gravity and tank's cross-sectional area are known. A support structure with one or more load sensors needs to be designed to accommodate the fluid container. Special attention needs to be paid to the container's plumbing and connections in order prevent level reading inaccuracies.

“Capacitance transmitters operate under the fact that fluids usually have a significantly different dielectric constant ( $\epsilon$ ) as that of the air” (Hambrice 5). Level changes can be detected with a capacitor probe made of two metal plates using the fluid as the dielectric. “Changes in capacitance can be equated to linear level changes” (Fardo 194).

Time of Flight (TOF) transducers measure the distance to a target surface by measuring the time required for a pulse emitted by the sensor antenna or transmitter to travel from the source to

the target surface and back. Ultrasonic, microwave and light pulses are commonly used on these sensors. A timing circuit measures the elapsed time and calculates the distance based on the speed of sound or light according to the type of pulse being emitted.

## **2.3 LASER TRIANGULATION LEVEL SENSOR**

### **2.3.1 Introduction**

Laser triangulation sensors' heads emit lasers that reflect light to form a triangle. In laser triangulation sensing, a laser beam is projected through a series of optical lenses collimating the beam to a specific standoff range and beam size. A set of optical lenses then collect the reflected beam and collimate it onto a photosensitive receiving element. "Distance changes between the sensor and target surface modify the angle on the return beam changing the beam position within the photosensitive receiving element. A microcontroller then processes the position of the beam on the receiving element and outputs the measured value in an analog or digital format" (Duval 5).

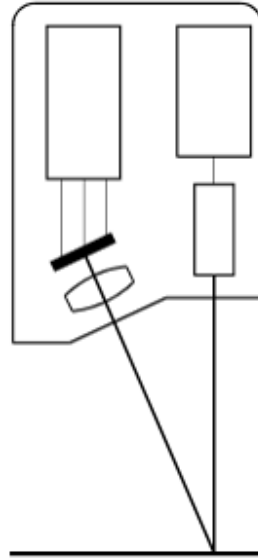


**Figure 2.2 Laser Triangulation Sensor Head**

**(MTI Instruments, Inc. Microtrak 7000<sup>TM</sup> – User Manual 29)**

One of the benefits of the laser triangulation distance sensing is the ability to maintain a high resolution over relatively long ranges. Many sensors offer resolutions of  $<1$  mm and ranges of  $>1$  micron, but in turn the higher resolutions occur at relatively small windows and at shorter ranges. In order to function, laser triangulation sensors require the laser light to reflect from the target's surface. To optimize measurement accuracy, the laser power level and the surrounding ambient light exposure levels need to be controlled. Device sensitivity is defined by the amount of light needed to provide an accurate reading. The most sensitive devices are most costly, and high sample rates require a stronger reflection. "In addition to the amount of light a surface reflects, the way it is reflected affects the optical sensor's performance. Partially specular or diffuse surfaces are difficult to measure" (Haus 71). "These sensors are employed for

contactless measurements of deformable, very rough, sensitive, hot, moving, solid or liquid surfaces” (Grote 813; Singh 306).

“Most of the laser measurement sensors perform an internal sample averaging called sample integration. This sampling or integration helps reduce the signal noise which results in a smoother and more accurate output. Resolution increases with the number of samples averaged or integrated. Response time increases proportionally to the resolution” (Duval 4).

Some advantages to laser level measurement sensing include its non-contact nature, suitability for vacuum medium since a propagation media is not required, compatibility with interfering reflections, ease of calibration and setup, low cost and commercial availability (Singh 306; Sharpe 831). Laser level sensors are not well suited for the measurement of transparent liquids as the sensor might detect the bottom of the container instead of the liquid surface. Very shiny and black surfaces can cause measurement errors due to lateral or weak reflection. Dense or light absorbing measuring medium such as steam, dust or fog can absorb the signal producing fault readings (Singh 306).

### **2.3.2 Operating Principle**

The information provided by laser triangulation displacement sensors is similar to that provided by a Linear Variable Differential Transformer (LVDT) or a contact probe but in a non-contact manner. “The sensor projects a laser beam onto the target surface and makes the distance calculation by defining where the reflected light falls on the detector (see Figure 2.3). The spot’s position on the detector changes with the movement of the target surface” (Sharpe

831; Haus 69). Triangulation can be classified as diffuse or specular depending on the reflective characteristics of the materials being measured.

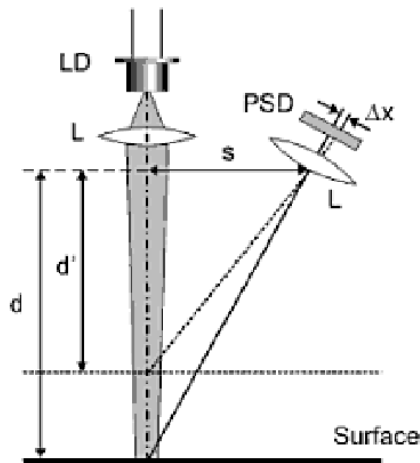


**Figure 2.3 Triangulation sensor operating principle (Haus 70)**

Triangulation sensors are composed of three subsystems: transmitter, receiver, and electronic processor. The electronic processor controls the transmitter that emits the laser beam. The beam illuminates the target object and reflects light into the receiver. The receiver transmits data back to the processor which interprets the data and outputs a measurement. The transmitter is typically a laser diode.

“The diode optics create a small spot at the standoff distance and set the target feature size detection limit. Sensor resolution is defined by the beam diameter. The beam diameter should be smaller than the smallest feature that needs to be measured. This diameter is specified in the center of the working range, increasing towards both extremes of the working range, changing with this the feature of size detection limit” (Clark 1).



An optical lens system focuses the light reflected off from the target surfaces into the receiver. Signal-conditioning electronics detect the spot's position on the receiving element. The most critical component in an optical triangulation system is the light receiving element which can be a Position-Sensing Detector (PSD) or a Charged Coupled Device (CCD). PSDs are analog detectors that rely on current generated by the photodiode. "PSDs output two currents that are proportional to the position of the image within the PSD" (Clark 1). These currents are generally converted first to a voltage and then to digital signals. A symmetric output occurs when the reflected spot falls in the middle of the receiving element. As the spot moves off center, the outputs will change allowing for sensor's electronics to calculate an equivalent surface position. These digital signals can finally be used individually, or summed together allowing for various post-processing techniques. The amount of post-processing performed depends on the amount of information available from the detector. Speed is one advantage of PSD-based systems. Sampling rates are usually in the 200 kHz range.

### **2.3.3 Accuracy, Resolution and Repeatability**

The expected difference between an instrument's reading and the actual variable value is known as "instrument's accuracy". The term linearity can occasionally be used like accuracy. Linearity usually refers to analog devices. Resolution is typically smaller than the instrument's accuracy and is known as the smallest detectable change that an instrument can observe. In laser triangulation sensors, temperature, surface reflectance and ambient light affect accuracy but generally will not affect resolution. In many applications, resolution is preferred over absolute accuracy.

Repeatability indicates the instrument's reading stability over time. Sample rate affects the instrument's repeatability. Longer sample times or smaller sample sizes usually yield improved repeatability. In laser triangulation sensors, excessively long sampling times can worsen repeatability due to component drift and temperature changes. The time for a change in the instrument's output signal from 10% to 90% is known as the "reaction time". In digital signal outputs, this time is the time required for a stable measurement output.

## **2.4 SERIAL COMMUNICATION**

The National Instruments<sup>TM</sup> Serial Communication General Concepts (1M9E1L6Q) document provides a clear description on serial communication:

Serial is a common communication protocol that is used on almost every personal computer and by many instrumentation, data acquisition and remote sampling devices. Although serial communication is slower than parallel communication, it is simpler and can be used over longer distances. The serial communication sends and receives one bit of information at a time and can extend as much as 1200 meters. In contrast parallel communication allows the transmission of an entire byte at once but for a distance no more than 20 meters. Serial communication is typically used for ASCII data transmission. Communication is possible thru the Ground, Transmit and the Receive transmission lines.

The asynchronous nature of serial communication allows transmission on thru a line while receiving on another. To make communication possible among two ports, parameters such as baud rate, data bits, stop bits, and parity must match. Baud rate

is a speed measure for communication indicating the number of bits transferred per second. Data bits, denotes the actual bits transmitted during transmission. Standard ASCII has uses values from 0 to 127 or 7 bits while extended ASCII uses values from 0 to 255 or 8 bits. Stop bits denote the end of transmission and also compensate for speed clock errors. Parity assists to check serial communication error. Parity can be even, odd, marked, spaced or no-parity

RS-232 (Recommended Standard – 232) and other EIA (Electronic Industries Association) standards define the electrical and mechanical details of the interface. RS-232 was initially designed to connect a digital computer to a modem for conversion and transmission in analog form (Bailey 183). The RS-232 standard defines the interface's electrical signal and mechanical characteristics and provides a functional description of interchange circuits (Reynders 71-72). Presently RS-232 it is widely used to connect computers to peripheral devices, such as mouse and printer as well as industrial instrumentation. Improvements in line drivers and cables, applications often increase the performance of RS-232 beyond the distance and speed listed in the standard up to 50 feet.

## **2.5 PROCESS CONTROL**

### **2.5.1 Classical Control Theory**

An important first step in the analysis and design of a control system is the mathematical description and modeling of the process that needs to be controlled. A mathematical model of the controlled process is essential if the controller will be designed by analytical means (Astrom 27). In a given controlled process, the set of variables that identify the dynamic characteristics of the process should first be defined. These variables are interrelated through established physical laws which lead to mathematical equations of various forms. Depending upon the nature of the process, as well as the operating condition of the system, some or all the system equations may be linear or nonlinear, time-varying or time-invariant. In addition, these equations can be algebraic equations, differential equations, or a combination of each.

The physical laws that govern the principles of operation of systems in real life are often complex. A realistic characterization of the systems may require nonlinear and/or time-varying equations that are generally complex to solve. For practical reasons, assumptions and approximations have to be applied to the physical systems to suit them for the application into linear systems theory (Astrom 38). In this fashion, applicable control systems analysis classes and design tools can be established. One assumption is that the system is basically linear, or that the system operates in the linear region so that the conditions of linearity are satisfied. Another assumption is that the system is basically nonlinear. In order to apply the linear theory of analysis and design the system is linearized to a rough nominal operating point. Under this

assumption, it should be considered that the analysis is applicable only for the range of the variables in which the linearization is valid.

### **2.5.2 Model Philosophies**

There are two main approaches to designing a control system. The traditional approach is where a control strategy and the system hardware are selected based on the knowledge, experience and insight of a process. After the control system is installed the controller settings are adjusted or tuned. In the model-based approach (Liptak, Process Control and Optimization, 671) a process model of a system is developed, followed a suitable control strategy and system hardware. A process model can be used as the basis for classical controller design methods. It can be incorporated directly in the control law. This approach is used as the starting point for many advanced control techniques. It can be used to develop a computer simulation of the process allowing the exploration of alternative control strategies and the calculation of preliminary values for the controller setting.

### **2.5.3 Modeling of Processes**

A process model is a mathematical abstraction of a real process. An equation or set of equations characterize the process and are meant to best approximate the true process (Astrom 38). The main objectives of a mathematical model are: to improve the understanding of the process, design a controller strategy for a new process, assist in the selection for controller settings, design the control law and to optimize process operating conditions. Process models are

usually classified by the way in which they are derived: by using the applicable physical principles or from a theoretical model. Derived from an empirical model or obtained from the statistical analysis of the operating process data, is also known as process identification. Or, a combination of both models, known as a “semi-empirical” model.

In general, the principles of mass (Equation 2.1) and energy (Equation 2.2) conservation can be applied and serve as a basis for the modeling of physical systems and processes.

$$\left\{ \begin{array}{l} \text{Rate of mass} \\ \text{accumulation} \end{array} \right\} = \left\{ \begin{array}{l} \text{Rate of} \\ \text{mass in} \end{array} \right\} - \left\{ \begin{array}{l} \text{Rate of} \\ \text{mass out} \end{array} \right\}$$

**Equation 2.1. Fundamental Law of Mass Conservation**

$$\left\{ \begin{array}{l} \text{Rate of energy} \\ \text{accumulation} \end{array} \right\} = \left\{ \begin{array}{l} \text{Rate of energy in} \\ \text{by flow or convection} \end{array} \right\} - \left\{ \begin{array}{l} \text{Rate of energy out} \\ \text{by flow or convection} \end{array} \right\} + \left\{ \begin{array}{l} \text{Net rate of heat addition to} \\ \text{system from surroundings} \end{array} \right\}$$

**Equation 2.2. Fundamental Law of Energy Conservation**

## 2.5.4 Closed Loop Control Systems

A more accurate control can be achieved by closing the system with a feedback signal. A sensor is used to measure the controlled output signal. The measured signal is then fed-back and compared with the reference input (Dorf 3). An actuating signal proportional to the difference between the input and the output is sent through the system to correct the error (Dorf 193). Finally, the resulting control signal is used as input to the process closing the loop. Systems with one or more feedback paths are called, “closed loop” systems. Closed-loop over Open-loop

controllers provide benefits such as disturbance rejection, guaranteed performance even with uncertainties, stabilization of open loop unstable processes and increased sensitivity with reduction over parameter variation (Dorf 194).

A good closed loop system has the ability to establish a tight concordance between the process variable and the set-point. In other words, a good system reduces to zero, or nearly zero the error signal. The final difference between the process variable and the set-point allowed by the system is called, “offset”. A good control system has a low offset. Response time is an important closed loop characteristic, sometimes more important than a low offset. If a disturbance occurs, a good control system will settle quickly.

It is possible to design systems with a low offset and high response times. This sometimes creates an unstable process with large and violent output variables variations. This is caused when the system has an excessive reaction to errors, creating a greater error in the opposite direction. Such types of events are called, ”system oscillations”. Oscillations usually disappear and the system then stabilizes at a good control variable. In the interim, the system goes out of control, which can turn into unexpected, undesirable outcomes. On occasions, oscillations do not lessen, but can keep on increasing until the process permanently goes out of control.

Control systems generally fall within one of the following five basic control methods, arranged in order of complexity: On-Off, Proportional plus Integral (PI), Proportional plus Derivative (PD) and Proportional plus Integral plus Derivative (PID).

### 2.5.5 On-Off Controllers

An “on-off” controller can be considered to be a special case of a proportional (P) controller with a very high controller gain. On-off controllers are usually simple and inexpensive controllers, but they lack versatility and are not very effective. Continuous cycling of the controlled variable and excessive wear affect the final control element. Its usage is limited to domestic and non-critical industrial applications. The controller output of an ideal on-off controller can be written as:

$$u_{on-off}(t) = \begin{cases} u_{\max} \\ u_{\min} \end{cases}$$

**Equation 2.3. Output of an ideal On-Off controller**

Where  $u_{\max}$  and  $u_{\min}$  denote the on and off values, respectively.

### 2.5.6 Proportional Part

The proportional part provides an immediate corrective action as well as a steady-state error or offset (Zhong 19). It can be applied when the steady-state error is acceptable to the process. Proportional-only controllers are desirable for simplicity reasons, but are not often used by themselves. To remove the steady-state error or offset from the proportional controller, an integral control action needs to be introduced into the feedback control.

Generally, the proportional band is expressed as a percentage of the controller’s whole scale range. Proportional band is the controller’s percentage of the full range that the measured variable must change to produce a 100% change. Most of the proportional controllers have a



proportional adjustable band. Proportional control eliminates the on-off permanent oscillation. A tight proportional band can make the controller respond as an on-off creating temporary oscillation close to the final control point. Proportional control provides a more controlled precision with less violent reaction, thus reducing mechanical components wear.

Given that the control output ( $u_p(t)$ ) is proportional to the error ( $y_s(t) - y(t)$ ), the proportional part drives the process output to the set-point as much as the error drives the process output away from the set-point. The transfer function for a Proportional Controller is:

$$\frac{U_P(s)}{E(s)} = k_c$$

**Equation 2.4. Proportional controller transfer function**

### **2.5.7 Integral part**

As the proportional part is not zero even when the error at steady-state is zero, the integral part has a significant function in rejecting the inherent controller offset. Due to its dependence to the accumulated past error, it provides a slow action in the control signal. The integral part (I) is not good for closed-loop stability and can cause large overshoot (Zhong 18). Given that the Integral part does not provide an immediate corrective action, it is generally used with the form of a PI controller. Integral control usually has an oscillatory response, and as a result it reduces the stability of the system. Proper control tuning or the introduction of a derivative control action tends to counteract the system's usual instability effects. The transfer function for an Integral Controller is:

$$\frac{U_I(s)}{E(s)} = \frac{k_c}{\tau_I} \cdot \frac{1}{s}$$

**Equation 2.5. Integral controller transfer function**

### **2.5.8 Proportional Plus Integral Control**

In the Proportional plus Integral Control, the controller's output is determined by the magnitude of the error signal. This is error magnitude is the proportional part. The integral part is the time integral of the error signal, or the magnitude of the error multiplied by the time in which the error has existed. Since the control reacts to the error's time integral, any offset error resulting from the proportional control in any given time is corrected with time. This can be viewed as a proportional positioning of the controller to the error. Then the integral part detects the permanence of the small error or offset. As time increases, the integral part separates the controller in the same direction helping reduce the offset. The longer the error lasts, the more distance the controller will move. Eventually, the error will come to zero or will equal the preset acceptable error and the controller's movement will cease. As time passes, the time integral no longer increases, since the error is zero, and in consequence the controller stops.

### **2.5.9 Derivative Part**

Given that the derivative part represents the approximate error increase after time  $\tau_d$  from the present time  $t$ , it plays an important role in rejecting the future error in advance by increasing

the control output proportional to the future incremental error (Zhong 18). The derivative part enhances the robustness of the PID controller by taking into account the abrupt error changes. If the process measurement is noisy, the derivative term will change widely and amplify the noise unless the measurement is filtered. The transfer function for a Derivative Controller is:

$$\frac{U_D(s)}{E(s)} = k_c \tau_D \cdot s$$

**Equation 2.6. Transfer function for a derivative controller**

### 2.5.10 PID Controller

“Many industrial processes are controlled using proportional-integral-derivative (PID) controllers. The popularity of PID controllers can be attributed partially to their good performance in a wide range of operating conditions and partly to their functional simplicity that allows for a simple and straightforward operation” (Dorf 391). “The PID controller is very simple and can be implemented using pneumatic, hydraulic, mechanical and electronic devices and software. Moreover PID controllers are very robust to plant uncertainties” (Zhong 17-18)

The transfer function for an ideal PID controller can be written as follows:

$$\frac{U_{PID}(s)}{E(s)} = k_c \left[ 1 + \frac{1}{\tau_I s} + \tau_D s \right]$$

**Equation 2.7. Transfer function for an ideal PID controller**

Common industrial controllers approximate the ideal behavior as follows.

$$\frac{U_{PID}(s)}{E(s)} = k_c \left[ \frac{\tau_I s + 1}{\tau_I s} \right] \left[ \frac{\tau_D s + 1}{\alpha \tau_D s + 1} \right]$$

**Equation 2.8. PID physical approximation to an ideal controller**

### 2.5.11 Typical Responses of feedback control systems

Figure 2.4 illustrates the typical feedback control responses. An open loop system slowly makes the process reach steady state. A proportional control reduces the system offset and creates a rapid response. An integral control produces an oscillatory response and removes the offset. A derivative control lessens response times and system oscillations. Figure 2.4 displays the Typical feedback control system responses.

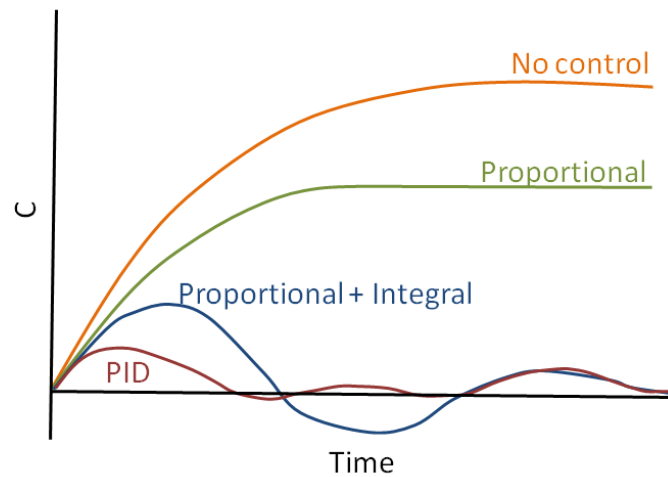


**Figure 2.4 Typical feedback control system responses**

### 2.5.12 Effect of controller gain

Increasing the controller gain turns into a less sluggish process response. Too much controller gain turns into an undesirable degree of oscillation or an unstable response. An intermediate value of the controller gain provides the best control result. Figure 2.5 displays the effect of controller gain in process response.

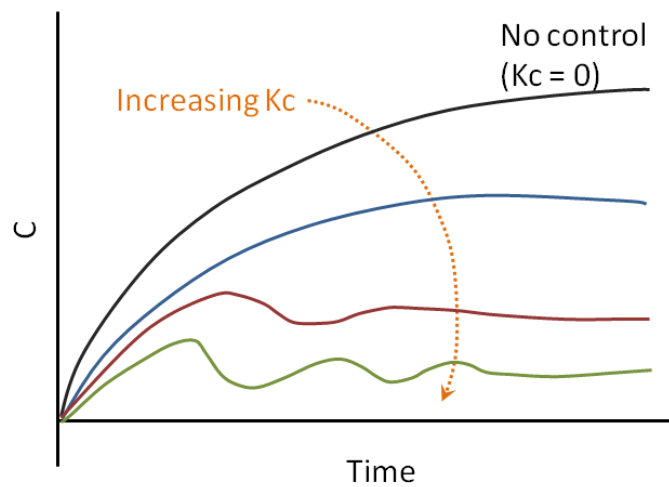


Figure 2.5 Effect of controller gain in process response

### 2.5.13 Laplace Transform

Laplace transform is a mathematical tool that significantly aids in solving a linear differential equation model. This transformation converts differential equations to algebraic equations, which can simplify the mathematical manipulations required to obtain a solution. In a wide variety of processes, the dynamic behavior on the process variables develops in a non-

linear fashion. The Laplace transform cannot be applied directly to these non-linear processes which must undergo a linearization routine such as the Taylor series expansion.

#### **2.5.14 The Transfer Function**

The Transfer Function is an algebraic expression for the dynamic relation between the input and output of the process model. It is defined as independent of the initial conditions and of the particular selection of forcing functions. A transfer function can be derived only for a linear differential equation model, because the Laplace transform can be applied only to linear equations. A transfer function provides a simple way to estimate and interpret the output response for a given input adjustment.

#### **2.5.15 Control Tuning**

“Tuning is the process of setting controller gains to achieve a desired performance. The goal of tuning is to determine the gains that optimize system response. Control systems have inherent limitations in response and stability” (Ellis 31). Compromises between the desirable outputs need to be made in order for successful tuning (Liptak. Process Control and Optimization. 671). “A PID controller can be tuned by many methods, such as trial-and-error tuning, empirical tuning such as Zeigler-Nichols method, analytical tuning, optimized tuning and auto-tuning with plant model identification” (Zhong 18). Tuning when all the system components are operating correctly ensures maximum system and equipment efficiency.

## **2.6 RAPID PROTOTYPING**

In recent years, the use of Computer Aided Design (CAD) has evolved into Computer Aided Manufacturing (CAM) technologies closing the gap between model design and prototype production phases. A manufacturing branch of such evolution is Rapid Prototyping (RP). RP manufacturing has the primary characteristic of constructing parts directly from CAD models, by following an additive process. In stereolithography, one of the RP processes, layers derived and converted from an original CAD file are scanned over the surface of photosensitive resin material. The total solidified stack of the individual model layers forms the complete part. The most widely recognized RP techniques are: Stereolithography (SL), Selective Laser Sintering (SLS), Fused Deposition Modeling (FDM) and 3D Printing (Grimm 162).

### **2.6.1 The SL Process**

Stereolithography (SL) is one of the simplest and most common Rapid Prototyping (RP) technologies (Bidanda 184). SL is an additive fabrication process based on the photopolymerization of liquid photosensitive resins to build models one layer at a time. A laser beam traces the cross sectional patterns defined by the CAD model geometry on the surface of a liquid plastic or resin (Grimm 164-165).

In SL, a CAD model of a part to be reproduced is converted into a stack model of equally spaced layers or cross sections. Each of these layers represents a specific, vertical model location and can be treated as an independent individual element. These individual layers are sequentially traced over the resin's surface to form a complete 3D replica of the original CAD model. In some cases, the model is composed of overhangs elements at any stage of layer

construction. In these cases, the CAD- to- Vector conversion software allows for the addition of support structures that hold the overhanging layers. During the building process, these supports are treated as elements of the original CAD model. Upon completion of the model, these supports need to be removed and cleaned off affecting the complete parts' surface finish. It is standard practice to utilize such built structures to keep the model from being built directly on the SL platform and guarantee the proper removal. This step also allows for the creation of a leveled structure which guarantees a consistent and uniform layer thickness throughout the building process. Some of the most relevant issues that arise during the SL building process include the control of the resin surface level, material handling and material purity. Figure 2.6 illustrates the standard SL machine elements and process.

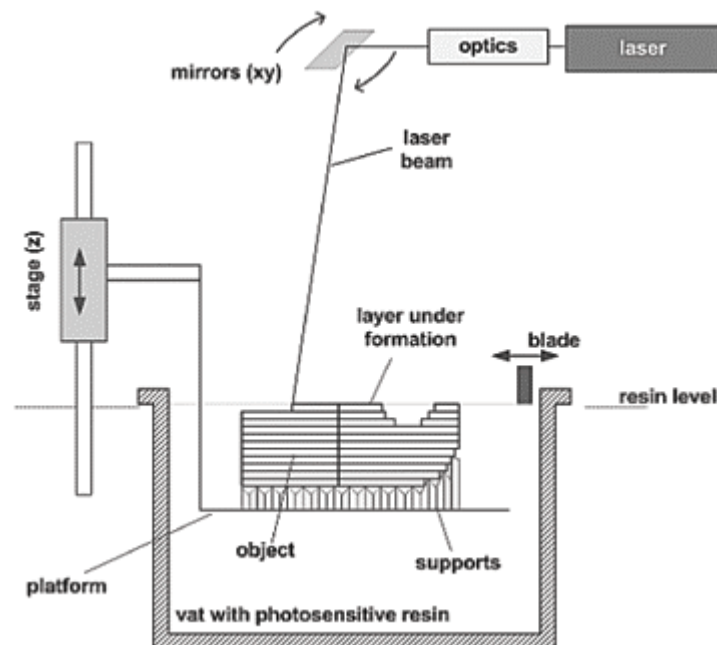


**Figure 2.6 “Sketch of the stereolithography process” (Beal 40).**



## **2.6.2 RP influence to other disciplines**

Advances in SL technologies combined with developments of photosensitive materials allow the fabrication of assemblies and functional models with function-specific SL properties such as thermal, optical and structural strength. These advances and developments make SL a more promising alternative which can be extended to diverse fields of study. RP structures can be used in research, science and several other fields, opening an opportunity to consider design alternatives not possible with traditional manufacturing techniques. Assembled components, mathematically derived structures, and biological bodies are examples of the possibilities that this technology provides.

“Earlier RP materials and technologies were used to provide product designers with the ability to visualize the product, but with limited ability to assess the functional performance of the product. Recent advances in RP have technologies have allowed the use of production type polymers that can be used to assess the functional behavior of these materials” (Kamrani 1).

Kochan suggests that the new developments in RP could drive its usage from prototype-only to small production batches (295-299). Karalekas describes the effects of the addition of nonwoven glass fibre mats on the mechanical properties of SL specimens (526-530). Sandoval describes the effects of multi-walled carbon nanotubes fillers on the physical polymerized SL resins (513-524). Dobson demonstrated the reproduction and mechanical testing of cancellous bone structures for the validation of Finite Element Analysis (FEA) results of these structures (481-484). Arcaute demonstrated the use of SL for the creation of complex scaffolds for applications in tissue engineering (1429). Beal evaluated the use of rapid tooling technique in powder metal injection molding (40-46). Kamrari highlights the use of RP on reverse

engineering, describing that today reverse engineering is used as a practical methodology to new challenges of unique parts (88).

## **3.0 EXPERIMENTAL SETUP**

### **3.1 PERISTALTIC PUMP**

An essential element of the fluid leveling system is the fluid handling unit, which can be either a control valve, or in this the case, a pump. The original concept disclosed by Wicker (“Multi-Material Stereolithography ...” US 7,556,490 B2) recommended a peristaltic pump due to the fluid isolation from the pump’s mechanical elements and the bi-directional flow capability. Characteristics accounted for were: pump accuracy, flow rates, and pressure capacity. Several pumping strategies considered were: using a combination of high-flow and high accuracy pumps(including a combination of normally open and normally closed valves), using a peristaltic pump for high flow and better fluid handling in combination with a syringe pump for increased accuracy.

A review of the desirable pump performance against common commercially available peristaltic pumps was made. A MasterFlex® L/S® 7550-50 peristaltic pump with a computer-compatible console drive in combination (Figure 3.1) with an MasterFlex® EasyLoad® peristaltic pump head (Figure 3.2) and using various tubing sizes offered an adequate performance combination. The pump drive has the ability to manipulate speed, or flow rate and flow direction. It can be manipulated at the drive’s front panel interface, or from a remote computer using either the factory software or other standard computer code.



**Figure 3.1 MasterFlex® L/S® 7550 Console Drive (Cole Palmer® MasterFlex® L/S® Operating Manual: Pump Drives 1)**



**Figure 3.2 MasterFlex® L/S® Easy-Load Peristaltic Pump Head (Cole Palmer® MasterFlex® L/S® Operating Manual: Easy-Load® Pump Heads)**

The pump head accepts a considerable range of tubing sizes as shown in Table 4.5. Figure 3.3 shows the recommended tubing material for specific viscosity and flow combinations. This combination offered computer control, reversible flow, variable flow ranging from 0.6 to 2300 mL/min. 0 contains the specifications, setup and operation of the peristaltic pump.

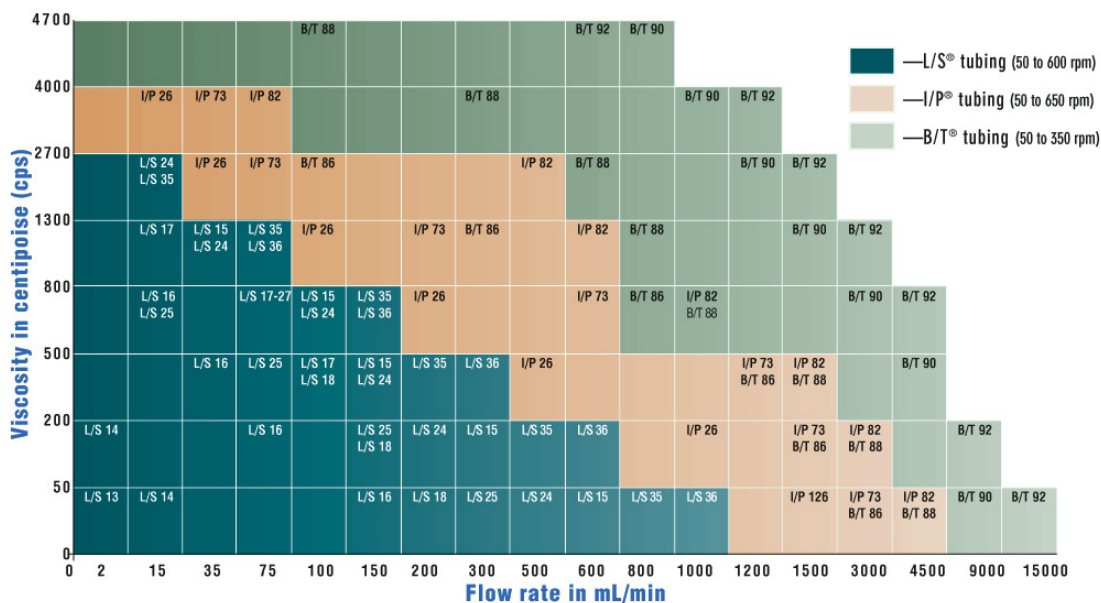
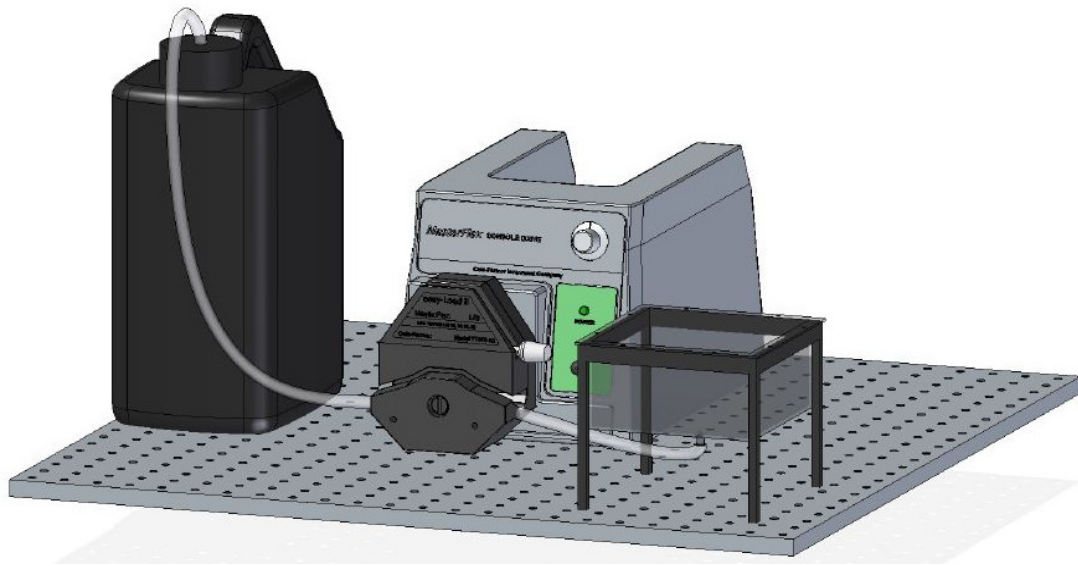


**Figure 3.3 MasterFlex® Peristaltic Pump Tubing Selection Guide (Cole-Palmer®. MasterFlex® Tubing Application Guide)**

### 3.1.1 Operation Curves

The following data was compiled using MasterFlex ® Norprene® tubing, and a MasterFlex ® Easy-Load® pump head. The fluid viscosities were taken at 25°C. The inlet and the outlet were 2.5 horizontal ft (0.75m) from the pump with no suction lift or discharge head.

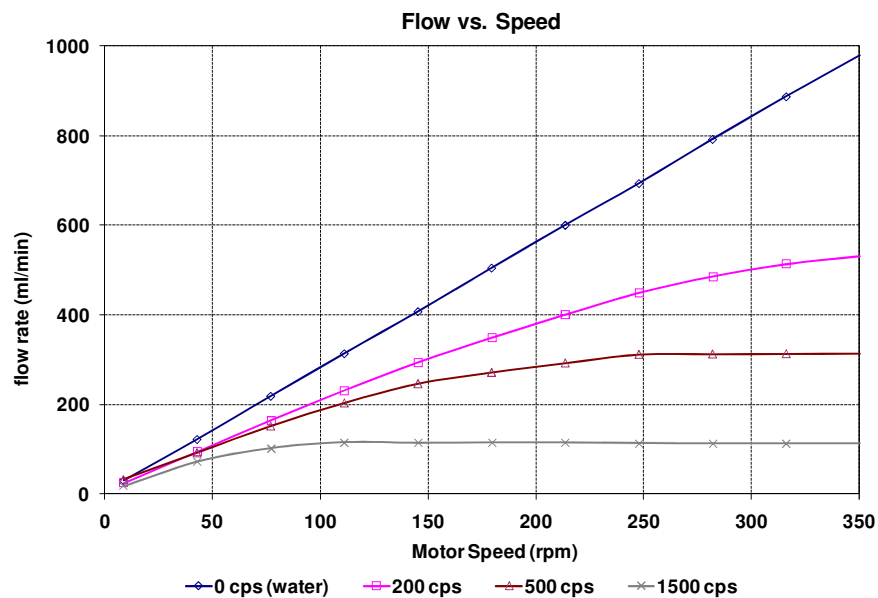
Figure 3.4 shows the system's stand-alone setup used for most tests performed with the peristaltic pump. A liquid container or reservoir was connected to the peristaltic pump via the peristaltic pump tubing, and finally connected to the working vat.



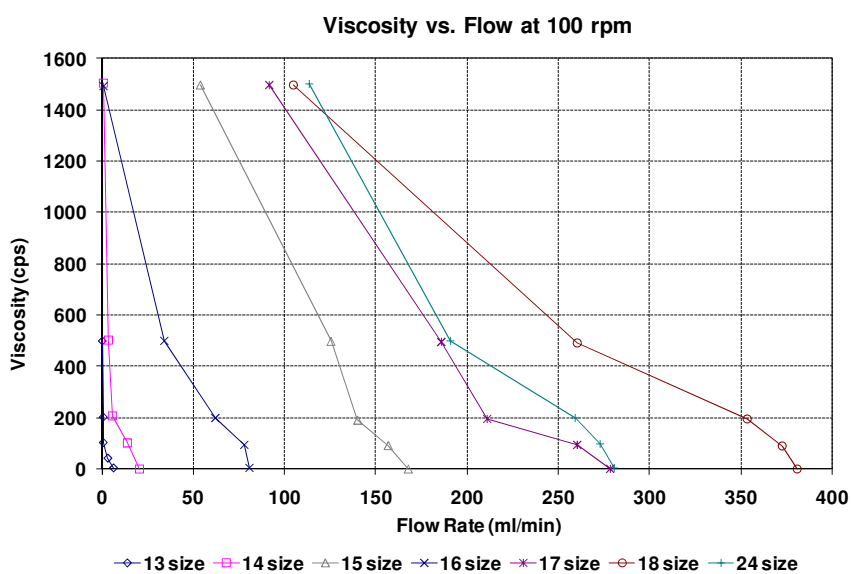
**Figure 3.4 Vat - Reservoir to Peristaltic Pump Setup**

Figure 3.5 discloses the characteristic pump flow rate function of pump speed for various fluid viscosities. Figure 3.6 shows the pump flow rates as a function of viscosity for various tubing sizes.

Figure 3.10 show the pump flow rate function of pump speed for various tubing sizes for fluid viscosities of 50, 100 and 1,500 cP respectively. This data were taken from the Cole-Palmer® Technical Library (Cole-Palmer® “Pumping Viscous Fluids Figures”).



**Figure 3.5 Peristaltic pump flow rate vs. speed for different viscosities (Cole-Palmer® “Pumping Viscous Fluids Figures”)**



**Figure 3.6 Peristaltic pump viscosity vs. flow rate for different tubing sizes at 100rpm (Cole-Palmer® “Pumping Viscous Fluids Figures”)**

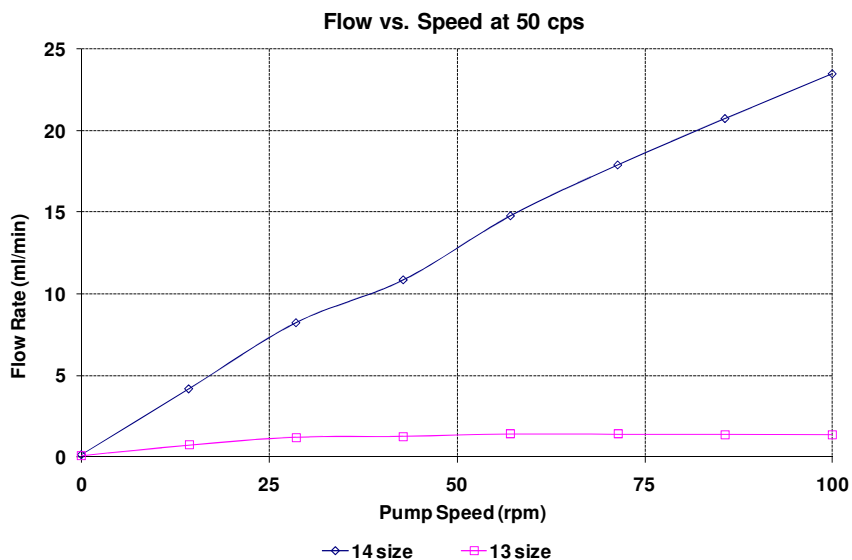


**Figure 3.7 Peristaltic pump flow rate vs. speed for different tubing sizes at 50cps (Cole-Palmer® “Pumping Viscous Fluids Figures”)**

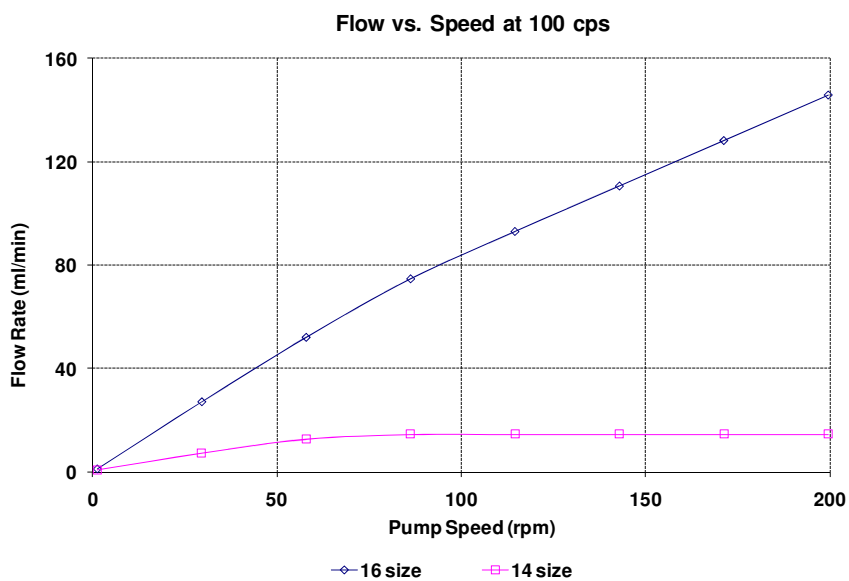


**Figure 3.8 Peristaltic pump flow rate vs. speed for different tubing sizes at 100cps (Cole-Palmer® “Pumping Viscous Fluids Figures”)**



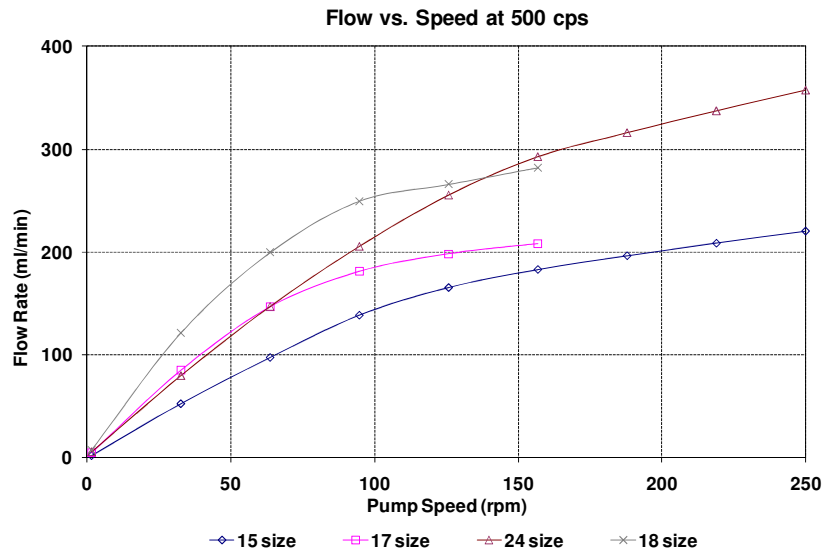


**Figure 3.9 Peristaltic pump flow rate vs. speed for different tubing sizes at 500cps (Cole-Palmer® “Pumping Viscous Fluids Figures”)**

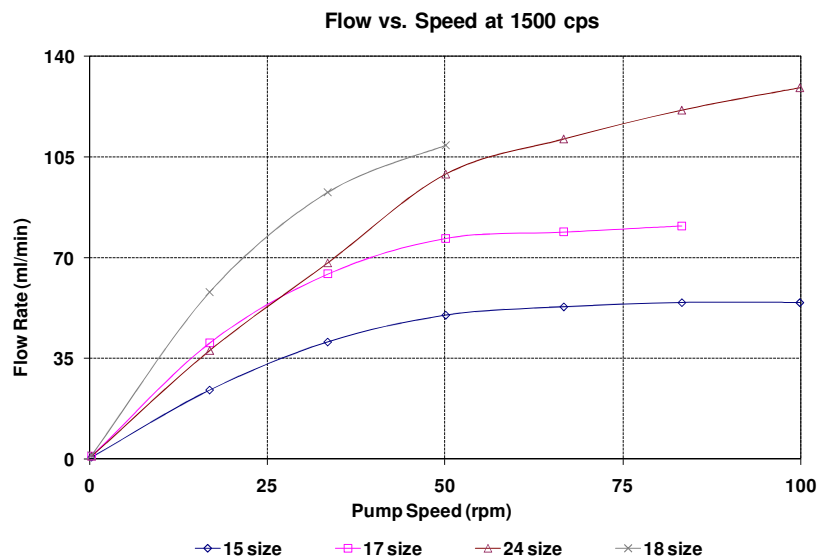


**Figure 3.10 Peristaltic pump flow rate vs. speed for different tubing sizes at 1500cps (Cole-Palmer® “Pumping Viscous Fluids Figures”)**

### 3.1.2 Drive communication specification

The information presented in this section (3.1.2) was taken directly from the Cole-Palmer® MasterFlex® L/S Operating Manual: Pump Drives (Doc 10A000194)

The Linkable Instrument Network is a serial communication system consisting of a control computer with one RS-232C port and one or more satellite units. A satellite unit can be a pump drive (7550-30, -50), mixer controller (50003-00, -05), or other product with similar communications protocol. This section describes the information needed to communicate with a pump drive. The term, “satellite unit” is used as a generic term for devices compatible with the Linkable Instrument Network. The term “pump drive” applies to MASTERFLEX Computerized Drives (7550-30, -50).

All communications between the control computer and satellite units is based on a pseudo daisy-chain principle. The transmission line of the control computer will pass through the input and output buffers in each of the satellite units. Each satellite unit will have the ability to turn the buffers on and off to block communications from other units below it in the daisy-chain. The output of the control computer would pass through each of the pump drives without software assistance from the pump drive. All pump drives in the daisy-chain must be powered up to enable communications with all drives.

The receive line of the control computer will originate in the transmitter of the last satellite in the chain. It will also be double buffered through each satellite. Each of the pump drives will have the ability to turn off its input receive line and place its own transmitter on the receive line to the control computer.

A third line, the Request to Send (RTS) will be a similarly buffered line. Each satellite will have the ability to set this line to signal the computer its request to send.

The maximum number of satellites is limited to 25 by the Linkable Instrument Network software to minimize communication time. However, up to 89 satellites could be controlled by a single RS-232C port using custom software since satellite units can be assigned any number from 01 to 89.

The 7550 Digital PWM BLDC Drives communicate with each other and a PC via a standard DB-9 modem cable (Cat. #22050-54). Older satellite units have a dual six position modular phone jack labeled, “IN” and “OUT”. Pin 1 on both jacks is located towards the top of the drive. The control computer has a standard DB-25 plug as found on most RS-232C connections.

The serial lines between units pass from unit to unit by a hardware buffer on the input and connecting it directly to the output driver through a hardware gate. This way any output only sees one input load. If power is turned off on any pump drive, all drives below it in the daisy-chain cannot communicate

The serial data format is full duplex or with simultaneous transmit and receive, 1 start bit, 7 data bits, one odd parity bit, and one stop bit at 4800 bits per second. All data transmitted will consist of characters from the standard ASCII character set. Odd parity is defined such that the sum of the eight individual bits is an odd number (1, 3, 5 or 7).

All transmissions originate, or are requested by the control computer (master). It may issue commands directly and it may request that the satellites report. When asked to report, the satellite would send the data requested. Should a satellite require communication with the computer, it has the ability to operate the request to send (RTS) line. Upon receiving the request, the computer would respond via the serial line.

### **3.2 LASER TRIANGULATION LEVEL SENSOR**

A key function of the leveling system is to consistently maintain an accurate fluid level, which in some cases will be subject to disturbances and possible target changes. Some of the items that had to be understood in order to adequately complete a sensor specification were: target material, standoff range, required resolution, mounting needs, available footprint, interface requirements, desired signal output, fixed or moving target, target speed, desired response time and degree of environmental protection.

There are several commercially available level sensing technologies shaped to fit application-specific conditions. In this particular application, fluid isolation was greatly desired, leading toward a non-contact sensor. Since the sensor would serve as the feedback or the loop closing for the control system, the ability to communicate directly to a central computer was an essential feature. Various sensing units were evaluated weighing cost against desirable features such as resolution, standoff range and target surface compatibility. A computer-compatible MTI Instruments MTI Microtrak 7000 with the MT-600 sensor head (Figure 3.11) was selected. This

combination offered a sensing resolution of  $1.27\mu\text{m}$  ( $50.0\mu\text{in.}$ ) and a standoff distance of  $152.4\text{mm}$  (6 in), with a diffuse laser spot of  $150 \times 250\mu\text{m}$ . 0 includes the sensor and sensor head full specifications detail.



**Figure 3.11 Laser Sensor Processing Unit and Head by Microtrak (MTI Instruments, Inc. Microtrak 7000<sup>TM</sup> – User Manual)**

### **3.3 SENSOR CALIBRATION, SETUP AND HEAD ALIGNMENT**

The information presented in this section (3.3) was taken directly from the MTI Instruments, Inc. Microtrak 7000<sup>TM</sup> – User Manual (Doc 10A000194).

Each laser sensor head has its own calibration data stored in nonvolatile memory. A sensor head can be disconnected and connected to another channel or controller without recalibrating either the sensor or the controller. The calibration table contains a factory-set default slope, offset, range, linearity table, user slope, electronic serial number and electronic checksum (used to verify correct data download). A factory-supplied head has the factory-generated slope factor preprogrammed into the user calibration memory location. When the controller is first turned on, the controller will download the calibration data from the head(s) and store it in its own nonvolatile memory. When the controller is activated again and the head has not been changed, the controller will not download the calibration data. If a different head is detected, the controller will re-download the calibration data. While the user calibration can reset, the factory calibration cannot be overwritten. It can be returned to the original factory default calibration by selecting the factory calibration option. A user calibration factor is included so the head can be field calibrated for greater accuracy. This allows the head to be adapted to targets with surface finishes that are significantly different than that of diffuse white paper.

To calibrate the instrument:

- Select “Normal” mode.
- Set the display value to zero either by moving the target to the zero position or by pushing the ZERO button.
- Press PARAM and select the “Calibrate” menu item.

- Move the target (or the laser sensor head) to a known location. (You must know the distance of the point relative to the zero starting point.) . Press ENTER.
- Adjust the displacement value to the step displacement value obtained in Step 2. This calibration will not affect the original factory calibration.
- The user calibration is then stored in the sensor's nonvolatile memory. It will always be loaded into the controller on power up unless a factory default calibration is performed.
- "Factory Default" overwrites the user calibration.
- To restore factory default calibration to the instrument:
- Select "Normal" mode.
- Press PARAM and select the "Calibrate" menu item.
- Select "Default." Press ENTER.
- "+/-" helps you set the correct orientation for target motion.
- To change the calibration sign to plus or minus:
- Select "Normal" mode.
- Press PARAM and select the "Calibrate" menu item.
- Select "+/-." Press ENTER. This toggles the sign function to the opposite of its current state.

Each laser sensor head model has a unique standoff and measuring range. Standoff is a point in front of the laser sensor head emission window, which is at the center of its linear range. When the head is positioned at its center of range the front panel

display will show a numeric 0.00. Installation should be such that operator does not have access to the laser beam or its reflection. Securely mount the laser sensor head so it is positioned at the standoff distance from the target. The laser sensor head view field should be clear of obstructions, dust, dirt, and fluids. The head should have an unobstructed view of the target surface, even if small right-angle steps or grooves are present. Once the sensor head is properly mounted and the system is ready to use, the aperture cover should be rotated out of the way. Replace the cover for safety when servicing the sensor or the target. Never stare into the laser beam or its reflection.

The sensor head should be exactly perpendicular over the surface being measured. Even very slight tilts will create a considerable offset. Normally, the head is considered perpendicular to the measured plane when the intensity is greatest. In addition, when the intensity is greater, the noise is lower.

Figure 3.12 shows the triangulation sensor head setup configuration. The head was affixed to an aluminum frame (Bosch-Rexroth 2x2in) via a Linear Ball Guide X-Axis Stage Micrometer Head (Misumi-XSG25) with the aid of two custom aluminum plates, one to mate with the X-Axis Stage and another to mate with the Sensor Head.



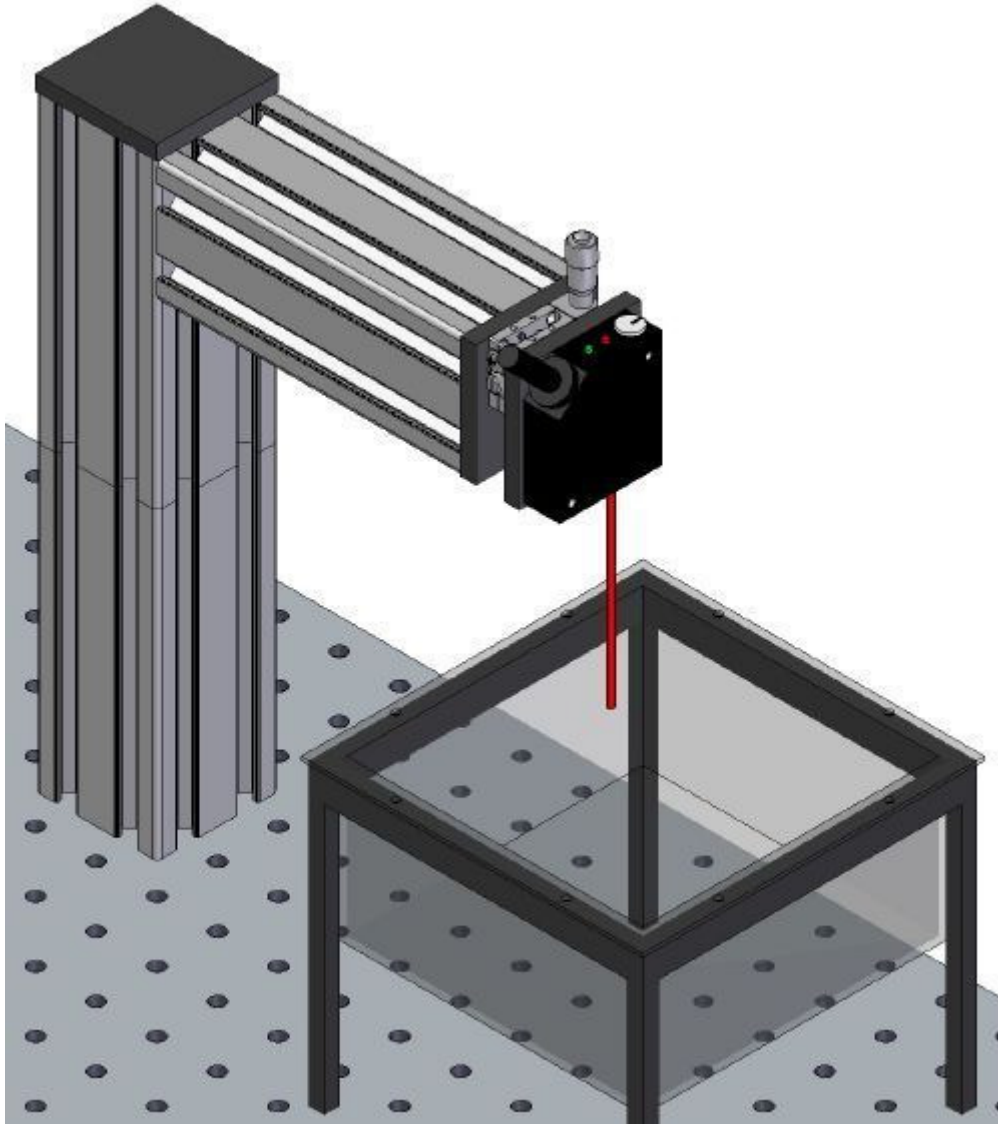


**Figure 3.12 Displacement Sensor Head and Vat Experimental Setup**

### **3.4 EXISTING LEVELING SYSTEM**

In the SL process, parts are constructed by sinking a build platform into a vat filled with resin. The build process comprehends the movement of the platform by a distance equal to the predefined layer thickness. Each layer is consecutively submitted to the polymerization process. This displacement is achieved by means of a vertical linear stage where the build platform is affixed. The stage displacement is commanded by a control computer as specified by the build parameters of the part under construction. After the platform is positioned to the build location, the resin level is sensed using a Helium Neon Diode laser level sensor. At this stage in the process, minor vertical adjustments can be performed to match the required surface level for layer construction.

### **3.5 FLUID VAT**

The vat geometry and dimensions were defined by the build platform cross sectional area and by the SL process chamber space restrains. Vats were designed to provide an adequate area for the SL build platform. Given that the vat's depth defines the height of the SL build models, vats were designed to accommodate standard model heights. To support accurate displaced volume to level correlation, the vats were designed to maintain a uniform cross sectional area. The resin was fed through the base of the vat which was designed with sufficient slope to allow for adequate resin draining and included a mating connector for the proper tubing and fitting size. In order to prevent the intrusion of air bubbles, a screen can be incorporated within the vat to isolate bubbles and force them away from the platform build area.

The use of peristaltic pumps reduces resin contamination, supports a multiple vat / multiple resin approach and eliminates the need for control or re-directional valves. Figure 3.13 is a graphical representation of a vat model employed for the manufacture of custom SL material vats.

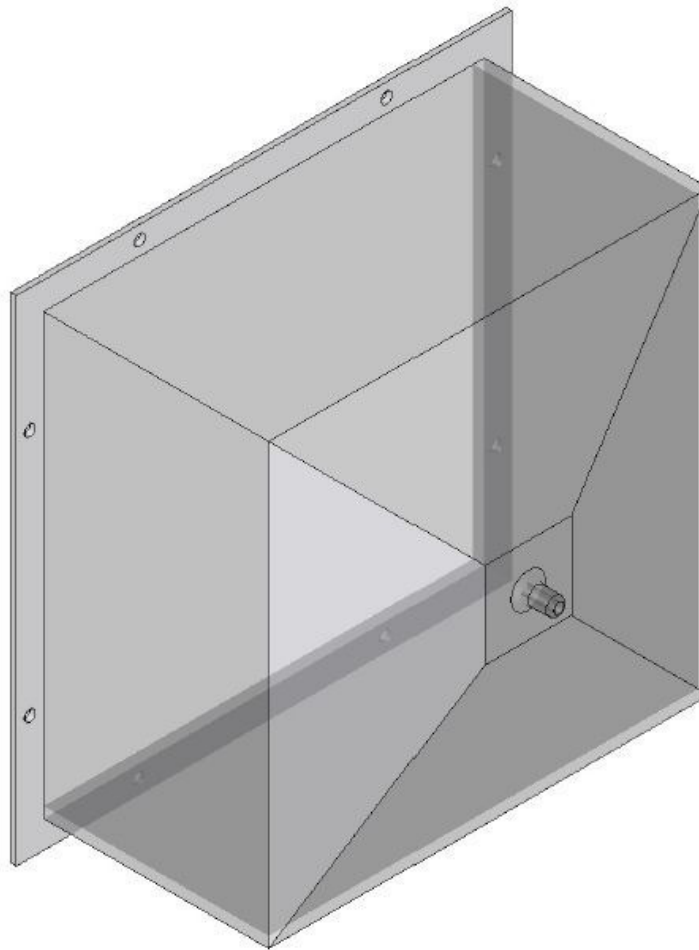


**Figure 3.13 Vat model used for Experiments**

### **3.6 RESINS**

Given that one of the main goals of this project was to develop a multiple-fluid leveling system for SL applications, particular attention had to be paid to the flow properties of the

working fluids. From the variety of physical properties of the commonly used materials, viscosity is one of the properties having the greatest impact on a fluid system design.

Experiments were carried out using DSM Somos® NanoForm™ 15120 which is one of the higher viscosity materials ( $\approx 570$  cps at  $30^{\circ}\text{C}$ ) used to represent the high viscosity materials group. On the other hand, natural water ( $\approx 0.8$  cps at  $30^{\circ}\text{C}$ ) was used to represent the lower viscosity materials group. DSM Somos® NanoForm™ 15120 is a resin developed by DSM Somos®. It is a liquid suspension of nanoparticles that help create superior stiffness and high heat deflection temperature components. In the DSM Somos® data sheet, NanoForm™ 15120 is described as a, “strong, stiff, high temperature nanocomposite resin for stereolithography” (NanoForm™ 15120 – Product Data Sheet).

## **4.0 SYSTEM OPERATION**

### **4.1 INTRODUCTION**

The primary goal of this project was to develop a leveling system capable to manipulate multiple fluid materials and be able to maintain a specific fluid level in spite of the volume changes or disturbances placed upon it. The control system needed to account for variable operational conditions, process variations and various kinds of perturbations or disturbances. The construction of a prototype system helped to demonstrate the feasibility of such a leveling system in the application to the MMSL technology. The information generated during the development of this prototype system served as a basis for the development and implementation of an automated fluid handling and leveling system into an automated MMSL system.

The system starts with an empty vat having a set-point close to 80% of the vat's level, allowing for a deeper build area and for sufficient overflow area to account for any system overshoot or oscillation and for level disturbances inherent to the build process. When started, the system begins filling by operating the pump at full speed until the fluid level reaches the sensor's reading range. Once in the sensor's reading range, the control system algorithm enters into operation controlling the pump's speed in relation to the fluid's level until the set-point is reached and the fluid's surface is stable. In the SL build process, a build platform is continuously being submerged into and retrieved from the working fluid, creating disturbances. Given that the level sensor is continuously reading, the control system constantly compensates for any level changes.

Figure 4.1 shows the complete prototype system setup. From left to right: the control computer, computer monitor, displacement sensor control unit, working fluid reservoir, peristaltic pump with head, vat and mounted displacement sensor head.

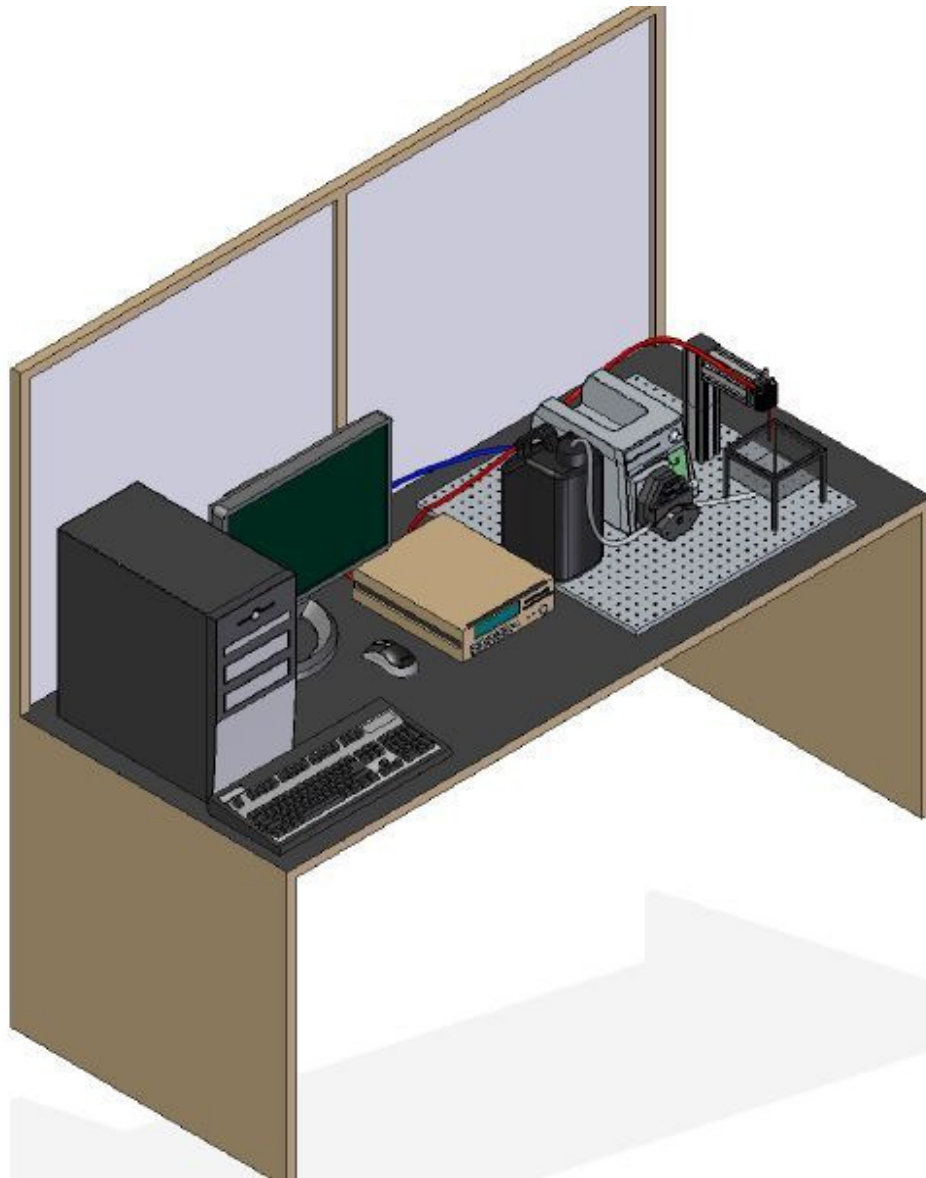


**Figure 4.1 Leveling System Experimental Setup**

## 4.2 PERISTALTIC PUMP

In addition to the factory communication system described in Section 3.1.2, a new communication system had to be developed in order to standardize the leveling system communication protocol for all the components, including pump and sensor, and to support the future integration of the leveling system into the MMSL apparatus as described by Wicker in the in the “Multi-Material Stereolithography” United States Patent (7,556,490 B2). The MasterFlex® L/S® Operating Manual: Pump Drives details the peristaltic pump operation using the factory communication software (11). Table 4.1 lists the commands and the required communication configuration. Table 4.2 Table 4.3 lists common pump commands and pump responses. Table 4.4 lists common ASCII characters used for pump communication. These commands and configuration codes served as a basis for the development of the LabVIEW™ subroutines to operate the peristaltic pump and integrate it to the leveling control algorithm.

**Table 4.1 Pump satellite commands (Cole Palmer® MasterFlex® L/S® Operating Manual: Pump Drives 13)**

COMMAND CHARACTERS FROM CONTROL COMPUTER TO PUMP		PARAMETER FIELD
A	Request auxiliary input status	none
B	Control auxiliary outputs when G command executed	xy, x = aux1, y = aux2, 0 = off, 1 = on
C	Request cumulative revolution counter	none
E	Request revolutions to go	none
G	Go Turn pump on and auxiliary output if preset	none = run for number of revolutions set by V command 0 = continuous run until Halt command
H	Halt (turn pump off)	none
I	Request status data	none
K	Request front panel switch pressed since last K command	none
L	Enable local operation	none
O	Control auxiliary outputs immediately without affecting drive	xy, x = aux1, y = aux2, 0 = off, 1 = on
R	Enable remote operation	none
S	Set motor direction and RPM	+xxx.x, -xxx.x, +xxxx, -xxxx, + = CW, – = CCW
S	Request motor direction & RPM	none
U	Change satellite number	nn (new satellite number)
V	Set number of revolutions to run	xxxxx.xx
Z	Zero revolutions to go counter	none
Z	Zero cumulative revolutions	0
<CAN>	Terminates line of data up to and including STX (used primarily for keyboard input)	none
<ENQ>	Enquire which satellite has activated its RTS line	none



**Table 4.2 Table 4.3 Sample pump commands and responses (Cole Palmer®  
MasterFlex® L/S® Operating Manual: Pump Drives 14)**

CONTROL COMPUTER COMMAND STRING	PUMP DRIVE RESPONSE
<STX>PnnA<CR>	<STX>Ax<CR> x: 0=open, 1=closed
<STX>PnnBxy<CR>, xy: 0 = off, 1 = on, x = aux1, y = aux2	<ACK> or none if P99
<STX>PnnC<CR>	<STX>Cxxxxxxx.xx<CR>
<STX>PnnE<CR>	<STX>Exxxxx.xx <CR>, x : revolutions to go (99,999.99 max), (-xxxx.xx if drive overshoots)
<STX>PnnG<CR>	<ACK> or none if P99
<STX>PnnH<CR>	<ACK> or none if P99
<STX>PnnI<CR>	<STX>Pnnlxxxx<CR> (see section 1.8)
<STX>PnnK<CR>	<STX>Kx<CR> (see section 1.12)
<STX>PnnL<CR>	<ACK> or none if P99
<STX>PnnOxy<CR>, xy: 0 = off, 1 = on, x = aux1, y = aux2	<ACK> or none if P99
<STX>PnnR<CR>	<ACK> or none if P99
<STX>PnnS+0130<CR> or	<ACK> or none if P99
<STX>PnnS+0130.0<CR>	<ACK> or none if P99
<STX>PnnS<CR>	<STX>S+0432.9<CR>
<STX>PnnUnn<CR>, nn = 01, 02, 03....87, 88, 89	<ACK>
<STX>PnnVxxxx.xx<CR>, V max = 99999.99	<ACK> or none if P99
<STX>PnnZ<CR>	<ACK> or none if P99
<STX>PnnZ0<CR>	<ACK> or none if P99
<CAN>	<ACK>
<ENQ>	<STX>P?x<CR> (on pump power up), <STX>Pnnlxxxx<CR> <STX>Pnnlxxxx<CR>

**Table 4.4 ASCII Control characters used (Cole Palmer® MasterFlex® L/S®  
Operating Manual: Pump Drives 14)**

DECIMAL	HEX	CHARACTER
2	02	STX Start of Text (CTRL - B)
6	06	ACK Acknowledge (CTRL - F)
5	05	ENQ Enquire (CTRL - E)
13	0D	CR Carriage Return (CTRL - M) (CR)
21	15	NAK Negative Acknowledge (CTRL - U)
24	18	CAN Cancel (CTRL - X)

### 4.2.1 Start Up Sequence

The Cole Palmer® MasterFlex® L/S® Operating Manual: Pump Drives (A-1299-0996)

describes the start up sequence as follows:

Normal start-up would consist of turning on all the satellite units first and then the control computer. Each satellite will enable it's receive and transmit buffers and activate its RTS line. The control computer would then send the enquire <ENQ> command in response to the active RTS line. Upon receiving the <ENQ> command, all satellites with an active RTS line would disable its receive and transmit buffers to the satellites below it in the daisy-chain. Next, the pump drives would respond with one of the following strings depending on its model number and version.

<STX>P?0<CR> = 600 RPM 7550 -30

<STX>P?2<CR> = 100 RPM 7550 -50

The control computer would only see the response from the first satellite in the chain since communications with the others is now blocked. The control computer would then send back <STX> Pnn<CR> with nn being a number starting with 01 for the first satellite and incrementing for each satellite up to 25 maximum. If the

pump drive receives the data without errors it will perform the following steps:1.

Deactivate its RTS line and enable the receive buffers to the next satellite.

2. Send an <ACK> to the control computer. 3. Enable the transmit buffer from the next satellite within 100 milliseconds after the last byte has been sent.

4. Put a P and the satellite number received in the first 3 positions on the satellite display.

After the control computer receives the <ACK> it will see the RTS from the next satellite and again issue the <ENQ> command. The process will repeat until all satellites are numbered.

If a satellite does not receive valid data from the control computer or detects a transmission error, it will send a <NAK>. When the control computer receives the <NAK> it will resend the <STX>Pnn<CR> to the satellite. Section 1.10 on error handling describes the maximum retries the control computer will perform.

If a satellite is turned on after all the other satellites have been numbered, it will be given the next available number if no commands have been sent to the other satellites. If commands have been issued, the satellite is assigned a temporary number starting with 89 and decrementing for each subsequent satellite. This will cause the satellite to release its RTS so normal communication can proceed. The operator will be alerted to the condition that another satellite has come on-line and needs to be numbered. The new satellite will be numbered so that it will appear correctly in the system. The control computer will use the following commands to renumber a satellite:

<STX>PooUnn<CR>

The “oo” is the old satellite number and “nn” the new number.

If a satellite is requesting to be numbered and the control computer has already issued 25 satellite numbers, the control computer will assign the satellite the number 89 and alert the operator to the situation. If a satellite is powered down after it has been numbered, it will be treated as a new unit when it is powered up again.

### **4.2.2 Command Format**

The Cole Palmer® MasterFlex® L/S® Operating Manual: Pump Drives (A-1299-0996) details the command format.

Commands from the control computer are preceded with the start of text <STX> character (02 hex), a satellite identification letter (P for Pump, M for mixer) and a two digit satellite number (01 through 89). Numbers 00 and 90 through 99 are reserved for special cases. When the same command is to be executed by all pump drives, 99 is sent for the satellite number. After the command character is the parameter field which varies in size from zero characters to 32 depending on the command. A carriage return <CR>, (0D hex) is used to indicate the end of a command string. Exceptions to this computer issued command format are <ENQ>, <ACK> and <NAK>. More than one command can be put in a command string as follows: <STX>P09S+0500.0V08255.37G <CR>. This command string example would set the speed at pump satellite 09 to 500.0 RPM, Clockwise direction, set 8255.37 revolutions and start the drive. The maximum number of characters allowed in one pump drive string is 38, including <STX>, Pnn and <CR>.

### 4.2.3 Pump Drive Communication Configuration

The first step to operate the peristaltic pump was to establish communication between the control computer and the digital pump drive. The digital pump drive connects to the control computer via a serial RS-232 port. Within LabVIEW™ subVI libraries the, “VISA Configure Serial Port” subVI can be found. The SubVI allows direct configuration of a serial port. In section 3.1.2, details can be found on the digital drive serial configuration as follows: full duplex data format, 1 start bit, 7 data bits, one odd parity bit, and one stop bit at 4800 bits per second, and all transmitted data should be in the form of standard ASCII characters. Figure 4.2 shows the standard, “VISA Configure Serial Port” VI block diagram with the appropriate serial configuration.

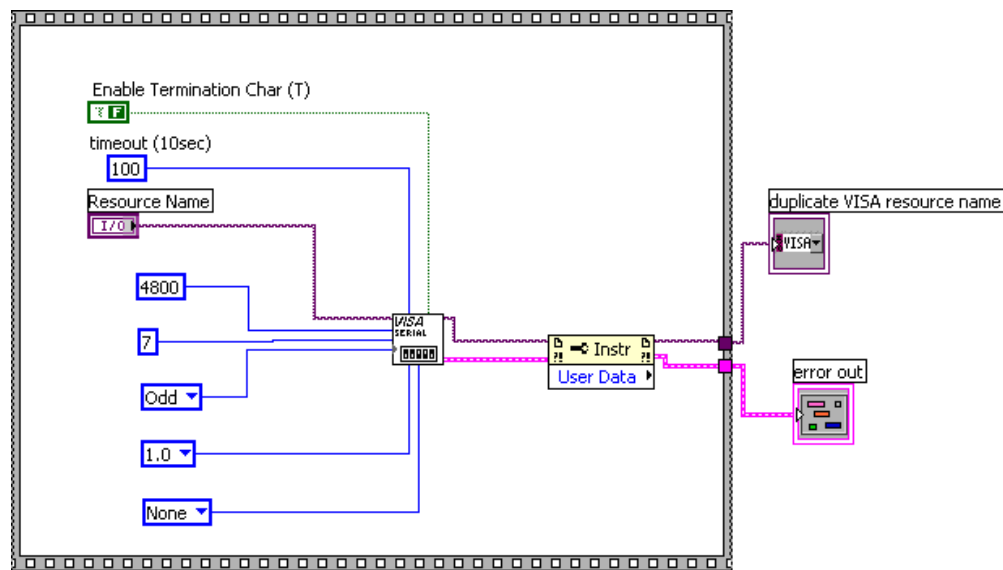


**Figure 4.2 Pump Drive LabVIEW™ VISA Configure Serial Port Block Diagram**

A pump drive, “Enquire VI” was made to serve as an initial means to verify the pump drive communication and to initiate the pump drive communication startup sequence as stated in section 0.0. This VI would later become a part of the control algorithm. Figure 4.3 shows the manual “Pump Enquire” VI front panel.

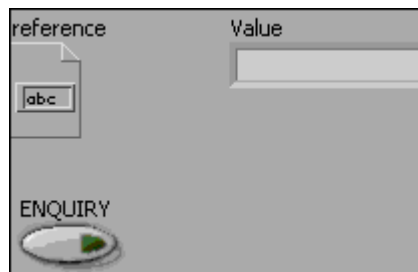


**Figure 4.3 Pump Enquire VI front panel.**

Once the appropriate communication configuration was established, single commands were sent to the pump to ensure proper operation. A simple VI was made to input the command string in Hexadecimal format, and send it to the pump drive via the established serial communication port. Figure 4.4 shows the, “direct write” VI front panel. A similar approach was followed to establish communication with the “Triangulation Sensor; in this case most of the communication was data read from the sensor with minimal commands sent.



**Figure 4.4 Direct Code Write SubVI front panel**

#### 4.2.4 Pump Drive Direction and Speed VI

Two key characteristics of the pump drive for a successful application on the control system were pump drive direction and pump speed. Drive direction defines the fluid flow direction, either filling into the build vat, or removing from the build vat. Pump drive speed provides excellent support in the implementation of a high accuracy control system. The control system was configured such that the pump drive speed would vary in proportion to the fluid level. Figure 4.5 shows the “Pump RPM and Direction” VI front panel. This VI manually operates the pump drive by directly entering the speed and direction parameters into the front panel interface, this VI then converts these inputs to Hexadecimal format, compiles them into a text string and sends them to the pump drive. During automatic pump drive operation this VI is in continuous operation as part of the control algorithm.

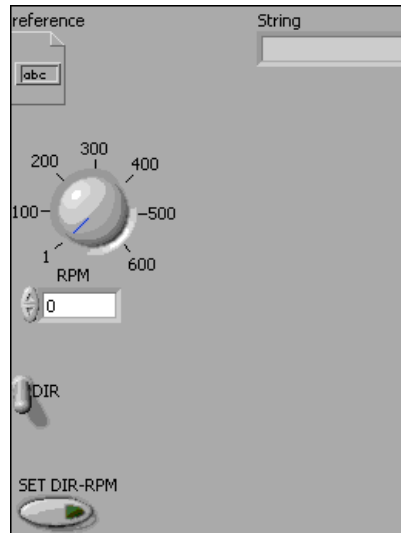


**Figure 4.5 Pump RPM and Direction VI front panel**

## 4.2.5 Pump Drive Volume Conversion VI

Given that the pump drive operates on a number of revolutions basis and not on a displacement or volume unit basis, each operation command had to be converted from a desired vat level in millimeters or microns to a specific number of revolutions. Assuming a constant vat's cross-sectional area and using the peristaltic tubing internal diameter the volume per revolution for a particular tubing size could be calculated. Table 4.5 lists the volume flow rates for a specific set of speeds, or speed range for various tubing sizes. With this information, the, "Level to Revolutions" conversion could be obtained as follows: Desired Level = Volume per Revolution / Vat Area. This relationship was incorporated in the control algorithm operation as a VI to link the sensed level to the pump's drive revolutions.

**Table 4.5 Flow rates for MasterFlex® L/S® Drive (Cole-Palmer®. "Peristaltic Pumps Offer Economical Multichannel Pumping")**

L/S Tubing	Compatible Pump Heads	Flow rates in mL/min at 10 to 600 rpm*
L/S 13		0.6 to 36
L/S 14		2.1 to 130
L/S 16		8 to 480
L/S 25		17 to 1000
L/S 17		28 to 1700
L/S 18		38 to 2300
L/S 15		17 to 1000 (18 to 1100)
L/S 24		28 to 1700 (30 to 1800)
L/S 35		38 to 2300 (43 to 2600)
L/S 36		48 to 2900 (58 to 3400)

Fits Standard, EASY-LOAD, EASY-LOAD II, QUICK LOAD, or Cartridge pump heads\*\*

Fits EASY-LOAD II or High-Performance pump heads

\* Flow rates in parenthesis can only be reached with the High-Performance pump head.



### 4.2.6 Pump Drive Stop VI

At a later stage in the development of the control structure, a VI was created, namely the “Pump Stop VI”. This was meant to halt the pump drive operation to control algorithm, or as a manual stop override for safety purposes. Figure 4.6 shows the “Pump Stop VI” front panel.



**Figure 4.6 Pump Stop Sub-VI front panel**

### 4.2.7 Pump Drive Control Front Panel

Figure 4.7 shows the, “Pump Drive Control” front panel. This panel compiles the several pump drive operating options and commands as described in the previous sections. Provided that communication to the triangulation sensor would take place in a similar fashion as with the pump drive, a “Resource Name” along with a “Device” had to be selected. The “Resource Name” refers to the serial port that connects and communicates with the pump drive. The “Device” menu, listed the pump number to be utilized. This allowed for the use of multiple pumps each designed under a different “Device Number” and each capable to be controlled independently.

In addition these are also shown in this front panel. The “Tubing Size” menu allowed for the selection of the most common standard peristaltic tubing sizes. A “Command” menu listed the usual single line pump drive commands. The “Pump Read” display would show the

commanded string in Hexadecimal Format. The “Read Pump” display would show any message sent by the pump.

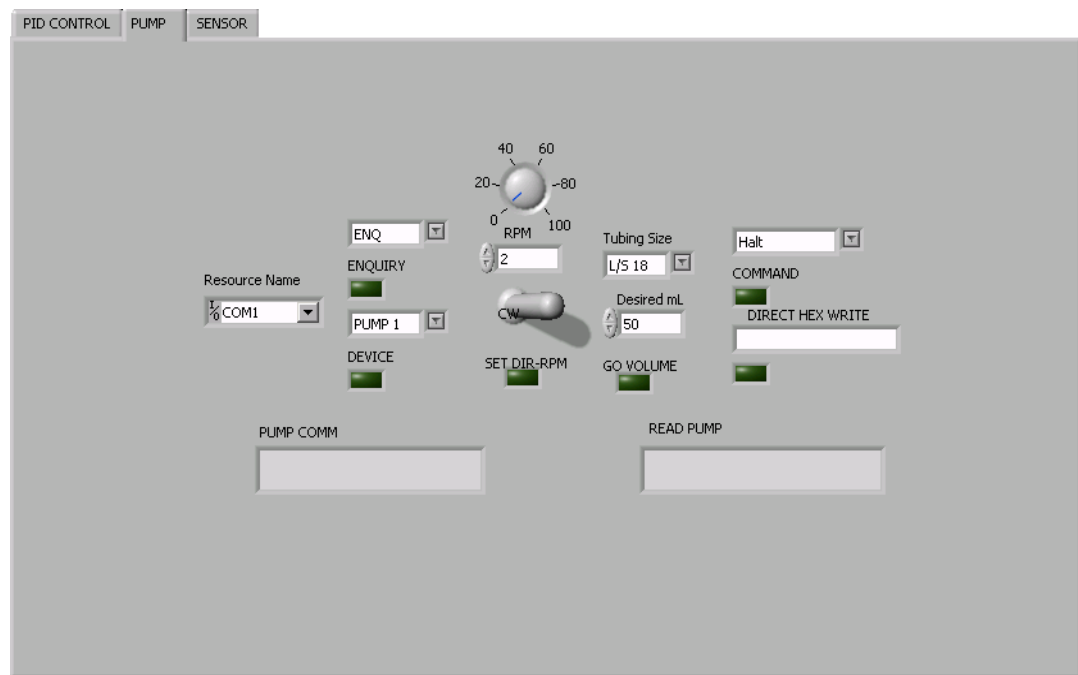


**Figure 4.7 Pump Drive Control Front Panel**

## 4.2.8 Operation Tests

Studies were performed to determine the pump's accuracy and precision across a wide range of volumes and at the highest pump's speed or revolutions per minute, which in turn defined the flow rate for each specific tubing size. The pump's accuracy (Figure 4.10) was assessed as the volume delivered compared to a target volume commanded to the pump (i.e. measured / pre-programmed). Precision (Figure 4.11) was assessed as the reproducibility of a commanded volume across a volume range. In order to measure the displaced volumes (Figure 4.8 and Figure 4.9), graduated cylinders were employed. For the range from 1 to 9 mL, a 10 mL graduated cylinder with 0.1 mL resolution was used. For the range from 10 to 75 mL, a 100 mL graduated cylinder with 1.0 mL resolution was used. For the range from 100 to 200 mL, a 250 mL graduated cylinder with 2.0 mL resolution was used. In the same manner, to measure the displaced mass, a 0.01g resolution and repeatability, "A&D GF-10K Industrial Balance" (A&D Company, Limited) scale was used.

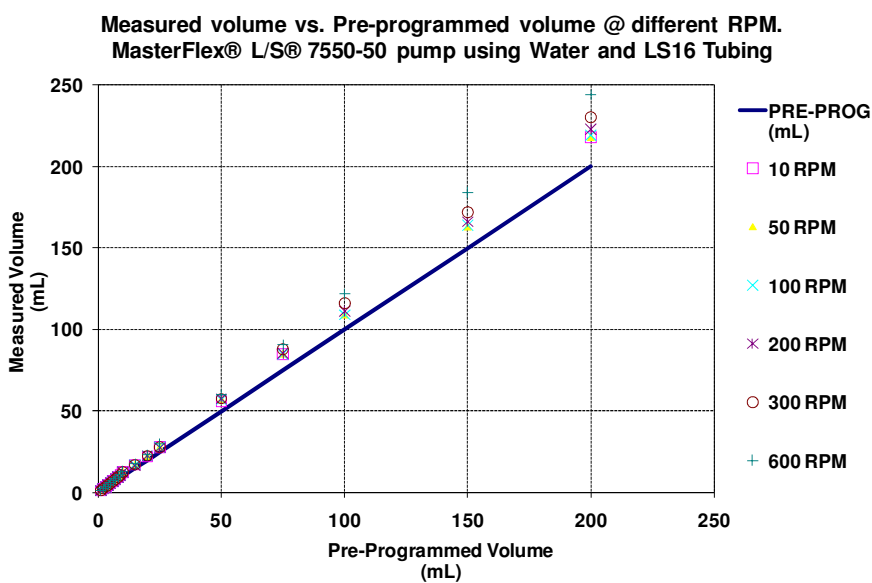
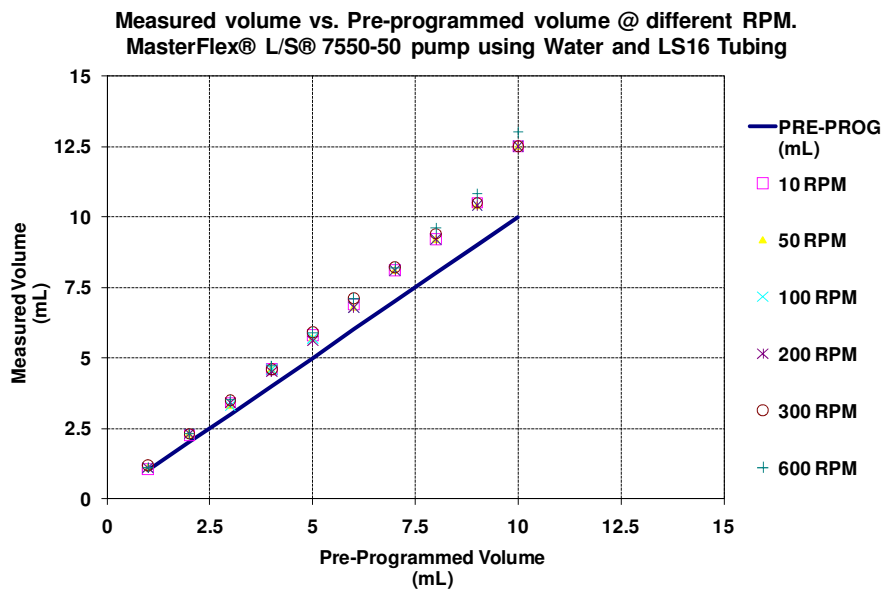
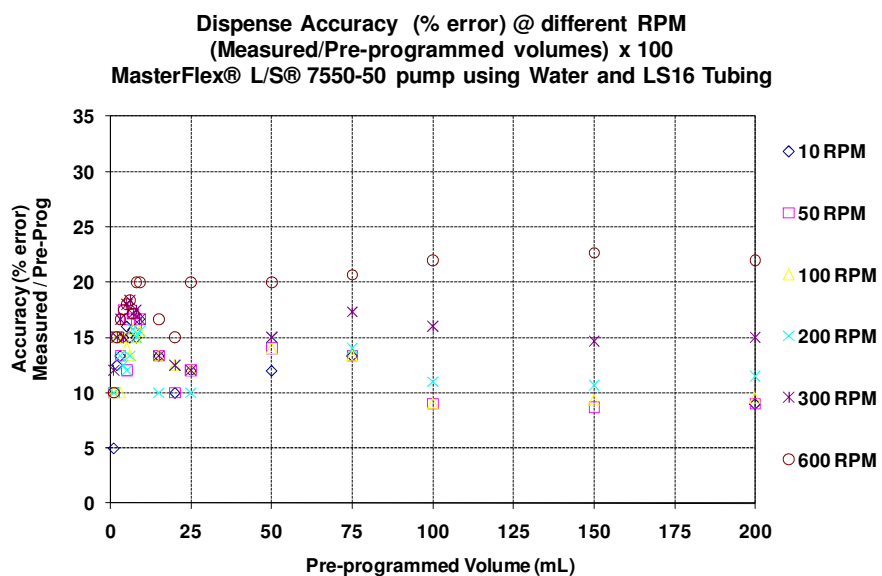


Figure 4.8 Pump measured vs. pre-programmed volume up to 200mL



**Figure 4.9 Pump measured vs. pre-programmed volume up to 10mL**



**Figure 4.10 Pump Dispense Accuracy (% error) for different RPM**

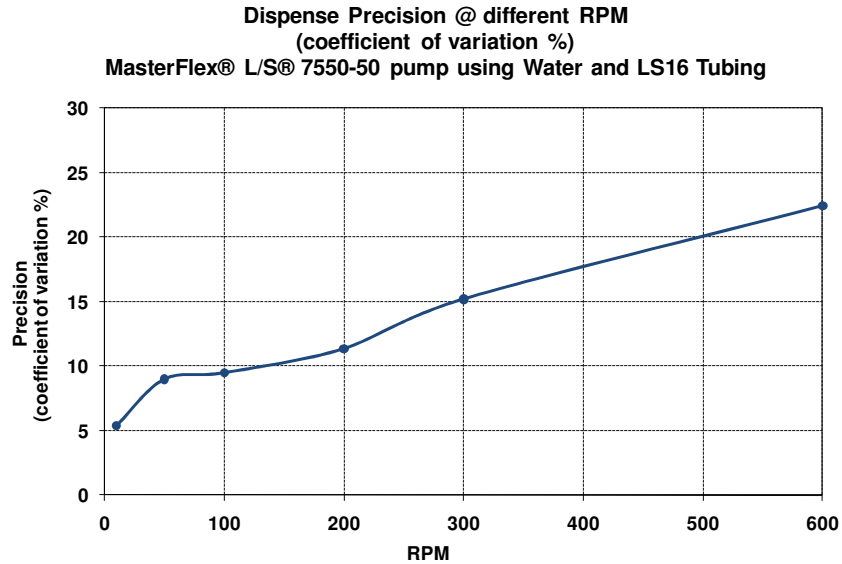


**Figure 4.11 Pump Dispense Precision at different RPM (coefficient of variation %)**

The pump showed a consistent increase of the dispensed volume ranging from roughly 8 to 24 % as compared to the pre-programmed volume, suggesting a pump or pump head calibration issue (Figure 4.10). Given that this accuracy deviation is relatively consistent, an alternative approach would be to apply of a compensation correction factor. Figure 4.11 reveals a reduction of the pump's precision when coupled with the pump's increase in speed. This data highlights the necessity of operating the pump at low speeds when high dispense accuracies are required.

Considering that this pump will operate within a controlled system, any specific correction factors can be incorporated in the control algorithm. In addition, since the control system will operate in a closed loop under a continuous high accuracy ( $\pm 2$ -micron) level feedback from the level sensor, a constant deviation correction or adjustment will take place, compensating for such inaccuracies. These performance results and design considerations (i.e. continuous closed loop

feedback) support the suitability of this pump configuration selection for the application in this filling and leveling system.

### **4.3 LASER TRIANGULATION SENSOR**

Similarly to the pump drive remote communication configuration, the laser displacement sensor processing unit can be configured for communication to a remote computer. This mode of communication supports data collection and parameter setting options. Likewise, a new communication protocol standard to the fluid handling and leveling system had to be developed. The Microtrak 7000<sup>TM</sup> – User Manual (Doc 10A000194) details the sensor operation and setup. The focus is made to the “front panel” operation mode and sensor head setup. To remotely operate the Microtrak 7000<sup>TM</sup> sensor, the sensor needs to be connected the remote computer via the RS-232 port, and matching parameters need to be set to the sensor and the control unit. Once these parameters are set control codes can be issued from the remote unit. Table 4.7 lists the control codes taken from the user manual. These codes served as a basis for the development of data collection LabVIEW<sup>TM</sup> subroutines and the integration to the leveling control algorithm.

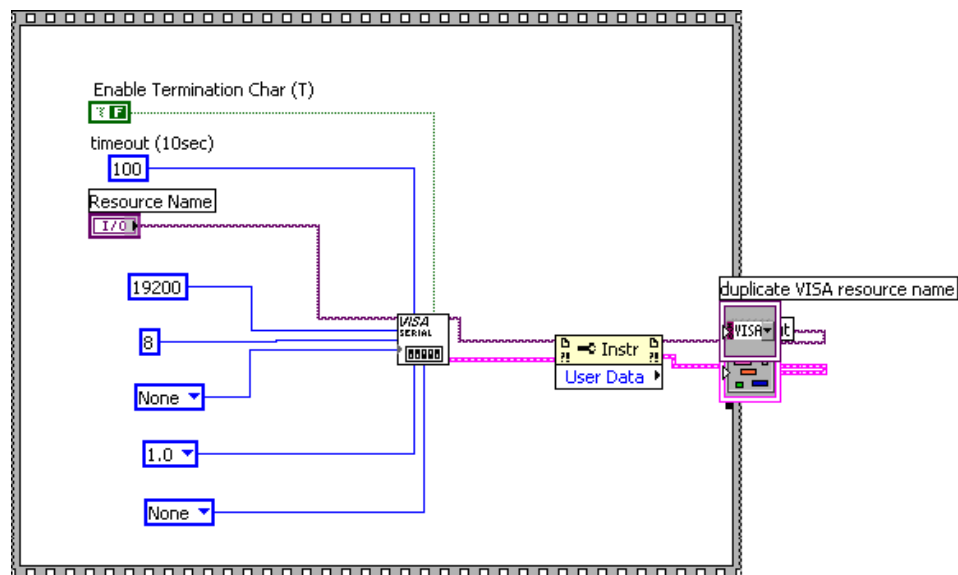
#### **4.3.1 Triangulation Sensor Communication Configuration**

Table 4.6 lists the RS-232 communication format. Figure 4.12 shows the standard, “VISA Configure Serial Port” VI block diagram with the appropriate serial configuration. There are two types of control codes: 1) Data query and 2) Parameter setting codes. Data query includes measurement data and system parameters. To query data, a control code is sent to the sensor to

which the sensor will send back the parameter or measurement. To set the system parameters, a control code followed by the parameter value and ending with “Carriage Return” (ASCII 0Dh) is sent to the sensor. Table 4.7 lists the RS-232 control codes.

**Table 4.6 Triangulation Sensor RS-232 Communication Format (MTI Instruments, Inc. Microtrak 7000™ – User Manual 22)**

Parity	Data	Stop
n	8	1
n	8	2
e	8	1
e	8	2
o	8	1
o	8	2
e	7	1
e	7	2
o	7	1
o	7	2



**Figure 4.12 Sensor LabVIEW™ VISA Configure Serial Port Block Diagram**

**Table 4.7 Microtrak 7000 Displacement Sensor RS-232 Control Codes (MTI Instruments, Inc. Microtrak 7000™ – User Manual)**

Character Code	ASCII Code	Setting Parameter	Type	Character Code	ASCII Code	Setting Parameter	Type
"	22	Software version query	Inquire	U	55	measure light intensity	Panel
#	23	mils	Units	V	56	unit of inch	Units
\$	24	microns		W	57	unit of mm	
%	25	1		X	58	Head 1	
@	26	0.5	Filter Setting (Hz)	Y	59	Head 2	Display
	27	0.2		Z	5A	Head 1, Head 2 alternative	
(	28	0.1		[	5B	Head 1- Head 2	
)	29	0.06		\	5C	Head 1 + Head 2	
*	2A	0.03		]	5D	Head 1- Head 2 (no cross talk)	
:	3A	1	Gain	^	5E	Head 1+ Head 2 (no cross talk)	Limits
;	3B	10		_	5F	Volts Mode	
<	3C	100		a	60	set up limit	
=	3D	auto		b	61	set low limit	
>	3E	normal	Mode		62	set offset	Cut Levels
?	3F	peak		d	64	dark cut level	
@	40	bottom		e	65	level cut time	
A	41	pk-pk		f	66	bright cut level	READ
B	42	pk-pk /w decay		g	67	output measure value once	
C	43	No smooth		h	68	*output measure value continuously	
D	44	8000	Filter Setting (Hz)	i	69	stop continuous measure value out	Inquire
E	45	2500		k	6B	current engineering unit	
F	46	500		l	6C	current warning message	
G	47	250		m	6D	current gain	
H	48	125		n	6E	current mode	
I	49	60		o	6F	current average number	
J	4A	30		p	70	current offset	
K	4B	15		q	71	current up limit	
L	4C	8		r	72	current low limit	
M	4D	4		s	73	current dark cut level	
N	4E	2		t	74	current bright cut level	
O	4F	ZERO	ZERO	u	75	current level cut time	
P	50	reset ZERO		v	76	current ZERO status	
Q	51	HOLD	HOLD	w	77	current HOLD status	
R	52	reset HOLD		x	78	current display mode	
S	53	Panel invalid	Panel	y	79	inc. display digits	Display
T	54	reset Panel invalid		z	7A	dec. display digits	

\*Do not use with IEEE-488 interface

After the sensor communication configuration has been made, the “direct write” VI shown in Figure 4.13 can be employed to send single commands to the sensor console to verify configuration and to operate it.



**Figure 4.13 Direct Code Write SubVI front panel**



### 4.3.2 Triangulation Sensor Front Panel

Figure 4.14 displays the “Sensor” front panel. This panel shows an arrangement of pull-down menus compiling the most common, “data query” and “parameter setting” codes as listed in Table 4.7. Once a code was selected from any menu, activating the adjacent button would send the code to the sensor console. As with the pump interface panel, the, “Resource Name” box, defines the serial port to be used. When activating the, “Read Button” a code 68 was sent to the sensor console allowing for: “output measure value continuously”, or to obtain a continuous or live level reading. By deactivating the, “Read Button”, a code 69 was sent to the sensor console allowing to: “stop output measure value out”, or to stop the level data acquisition. The, “Sensor Comm” display box showed the commanded string in Hexadecimal Format, and the, “Read Sensor” display box showed any returned by the sensor and the continuous or live level reading.

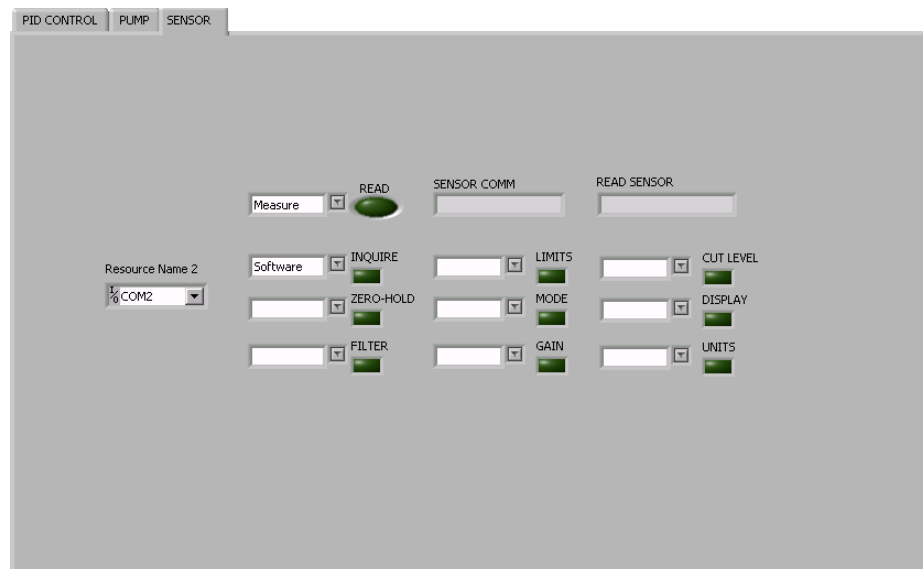


**Figure 4.14 Control-Sensor Front Panel**

### 4.3.3 Level Data Collection

In addition to providing a continuous live reading of the fluid's surface or, "Process Variable" to the control system, the sensed level data could be stored in a text file for post processing and control tuning. The, "Write to Spreadsheet File" is a LabVIEW® VI that converts 1D (1Dimensional) or 2D (2Dimensional) numerical data arrays into a text string and writes the string into a new or an existing file. This text file can be used by most spreadsheet applications (National Instruments™ LabVIEW™ 8.5 Help 2-7). In this particular application, the collected level data was stored in a 2D text string composed of time in tenths of second and level in microns. Figure 5.1 and Figure 5.2 are examples of the usage of the level collected data.

## 4.4 OPERATION TESTS

The data shown in figures Figure 4.16 through Figure 4.18 were compiled using a Laser Triangulation Micro Epsilon Level Sensor ILD 1800-(100) 10 which has a measuring range of 100-mm, with a resolution of 10-microns and a spot diameter of 60-microns (Micro-Epsilon® User Manual - CCD System optoNCDT 1800®). 0 details complete sensor specifications. A VP9000 one axis stepping motor/stage served as the control signal setting the displacement to be sensed or measured. The linear stage, "Scaled for Step" configuration option was used. This stepping motor to stage combination gave a step equivalency of 0.0003125 inches or 126 steps to 1mm (Velmex, Inc. User Manual - VP9000 Programmable Stepping Motor Controller). The Sensor was set up to average 128 data samples for each individual reading. Each data point was obtained by commanding the linear stage to move or displace by a predefined distance, then a corresponding sensor reading was obtained. Figure 4.15 shows the displacement sensor head and

stepping motor arrangement used during these tests. The head was affixed to the linear stage plate with the aid of a custom aluminum plate. The vat, or target material was placed directly below the sensor's laser beam. Sections 0.0 through 0.0 detail the observations made during these tests.

Figure 4.16 and Figure 4.17 exhibit an acceptable linear behavior with minor deviations when sensing the DSM Somos® NanoForm® 15120 resin and the black surface. Figure 4.18 emphasizes these inaccuracies mostly below the 1 mm range. The overall the performance of the Micro Epsilon Level Sensor ILD 1800-(100) 10 showed acceptable with limitations primarily on sensing resolution (10-microns). Ultimately, a Microtrak 7000™ laser displacement sensor processing unit with a MT 600 laser head (1.27-microns) was employed for the fluid handling and leveling system. It is anticipated that the tests, phenomena observed and data collected for either of these sensors would replicate with exception only to those specification differences.

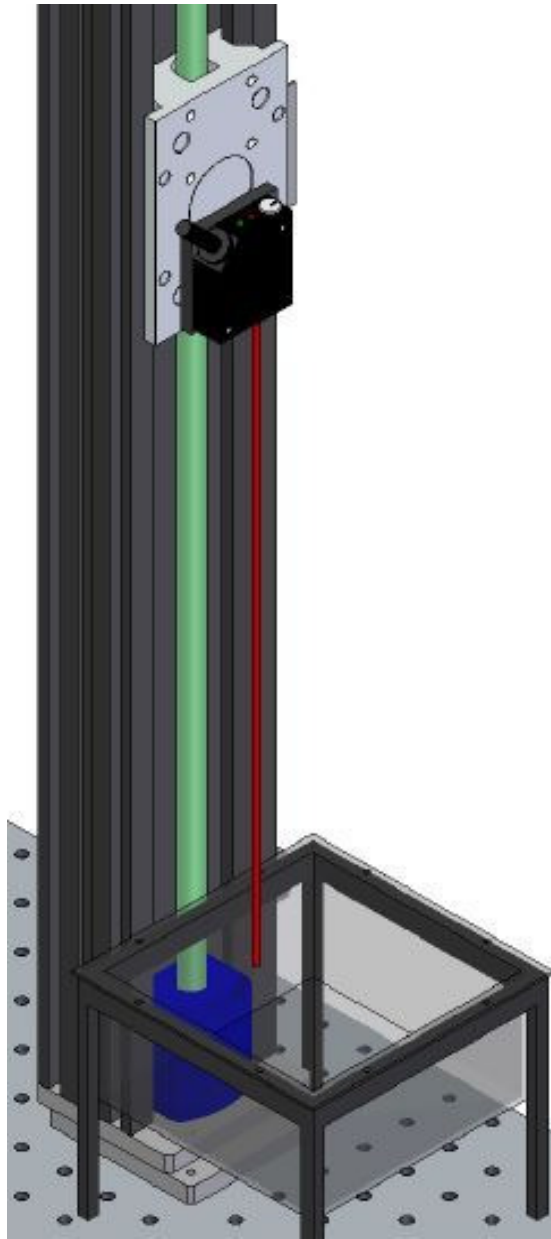


**Figure 4.15 Displacement Sensor Head to Linear Stage Setup**

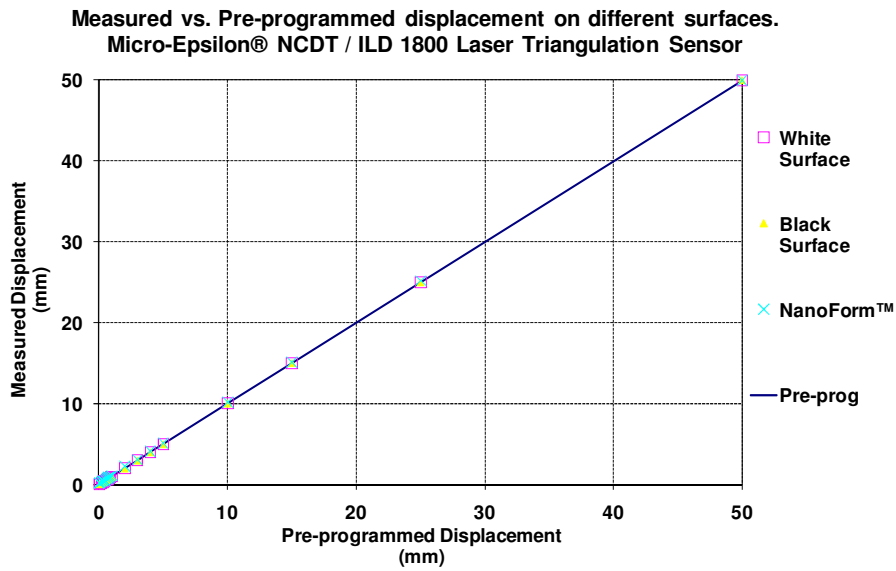


Figure 4.16 Sensor measured vs. pre-programmed displacement up to 50mm

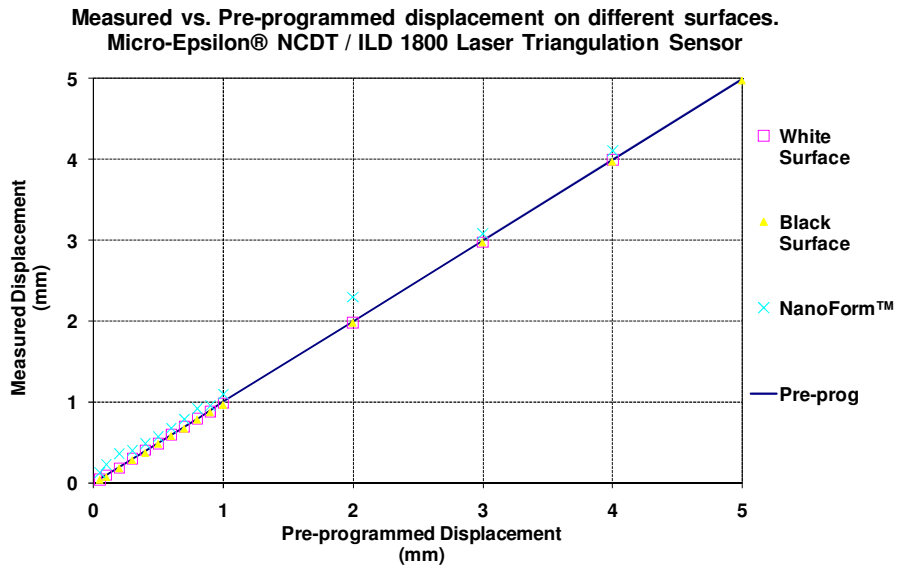
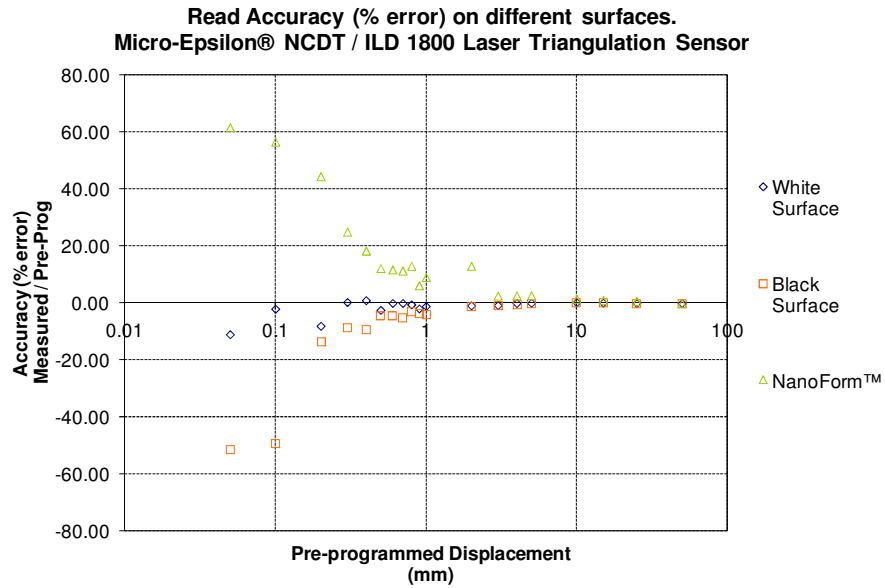


Figure 4.17 Sensor measured vs. pre-programmed displacement up to 5mm.



**Figure 4.18 Sensor Read Accuracy (% error) on different surfaces**

#### 4.4.1 Laser Beam Surface Penetration

The triangulation sensor was unable to sense the surface of the water and most clear resins. It was observed that the laser sensor's beam would penetrate into the fluid's surface producing inconsistent level readings. To address this phenomenon, in the instances where a clear and transparent fluid's surface needed to be sensed, a float element was implemented to provide a consistent surface than could support adequate laser triangulation sensing.

#### 4.4.2 Float and Guide

While the float solves the basic problem of locating the fluids surface, the actual reading of the float's position still needs to be made (Hambrice 2). When employing floats, a sensing

device is added to track the float's position, in this case, the laser triangulation level sensor. Because floats are allowed to move along with the fluid's surface, if not guided, it is likely for them to drift away from the laser sensor view losing the level reading. If the float has excessive lateral movement, float's surface inaccuracies or flatness variation can present erroneous level readings. For this reason, an adequate float guide is recommended along with the use of the float. Liptak offers a detailed discussion of, "float-type devices" and "float and guide tube designs". A guide tube is positioned within the rising and falling of the fluid while containing the float element (Liptak, Bela G Instrument Engineers' Handbook – Process Measurement and Analysis 475-477). In its patent, "Laser Measurement of Liquid Level in a Holder" Wilkins describes several float and guide level measurement alternatives and their usage with laser level sensors. A tube or pipe houses a float, the laser sensor is mounted over pipe with the laser beam directed down the center of the tube, the float receives and reflects the beam back to the sensor providing a level reading (Wilkins "Laser Measurement of Liquid Level in a Holder." United States Patent US 7,082,828 B1).

To support the float and guide configuration, the vat described in section 3.5 Fluid Vat had to be modified to accommodate a float guide. The guide consisted of a 2.74-cm by 5.28-cm (1.08-inch by 2.08-inches) rectangular chamber extending from the upper face of the vat down to the start of the base slope, leaving enough clearance to permit free flow between the guide chamber and the vat's working area. Figure 4.19 details the float guide feature as it was incorporated in the existing prototype vat design.

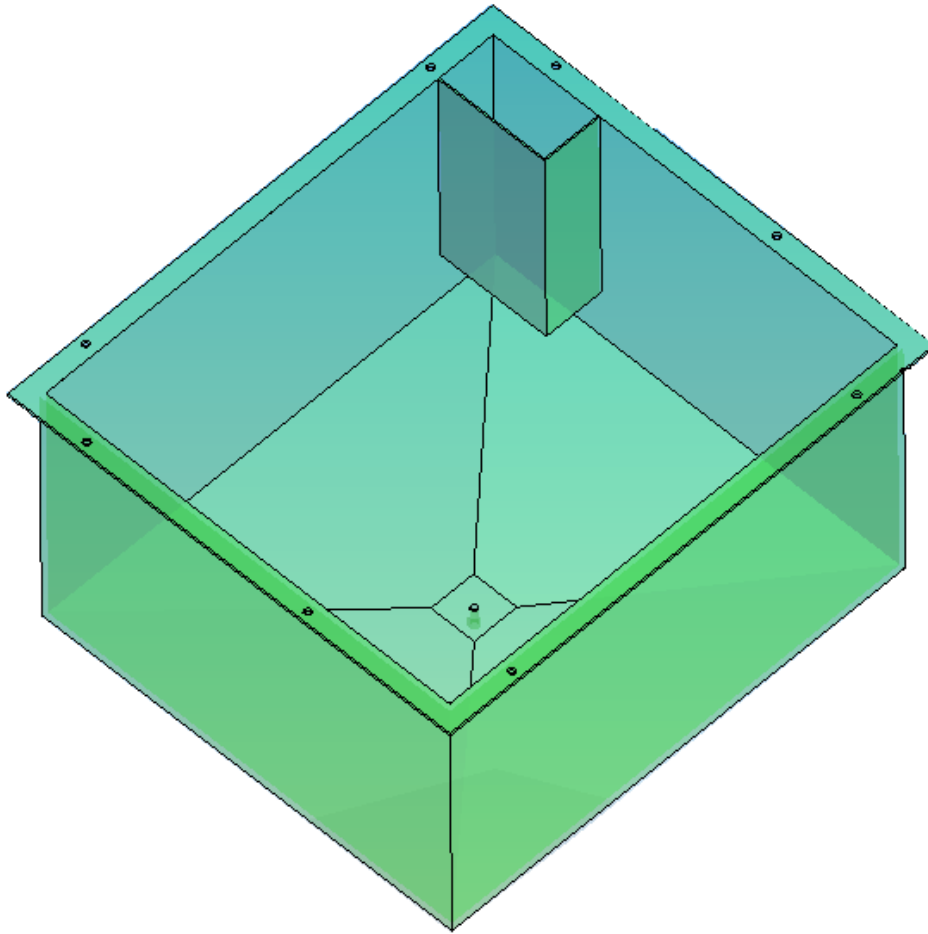


**Figure 4.19 Vat model with Float-Guide Element**

### **4.4.3 Float Calibration**

It was considered that a flat stainless steel metal sheet could easily be shaped and flattened to provide a more accurate reading along its surface. A stainless steel float would also support the leveling system cleanliness requirements. Similarly, it was also considered that a cellulose-acetate float, with its compatibility with the different resins, the difference in viscosity and optical appearance would greatly support the system requirements.



A simple 2.54-cm by 5.08-cm (1-inch by 2-inches) rectangular flat stainless steel 0.457-mm (0.018-inches) thick sheet (T304 Stainless Steel - #8 mirror finish 26ga), or a flat cellulose-acetate 1.19-mm (3/64-inches) thick sheet (Black Extruded Cellulose Acetate – Optical Grade Polished) were used as float elements. The fluid's surface tension property permitted the stainless steel sheet to float. While the cellulose-acetate density difference to that of the fluids used, would permit this element to float.

The following approaches were evaluated for the floats' calibration. A visual measurement of the float and liquid surfaces could be made by lateral viewing both surfaces thru a transparent sight. Magnified scales would function as the measuring device. Another approach was to start with an empty container of known cross sectional area. The float element would be placed directly on the bottom of the empty container. The laser displacement sensor would read the position of the float in the empty state defining a zero or reference point. A finite known fluid volume would be dispensed into the container increasing the fluid surface level by a known magnitude (i.e. "level gauge",  $\text{level} = \text{volume} / \text{area}$ ). The laser displacement sensor would then measure the change in the position of the float. The resulting fluid level and the float position would be compared defining the buoyancy characteristics for that specific float and fluid combination. An additional calibration approach was to make an analytical buoyancy calculation employing the fluid and float mechanical properties.

Due to its simplicity and accuracy, the second approach, the volume to level or "level gauge" approach was mostly utilized. The "magnified scale" and the "analytical" approaches were seldom used, and were typically used for confirmation and verification purposes.

#### **4.4.4 Surface reflective properties**

The triangulation sensor showed a continuous negative deviation of approximately 20 microns when reading a surface with low reflection properties such as black paper. The triangulation sensor showed an average variation of approximately 75 microns in all DSM Somos® NanoForm® 15120 resin readings. In addition, when reading DSM Somos® NanoForm® 15120 resins, an offset of approximately 4.6 mm from the fluid's surface to the sensor reading was observed. This suggested a finite and consistent penetration factor of the laser beam below the fluid's surface. This phenomenon was confirmed and eliminated by employing the “float device”.

### **4.5 LABVIEW CONTROL**

The basic idea behind a PID controller is to read the sensor signal, then compute the desired actuator output by calculating the proportional, integral and derivative responses and summing these three components. The sensor measures the process variable and provides feedback to the control system. The difference between the process variable and the set-point is used by the control system algorithm to determine the desired pump output. This loop of reading the sensor, providing constant feedback and calculating the desired output is called, “closed loop” and is continuously repeated.

The proportional component depends only on the difference between the set-point and the process variable or error term. This component determines the ratio of the output response to the error signal. A larger proportional gain increases the speed of the system's response. A gain too large creates oscillations. The integral component sums the error over time so the effect is to

drive the steady state error to zero. The derivative component is proportional to the rate of change of the process variable and causes the output to decrease.

### **4.5.1 PID Control Front Panel**

Figure 4.20 shows the, “Control Interface” front panel. This panel has input boxes for each of the tuning parameters. The set-point is defined as the midpoint of the upper and lower limit displayed in the interface; in this case, the total sensor reading range is 10-mm. Another key input to the control algorithm is the vats’ cross sectional area. As described in section 0.0 (4.2.5 Pump Drive Volume Conversion VI), the vat’s cross sectional area in conjunction with the peristaltic tubing size affects the control’s resolution. A small area vat in combination with a larger tubing size can cause coarse steps, or pulses with each pump revolution. The volume displaced in each revolution using the larger tubing size causes a large level increase for a small cross sectional area vat. A smaller tubing size in combination with a vat with large area will have an increased level resolution due to the smaller volume displaced per revolution distributed along the larger vat area. A compromise between level resolution and system response time needs to be made.

The “Auto Level” button initiates the automatic filling and leveling process. The “Stop Pump” button halts the pump regardless of the condition of the process as described in section 4.2.6 Pump Drive Stop VI. The “File Path” box opens a browse menu to define the location for the level data output file as described in section 4.3.3 Level Data Collection. The upper display window shows the fluid’s surface level live reading or process variable. The lower display

window shows the control's algorithm response as applied to the control system elements, in this case to the Peristaltic Pump.

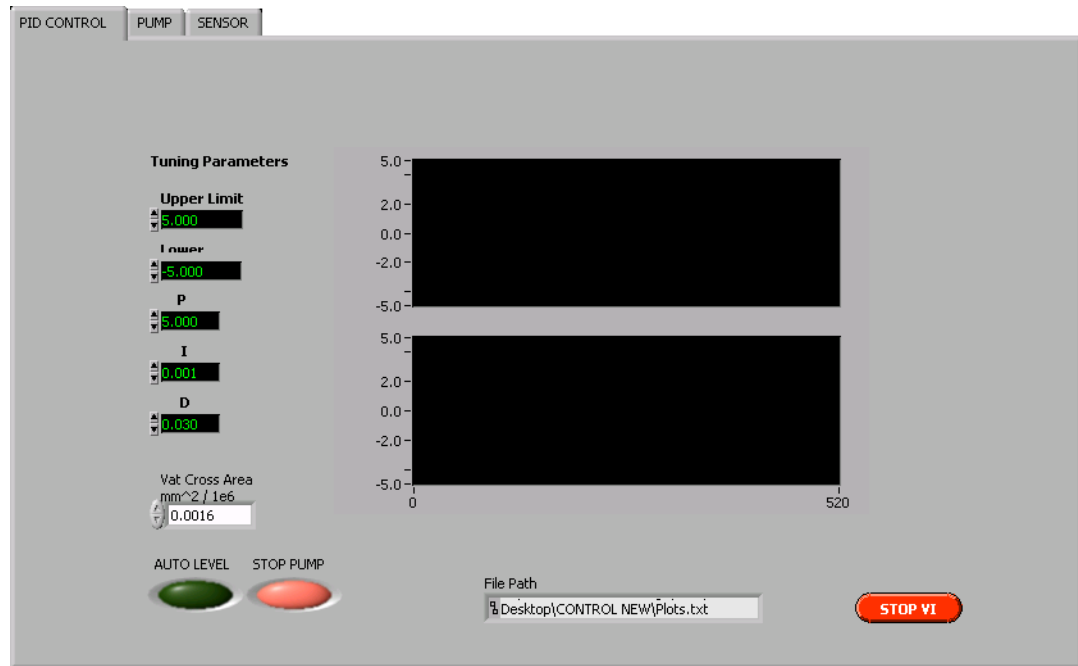


**Figure 4.20 Control Interface front panel**

## 5.0 SYSTEM DEMONSTRATION

### 5.1 SEMI-AUTOMATED LEVELING SYSTEM STRATEGY

Wicker *et al.* (“Multi-Material Stereolithography ...” US 7,556,490 B2; “Multiple Material Micro-Fabrication...” 754-764) proposed a strategy for filling and removing SL material from one or multiple vats and for controlling the liquid level in each vat. A peristaltic pump provided a means to mechanically add or remove precise fluid quantities to and from each vat. A vat overflow drain system was employed to maintain a constant level within an associated vat by continuously pumping liquid into the vat. Each vat was configured with two fluid chambers one being the vat working area configured to fit the platform and an overflow drain chamber designed to drain the overflow material back to a material reservoir. The volume / level of the main vat chamber could be adjusted by repositioning a vertical leveling gate. Sandoval (“Nanotailoring Stereolithography ...” 513-524) and Lozoya (“Development and demonstration ...”) demonstrated successful fluid handling and accurate fluid leveling by employing a peristaltic pump jointly with a vat overflow drain approach.

This approach is subject to the fluid flow characteristics and to the system behavior through the build process. Conditions such as: leveling gate edge condition, fluid viscosity, system disturbances and pump flow rates affect the actual overflow fluid level. In addition, level estimation greatly depended on the system and fluid settling times creating a need to characterize build routines based on material and system variables.

## 5.2 SYSTEM DEMONSTRATION

The system described in sections 3.0-4.0 is capable of automatically filling and accurately controlling the level of one or more vats with a variety of fluids having different viscosities. The information collected during the system's setup and operation provided a confident foundation to implement the system into a fully automated MMSL apparatus as originally proposed by Wicker *et al.* ("Multi-Material Stereolithography ..." US 7,556,490 B2).

DSM Somos® Nanoform™ 15120 being one of the higher viscosity materials with  $\approx 570$  cps at 30°C was used to characterize the high viscosity materials group. Natural water with  $\approx 0.8$  cps at 30°C was used to characterize the lower viscosity materials group.

A stand alone stainless steel vat having 20.32-cm by 22.86-cm (8-inches by 9-inches) in area was chosen for these demonstrative experiments. A Masterflex® L/S 7550-50 peristaltic pump drive with an EasyLoad® 77201-60 L/S peristaltic pump head and MasterFlex® Tygon® L/S 18 flexible tubing were employed. Due to the vat's working volume it was preferred to use L/S 18 over L/S 15 tubing. Making reference to Table 4.1 the estimated fill times can be calculated. At 600 RPM using MasterFlex® L/S 18 it would take approximately 3 minutes and 50 seconds to displace a 9 liter volume. At 600 RPM using MasterFlex® L/S 15 it would take approximately 8 minutes and 10 seconds to displace a 9 liter volume. To reach 80% of the vat's volume it would take approximately 3 minutes 10 seconds with MasterFlex® L/S 18 and 6 minutes and 30 seconds to reach with and MasterFlex® L/S 15 tubing. A non-contact Microtrak 7000™ laser displacement sensor processing unit with a MT 600 laser head was utilized to sense the fluid's surface level.

The following figures (Figure 5.1 and Figure 5.2) compare the automated fluid handling and leveling system in operation under various Proportional Control values. The level reading

along with the control response is displayed for each fluid. These figures only display the sensors reading range and do not include the complete vat's height level increase.

Figure 5.1 compares the fluid level and control response for a proportional value of 1. A settling time difference of approximately 15 seconds can be observed between the two fluids. No overshoot is observed for the level or the control signal on neither of the fluids.

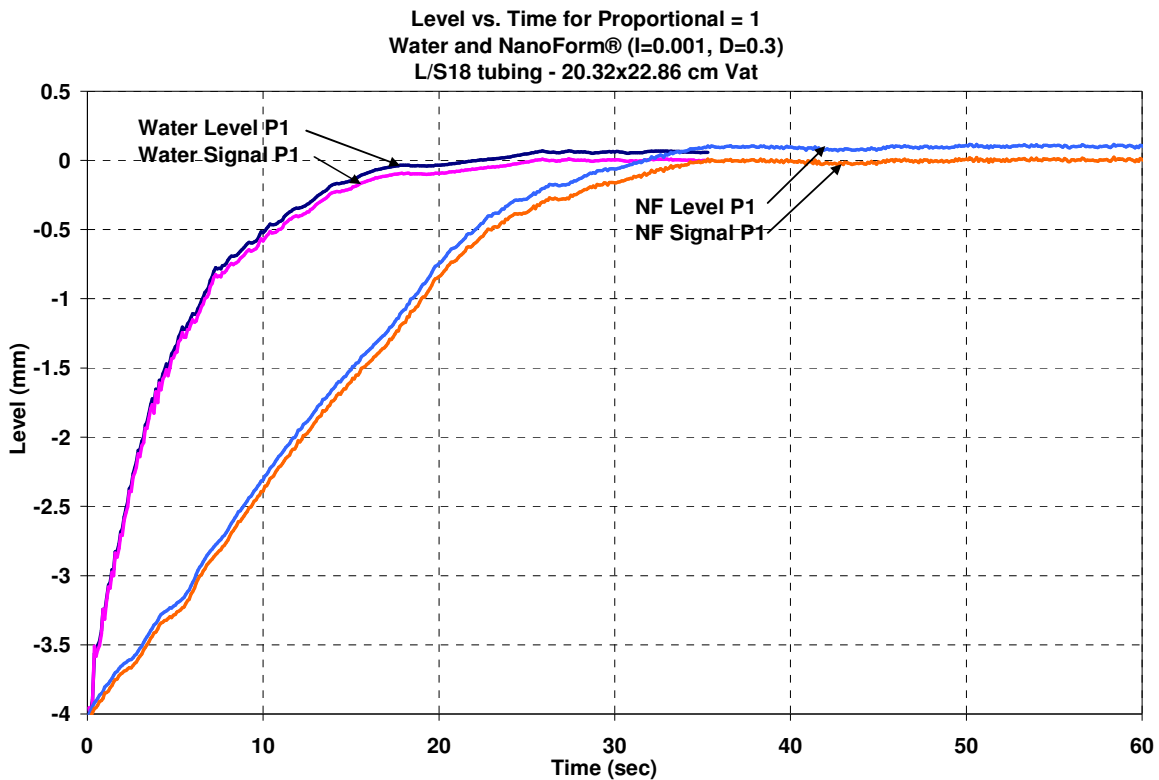


**Figure 5.1 Control and Level output using Water and DSM Somos® NanoForm® 15120 with PID values of P=1, I=0.001, D=0.3**

Figure 5.2 compares the fluid level and control response for a proportional value of 9. A settling time difference of approximately 20 seconds can be observed between the two fluids. Considerable overshoot and oscillation can be observed for the control signal on both fluids. The level signal has a slight overshoot more noticeable with water. Similarly, level oscillation is

more noticeable with water. Level response dampening can be observed with the increase of fluid viscosity.

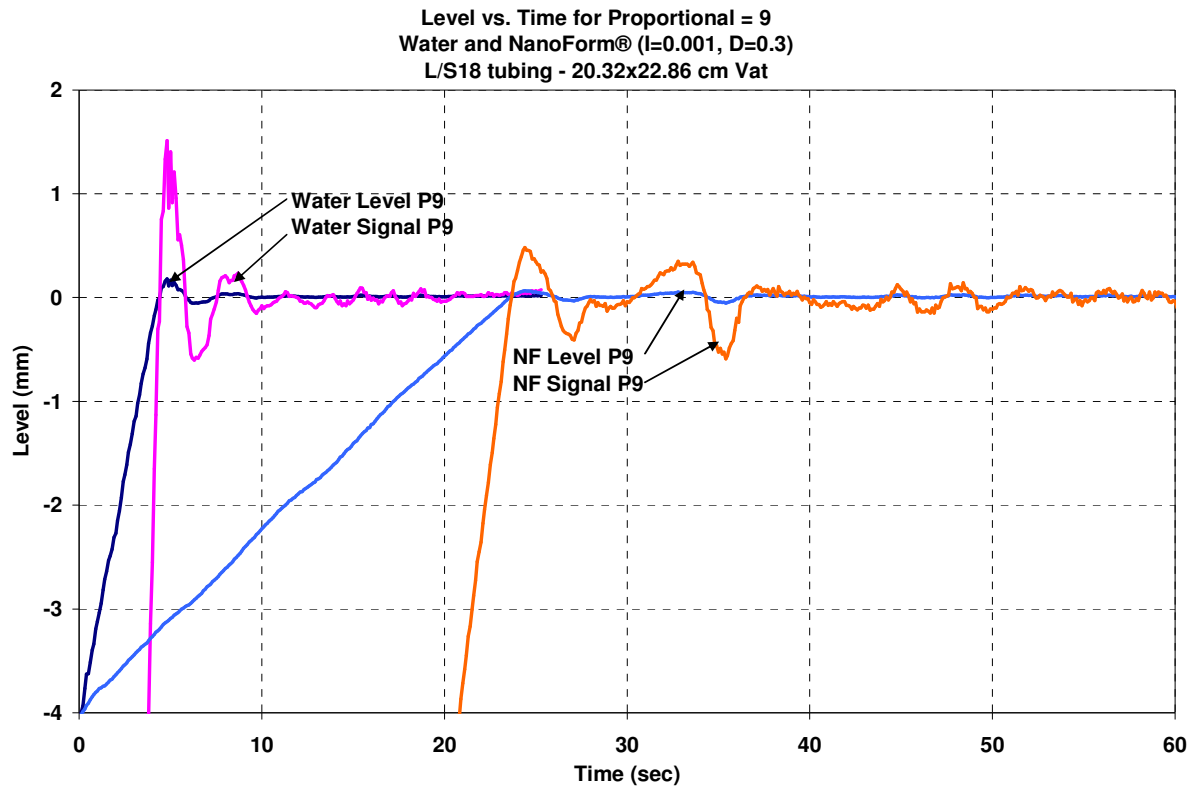


**Figure 5.2 Control and Level output using Water and DSM Somos® NanoForm® 15120 with PID values of P=9, I=0.001, D=0.3**

### 5.3 SYSTEM IMPLEMENTATION

As a concluding step the automated fluid handling and leveling system was incorporated into an automated MMSL machine. Inamdar *et al.* provide a detailed description of the development of an automated MMSL machine consisting of a control and a manufacturing center (“Development of an Automated ...” 624-635). This study offers an accurate summary of



the incorporation and utilization of the leveling system into an automated MMSL machine. In addition, the production of “simple multiple-material samples with vertical and horizontal orientations” validates the fluid handling and leveling system operation (Inamdar 629).

The manufacturing center included laser optics retrofitted from a 3D Systems® 250/50 SL machine, a rotating platform and carousel with four vats. The control center included an automated multi-pump fluid handling and leveling system, 3D Systems software, overall process control LabVIEW™ software custom routines, scanning mirror controller and signal conditioning module.

In this particular application, vat sizing was limited by the load capacity of the rotary stage used to drive the vat carousel. The carousel included four stainless steel vats 20.32-cm by 22.86-cm (8-inches by 9-inches) in area, each having a total of nine liters in volume.

The automatic multi-pump fluid handling and leveling system including a laser displacement sensor, peristaltic pumps, pump heads and flexible tubing was incorporated to handle the multiple fluids and control the fluid level in the individual vats with accuracies in the order of  $\pm 5\mu\text{m}$ . Four Masterflex® L/S peristaltic pump drives (Model MasterFlex® L/S® 7550-50) with the corresponding four EasyLoad® peristaltic pump heads (Model # 77201-60, L/S Easy- Load® II, Cole-Parmer Instrument Company) and MasterFlex® Tygon® L/S 18 flexible tubing were employed. A non-contact Microtrak 7000™ laser displacement sensor processing unit with a MT 600 laser head (Microtrak 7000™ – User Manual Doc 10A000194) was utilized to sense the fluid’s surface level.

A floating device calibrated for the various fluids' buoyancy parameters was employed to overcome the inaccuracies related to the fluid's surface reflective and laser absorption properties. In this application, a cellulose acetate floating device 1.19-mm (3/64-inches) in thickness was utilized due to its compatibility with the different resins, their difference in viscosity and optical appearance. The resins used ranged from a viscosity of 260 cps at 30°C for DSM Somos® Watershed™ 11120 (DSM Somos® WaterShed™ 11120 – Product Data Sheet) to 570 cps at 30°C for DSM Somos® Nanoform™ 15120 (DSM Somos® NanoForm™ 15120 – Product Data Sheet) and from an optically clear for DSM Somos® Watershed™ 11120 to an opaque gray for DSM Somos® Nanoform™ 15120. The float calibration values or offset above the resin level ranged from 300 µm for DSM Somos® Watershed™ 11120 to 460 µm for DSM Somos® Nanoform™ 15120. These offset or calibration factors, were incorporated into the LabVIEW® programming containing particular settings specific for the different fluid properties for the different fluids used.

## **6.0 RESULTS OF STUDY**

### **6.1 INTRODUCTION**

System identification is a determination in the basis of inputs and outputs of an equivalent system made-up of a collection of components coordinated together to perform a function equivalent to the system under test. System identification can start with an experimental design followed by data collection and data processing. A suitable model structure can be selected then important parameters of the model can be estimated. Models will seldom emulate their actual physical counterparts perfectly. In general, these studies provide a means of tuning the controller parameters and aid in process optimization.

### **6.2 SYSTEM DESCRIPTION AND MODELING**

The system starts operation when the peristaltic pump displaces the fluid from the reservoir filling into the bottom of the vat. The peristaltic pump is capable of bi-directional flow and variable speeds in both directions. The system is setup to operate at full speed in either direction while the fluid level is out of reach of the sensor's reading range. Once the level enters the sensing range, the control system algorithm enters into operation calculating the pump speed and direction in relation to the fluid's level until the set-point is reached and the fluid's surface is stable. Live level feedback allows for continuous level disturbance compensation. Figure 6.1 shows the fluid handling elements of the system. Specific details on each of the elements have been given in preceding sections.

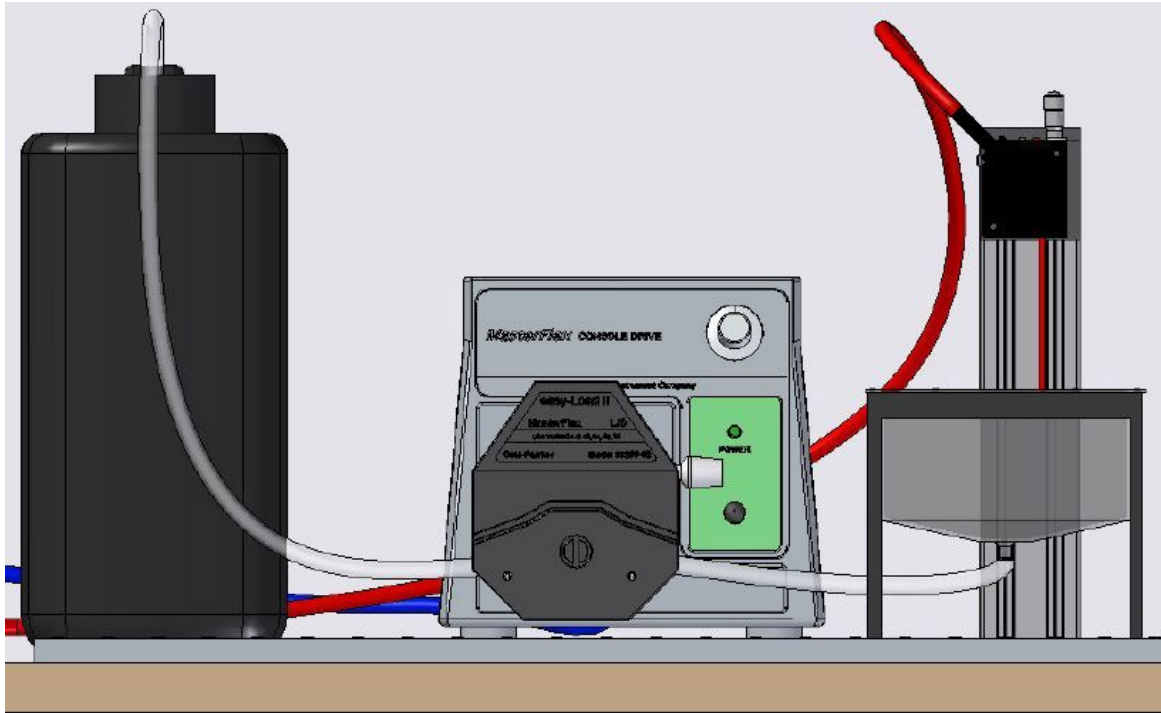


**Figure 6.1 Fluid handling experimental Setup**

The vat acts as a fluid capacitor where the fluid enters and leaves the vat. The mass balance is: [Accumulation] = [In]-[Out]. Due to the use of a single flow port in and out of the vat and the use of a bidirectional peristaltic pump to control flow the mass balance can be rewritten as follows: [Accumulation] = [Pump Flow] or:

$$A \frac{dh}{dt} = Q_{i/o}$$

**Equation 6.1. Mass Balance**

Where A is the vat cross sectional area = 464.5cm<sup>2</sup> (72in<sup>2</sup>), h is the fluid level in mm and Q<sub>i/o</sub> is the flow rate in-out of the vat.

From Figure 3.5 the pump characteristic equations can be obtained. For 500 cps a linear behavior can be observed above 250 RPM. The following linear equation can be estimated to support the system analysis:

$$y = 0.01x + 500$$

**Equation 6.2. Pump linear characteristic equation for a 500 cps fluid above 250RPM**

Where  $y(x)$  is the volume displaced in  $\text{mm}^3$  function of revolutions per minute. For small changes in the pump speed Equation 6.2 can be rewritten as follows:

$$Q_{\text{pump}} = (0.01 \text{ rev} + 500) \frac{d \text{ rev}}{dt}$$

**Equation 6.3. Pump equation for small changes in speed**

Given that the fluid entering and leaving the vat is the same fluid being displaced by the pump, Equation 6.1 and Equation 6.3 can be combined to form:

$$A \frac{dh}{dt} = (0.01 \text{ rev} + 500) \frac{d \text{ rev}}{dt}$$

**Equation 6.4. Mass – Flow balance between vat and pump**

Applying the Laplace transform on both sides of the equation:

$$\frac{A}{s} h(s) = \left( \frac{0.01}{s^2} + \frac{500}{s} \right) \text{rev}(s)$$

And solving, the plant transfer function can be obtained as follows:

$$\frac{h(s)}{\text{rev}(s)} = \frac{500.01}{A(s+1)} = H(s)$$

### Equation 6.5. Transfer function for the pump – vat

The level sensor is a simple unit with proportional gains and no system dynamics.

The input – output relation of the sensor can be written as follows:

$$D_{Sensor} = K_s h$$

### Equation 6.6. Transfer function of the level sensor

Where  $D_{sensor}$  is the sensor reading,  $h$  is the fluid level in mm and  $K_s$  is a constant.

From Figure 4.16 and Figure 4.17 the gain of the level sensor can be obtained as follows:

$$K_s = 1$$

### Equation 6.7. Sensor gain

The block diagram of the system can be written as follows:

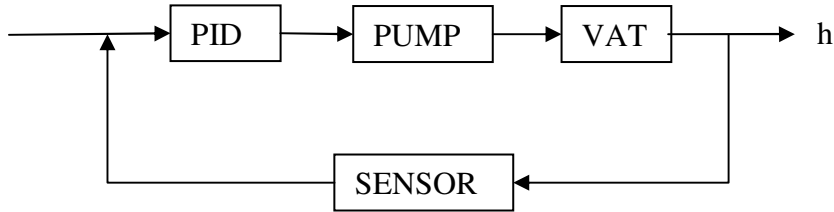


Figure 6.2 Block diagram of the system

From Equation 2.8 the PID controller equation can be rewritten as:

$$G(s, Kp, Ki, Kd) = \frac{Kp \cdot s + Kd \cdot s^2 + Ki}{s}$$

### Equation 6.8. Transfer function for a PID controller

To identify the system, a step response test is carried out by applying a step input in the form of:

$$F(s) = \frac{1}{s}$$

**Equation 6.9. Step function**

The closed loop transfer function is defined as:

$$T(s, Kp, Ki, Kd) = \frac{F(s) \cdot G(s, Kp, Ki, Kd) \cdot H(s)}{1 + G(s, Kp, Ki, Kd) \cdot H(s)}$$

**Equation 6.10. Closed loop transfer function**

## 6.3 TUNING

Controller gains can be obtained manually by trial and error. The I and D terms are set to zero and P is increased until the loop oscillates making the system faster. The integral term is then increased to reduce oscillations and steady state error increasing overshoot. The integral term is then adjusted to obtain minimum oscillation and reduce the overshoot. The derivative term is then increased until the loop has acceptable rate to the set-point. An increased derivative term makes the system more stable and sensitive to noise.

Another common method for tuning a PID controller is the Zeigler-Nichols method (Zhong 19). It is similar to the trial and error, where the I and D terms are set to zero and P is increased until oscillation appears. Then the critical gain  $K_c$  and the period of oscillation  $P_c$  are noted.

And finally P, I and D are adjusted per the following table (National Instruments<sup>TM</sup> LabVIEW<sup>TM</sup> – PID Control Toolkit User Manual).

**Table 6.1 Ziegler-Nichols tuning using the oscillation method**

Control	P	Ti	Td
P	$0.5K_c$	-	-
PI	$0.45K_c$	$P_c/1.2$	-
PID	$0.60K_c$	$0.5P_c$	$P_c/8$

These two methods are certainly not the only way to tune a PID controller but are recognized and accepted for their simplicity and ease of use. With the aid of MathCad® software the closed controller in Equation 6.10 can be tuned for the desired system response (Mathsoft Mathcad® “Mathcad Worksheet – Modeling a PID controller”).

Following the previously mentioned trial and error tuning routine PID values were chosen to provide the desired response as follows:  $K_p=1$ ,  $K_i=1$  and  $K_d=25$ . Figure 6.3 shows the closed loop system step response  $T(t)$  and the system response for these PID values  $T\text{-PID}(t)$ .



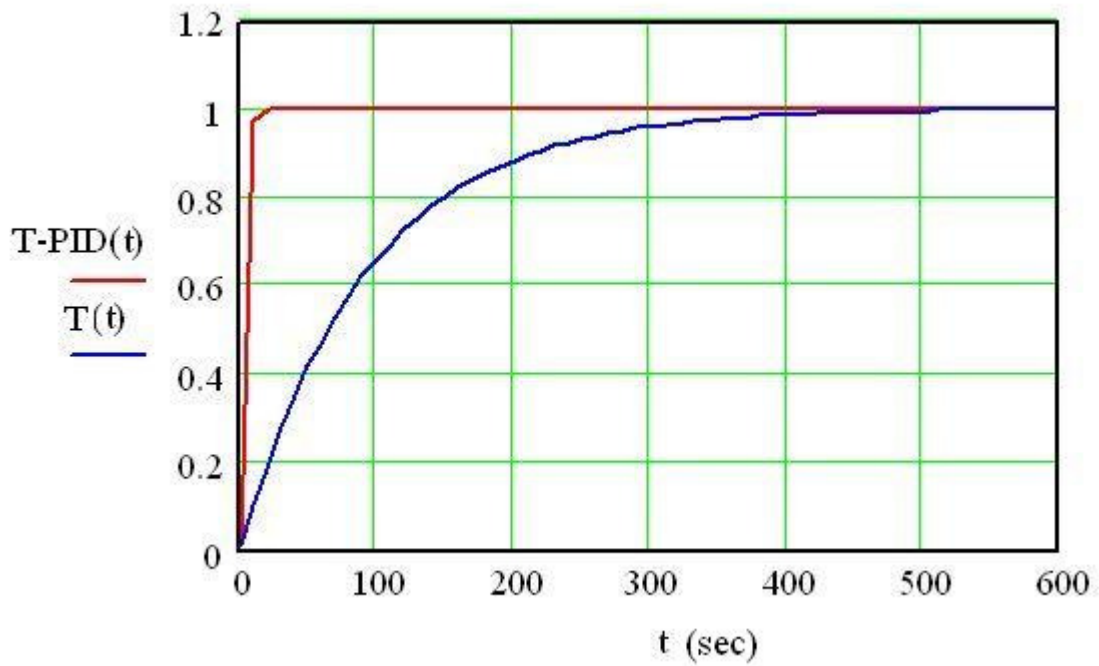


**Figure 6.3 System step response**

Although the case study in this section is simple, it illustrates the basic principles of designing a controller from the identification of the system to the implementation of a suitable controller algorithm. These results were only compared to the actual physical system but not implemented. Additional studies can be carried out to further refine the system for a variety of physical characteristics and system conditions. This is an activity recommended for future research.

## 7.0 CONCLUSIONS AND RECOMMENDATIONS

The work presented in this thesis addresses the development of an automated fluid leveling system for application in a multiple material stereolithography (MMSL) apparatus. The successful design, development and implementation of this system are described in detail. The system was designed to effectively handle multiple materials and vats which could be virtually configured in any arrangement while supporting a non-contaminating and potentially sterile environment. The system was developed and proven as a standalone independent unit. The system was finally incorporated into an automated MMSL machine demonstrating satisfactory system design and operating performance.

### 7.1 SUMMARY OF DESIGN

Following the original concept disclosed in the Wicker *et al.*, a peristaltic pump was utilized providing fluid isolation, bi-directional flow and flow control ( “Multi-Material Stereolithography ...” US 7,556,490 B2; “Multiple Material Micro-Fabrication...” 757). A MasterFlex® L/S® 7550-50 peristaltic pump drive with a MasterFlex® EasyLoad® peristaltic pump head were used. This combination produced flow rates from 5.8 to 2300 mL/min for MasterFlex ® L/S18 tubing and 0.28 to 130 mL/min for MasterFlex ® L/S14 tubing. When using a vat 20.32-cm by 22.86-cm (8-inches by 9-inches) in area, the resulting theoretical level increments were 7.8 and 3.7 microns per revolution, or an equivalent level resolution of 0.78 and 0.037 microns for MasterFlex® L/S18 and L/S14 correspondingly. Measured water pump flow accuracies ranged from  $\pm 5$ microns for low pump speeds or speeds below 50 rpm and up to  $\pm 100$

microns for high pump speeds or speeds above 500 rpm. A computer-compatible MTI Instruments - Microtrak 7000TM Laser Displacement Sensor with a MT 600 Laser Head was used serving as feedback for the closed loop control system.

The system development was completed as a standalone unit proving vat design flexibility for any particular application. Simple LabVIEW® programs were created to support flexibility and implementation

## **7.2 SUMMARY OF OPERATION**

The developed fluid handling and leveling system manipulated fluid materials with different characteristics and maintained a fluid level in spite of any disturbances placed upon the fluid. Communication routines were established between the control computer, pump drive and displacement sensor. Once adequate communication was established, software routines had to be created to configure and operate the pump drive and displacement sensor within its own array of capabilities. Some routines for the operation of the automated fluid handling system were pump direction, pump speed and continuous level reading. A PID controller was used to control system. The control algorithm adjusted the pump's speed in relation to the fluid's level and continuously compensated for any level changes or disturbances. Simple LabVIEW® routines were created supporting system flexibility and ease of incorporation into larger automated systems such as the automated MMSL stated in section 5.3 system implementation ).

Findings on the displacement sensor laser beam reaction to sensing a fluid surface are discussed in section 4.4.1 (Laser Beam Surface Penetration). The incidence of the laser beam into the fluids' surface resulted in laser beam penetration or reflection creating displacement

sensor reading inaccuracies. It was opted to use a simple float device which helped overcome these phenomena while preserve the sensor's original performance and supporting the system's cleanliness requirements. Calibration of the float device had to be performed for each of the float materials and working fluids combination. Float calibration data were then incorporated into LabVIEW® routines along with fluid specific characteristics.

### **7.3 SUMMARY OF RESULTS**

The vat's cross sectional area and the peristaltic tubing size affected the system's resolution. A large vat area to tubing size ratio is desirable since this reduces potential level pulsation and increases accuracy per revolution. A compromise between level resolution and system response time needs to be made. In addition, considerations need to be made on fluid viscosity to tubing size relationship. Increase in fluid viscosity increases the resistance to flow, creating limitations to the pumping speed for some fluid – tubing combinations. Guidelines for such conditions are provided by the pump and tubing supplier. Increased viscosities also provide a damping effect reducing fluid pulsation. Ultimately, each individual system needs to be carefully examined to comprehend these variables and define the best fill time and accuracy combination against the system requirements.

To characterize the system reaction under the expected range of operation, fluids at the viscosity extremes were employed. A range from 570 to 1 cps was covered by testing with DSM Somos® NanoForm™ 15120 resin for the higher viscosity and water for the lower viscosity. A single vat 20.32-cm by 22.86-cm (8-inches by 9-inches) in area, 9 liters in volume was chosen for these demonstrative experiments. An estimated fill-time difference of 4 minutes and 40

seconds was observed between these fluids using L/S 18 tubing. In addition, the proportional (P) parameter from the PID controller was changed from 1 to 9 creating different system reaction. Figure 5.1 and Figure 5.2 show the actual fluid level reading along with the control response signal. A settling time difference ranging from 15 to 20 seconds could be observed for this range of Proportional (P) values among the different fluids viscosity.

This implementation yielded simple multiple material parts with vertical and horizontal interface orientations with significantly different resin materials. These results showed successful system design and operation.

A mathematical characterization was carried out taking into account the pump and vat flow characteristics for specific conditions. Mathematical system modeling is a valuable tool for understanding the process and assisting in the selection of controller settings for specific conditions and outputs evaluation. This analysis yielded a simplified mathematical system representation or transfer function. This equation provides a means of tuning the controller parameters and aids in the process optimization.

## **7.4 RECOMMENDATIONS FOR FUTURE RESEARCH**

The results of the mathematical modeling illustrate the basic principles of designing a controller from the identification of the system to the implementation of a suitable controller algorithm. Additional studies can be carried out for further system refinement and process optimization for a variety of applications.

With the understanding of the system behavior under specific system variables that affect the level resolution and accuracy the build by layer technique as originally stated by Wicker *et*

*al.* (“Multi-Material Stereolithography ...” US 7,556,490 B2) can be further exploited. The fluid handling and leveling system can be setup to a high resolution and accuracy mode. Using smaller size high precision MasterFlex® L/S tubing (i.e. MasterFlex® L/S 14) together with a large vat cross sectional area (i.e. 20.32-cm by 22.86-cm vat) and low pump speeds (i.e. 50 rpm) will result in a significant increase in resolution of at least 0.04 microns and accuracies greater than 0.25 microns. The implementation of this approach would only require adjustments to the LabVIEW® routines that interact with the main SL program to allow the introduction of the desired fluid level steps to replace the standard SL routine Z linear stage steps.

Having a working system as a baseline and with the aim to improve the system accuracies alternative pump combinations can be pursued. Employing diverse tubing sizes supports either fast fill times by using large tubing sizes or high accuracies by employing smaller ones. These tubing or flow rate combinations can be achieved by: Using multiple single-headed peristaltic pumps, each with a different tubing size. By using a single multiple-headed peristaltic pump, each head carrying a different tubing size. This approach would require gate valves to control the different individual tubing circuits. Or by combining a low accuracy - high flow peristaltic pump with a high accuracy – low flow syringe pump. These are only some of several possible combinations which can be tailored to meet specific system needs.

These recommendations disclose general scenarios considered to have sufficient potential for continued development. Several other potential scenarios can certainly be identified during system implementation to specific applications or circumstances and/or through the continued utilization and acquaintance with the existing system.

## REFERENCES

- A&D Company, Limited. GX-K and GF-K series – High resolution industrial balance Instruction Manual. 2004. WM + PD4000775A.
- Arcaute, Karina, Brenda K. Mann and Ryan B. Wicker. “Stereolithography of Three-Dimensional Bioactive Poly (Ethylene Glycol) Constructs with Encapsulated Cells.” Annals of Biomedical Engineering. September 2006. 1429-1441.
- Astrom, Karl Johan and Richard Murray. Feedback Systems – An Introduction for Scientists and Engineers. New Jersey: Princeton University Press, 2008.
- Bailey, David and Edwin Wright. Practical SCADA for Industry. Ed. Newes. Massachusetts: Elsevier, 2003. 183-188.
- Beal, V. E., C. H. Ahrens and P. A. Wendhausen. “The Use of Stereolithography Rapid Tools in the Manufacturing of Metal Powder Injection Molding Parts.” Journal of the Brazilian Society of Mechanical Sciences and Engineering. Rio de Janeiro, March 2004. Vol. 26 No. 1. 40-46.
- Bishop, Robert H. Learning with LabView 2009. New Jersey: Pearson Education, 2010.
- Blais, Francois. “Review of 20 years of range sensor development.” Journal of Electronic Imaging. 13 (January 2004): 231-240.
- Bidanda, Bopaya and Paulo Bartolo. Virtual Prototyping & Bio Manufacturing in Medical Applications. New York: Springer, 2008. 153-155, 184-185.
- Choi, Jae-Won, Eric MacDonald and Ryan Wicker. “Multi-material microstereolithography.” International Journal of Advanced Manufacturing Technology. London: Springer, November 2009.

Clark, Robert R. “Triangulation Displacement Sensor.” United States Patent. US 6,624,899 B1.  
California: September 2003.

Cole Palmer®. MasterFlex® L/S® Operating Manual: Pump Drives. Ed. 04. A-1299-0996.

Cole Palmer®. MasterFlex® L/S® Operating Manual: Easy-Load® Pump Heads. Ed. 06. A-1299-0335.

Cole-Palmer®. MasterFlex® Tubing Application Guide. December 2006.

Cole-Palmer®. “Peristaltic Pumps Offer Economical Multichannel Pumping.” Cole-Palmer® Technical Library. April 2010.

[http://www.coleparmer.com/techinfo/techinfo.asp?htmlfile=ppumpsecon\\_WP.htm&id=578](http://www.coleparmer.com/techinfo/techinfo.asp?htmlfile=ppumpsecon_WP.htm&id=578)>.

Cole-Palmer®. “Peristaltic Pumps Offer Custom Fluid Solutions.” Cole-Palmer® Technical Library. April 2010.

[http://www.coleparmer.com/techinfo/print.asp?htmlfile=ppumpscustom\\_WP.htm&ID=577](http://www.coleparmer.com/techinfo/print.asp?htmlfile=ppumpscustom_WP.htm&ID=577)>.

Cole-Palmer®. “Pumping Viscous Fluids Figures.” Cole-Palmer® Technical Library. April 2010. <

<http://www.coleparmer.com/techinfo/techinfo.asp?htmlfile=PumpingViscousFluids.htm&ID=617>>.

Dobson, C. A., G. Sias, R. Phillips, M. J. Fagan and C. M. Langton. “Three dimensional stereolithography models of cancerous bone structures from CT data: testing and validation of finite element results.” Proceedings of the Institution of Mechanical Engineers. December 2006. Vol. 220 Part H. 481-484.



Dorf, Richard C. and Robert H. Bishop. Modern Control Systems. Ed. 11. New Jersey: Pearson Education, 2008. 83-91.

DSM Somos®. NanoForm™ 15120 – Product Data Sheet. Illinois: November 2005.

DSM Somos®. WaterShed 11120– Product Data Sheet. Illinois: October 2009.

DSM Somos®. Somos 14120 – Product Data Sheet. Illinois: October 2009.

Duval, Brian. “Advances in Analog Distance Sensing.” *Sensors Magazine*. September 2004.

<<http://www.sensorsmag.com/sensors/motion-velocity-displacement/advances-analog-distance-sensing-816>>.

Ellis, George. *Control System Design Guide – Using your Computer to Understand and Diagnose Feedback Controllers*. Ed. 3. California: Elsevier Academic Press, 2004. 31-32.

El-Mansi, E. M. T., C. F. A. Bryce, A. L. Demain and A. R. Allman. Fermentation, Microbiology and Biotechnology. Ed. 2. Florida: CRC Press, 2007. 428.

Fardo, Stephen and Dale Patrick. Industrial Process Control Systems. Ed. 2. Georgia: The Fairmont Press, 2009. 185-220.

Farnworth, Warren M. “Layer Thickness Control for Stereolithography Utilizing Variable Liquid Elevation and Laser Focal Length.” United States Patent. US 6,607,689 B1. Idaho: August 2003.

Gibaldi, Joseph. MLA Handbook for Writers of Research Papers. Ed. 6. New York: The Modern Language Association of America, 2003.

Girdhar, Paresh, Octo Moniz. Practical Centrifugal Pumps. Ed. Newes. Massachusetts: Elsevier, 2004. 1.

- Giuliani, Valerio, T. Freiheit and Peihua Gu. “Design and Realization of Multi-Material and Multi-Process Deposition Method.” Canadian Design Engineering Network. Alberta: University of Calgary, 2005.
- Golnaraghi, Farid and Benjamin C. Kuo. Automatic Control systems. New Jersey: John Wiley & Sons, 2010.
- Grimm, Todd. User’s Guide to Rapid Prototyping. Society of Manufacturing Engineers, 2004. 49-51, 161-172.
- Grote, Antonsson. Springer Handbook of Mechanical Engineering. New York: Springer, 2009. 813-816.
- Hambrice, Kevin and Henry Hopper. “A Dozen Ways to Measure Fluid Level and How They Work.” *Sensors Magazine - Sensor Technology and Design*. December 2004.  
<<http://www.sensorsmag.com/sensors/leak-level/a-dozen-ways-measure-fluid-level-and-how-they-work-1067>>
- Haus, Jorg. *Optical Sensors – Basics and Applications*. Wiley-VCH, 2010.
- Ibrahim, Dogan. Microcontroller Based Applied Digital Control. England: John Wiley & Sons, 2006. 269-282.
- Inamdar, Asim, Marco Magana, Frank Medina, Yinko Grajeda, and Ryan Wicker. “Development of an Automated Multiple Material Stereolithography Machine.” Proceedings of the 17<sup>th</sup> Annual Freeform Fabrication Symposium. Austin TX, August 2006. 624-635.
- Kamrani, Ali K. and Emad Abouel Nasr. Rapid Prototyping Theory and Practice. New York: Springer Science + Business Media, Inc., 2006. 1-2, 87-90.

- Karalekas, D. and K. Antoniou. "Composite rapid prototyping: overcoming the drawback of poor mechanical properties." Journal of Materials Processing Technology. Elsevier, April 2004. 526 – 530.
- Kochan, Anna. "Rapid Prototyping Gains Speed, Volume and Precision." Assembly Automation. 2000. Vol. 20. 295-299.
- Kotera, M. and Ochiai N. "Three-dimensional simulation of resist pattern deformation by surface tension at the drying process." Microelectronic Engineering. Elsevier, January 2005. 515-520.
- Liptak, Bela G. Instrument Engineers' Handbook – Process Measurement and Analysis. Ed. 4. Massachusetts: CRC Press, 2003. 474-485, 1404-1411.
- Liptak, Bela G. Instrument Engineers' Handbook – Process Control and Optimization. Ed. 4. Massachusetts: CRC Press, 2006. 96- 112.
- Lozoya, Oswaldo Alonso. "Development and demonstration of a multiple material stereolithography system." ETD Collection for University of Texas. El Paso TX, January 2006.
- Mathsoft Mathcad®. "Mathcad worksheet – Modeling a PID Controller." Mathsoft Mathcad® Enterprise Resource Center. October 2008.
- Micro-Epsilon®. User Manual - CCD System optoNCDT 1800®.
- Mohammed, Selma B., David A. Fields, Bettina Mittendorfer, Andrew R. Coggan, and Samuel Klein. "Are Peristaltic Pumps as Reliable as Syringe Pumps for Metabolic Research? Assessment of Accuracy, Precision, and Metabolic Kinetics." Metabolism. Elsevier, July 2004. 875-878.

MTI Instruments, Inc. Microtrak 7000<sup>TM</sup> – User Manual. Revision 5.5. Albany New York. Doc 10A000194.

Mulley, Raymond. Flow of industrial Fluids – Theory and Equations. Florida: CRC Press, 2004. 121-124.

National Instruments<sup>TM</sup>. LabVIEW<sup>TM</sup> 8.5 Help. National Instruments Corporation, August 2007. 371361D-01.

National Instruments<sup>TM</sup>. LabVIEW<sup>TM</sup> – PID Control Toolkit User Manual. National Instruments Corporation, June 2008. 372192C-01.

National Instruments<sup>TM</sup>. LabVIEW<sup>TM</sup> – PID Theory Explained. National Instruments Corporation, 2006.

National Instruments<sup>TM</sup>. Serial Communication General Concepts. National Instruments Corporation. May 2009. 1M9E1L6Q.

National Instruments<sup>TM</sup>. Serial Hardware and Software for Windows Help. National Instruments Corporation, August 2005.

Rahmat, Mohd Fua’ad and Sahazati Md Rozali. “Modeling and Controller Design for a Coupled Tank Liquid Level System: Analysis & Comparison.” Jurnal Teknologi. June 2008. 113-141.

Reynders, Deon, Steve Mackay and Edwin Wright. Practical Industrial Data Communications – Best Practice Techniques. Ed. Newes. Massachusetts: Elsevier, 2005. 71 – 74.

Sahu, G. K. Pumps. New Delhi: New Age International, 2006. 24 – 35.

Sandoval, J. H., L. Ochoa, A. Hernandez, O. Lozoya, K. F. Soto, L. E. Murr and R. B. Wicker. “Nanotailoring Stereolithography Resins for Unique Applications Using Carbon

- Nanotubes.” Proceedings of the 16<sup>th</sup> Annual Solid Freeform Fabrication Symposium. Austin TX, August 2005. 513 – 524.
- Seibel, Barry S. Phacodynamics – Mastering the Tools and Techniques of Phacoemulsification Surgery. Ed. 4. New Jersey: SLACK Incorporated, 2005. 16-29.
- Sharpe, William N. Experimental Solid Mechanics. New York: Springer Science + Business Media, 2008. 831.
- Singh, S. K. Industrial Instrumentation and Control. Ed. 3. New Delhi: Tata McGraw-Hill, 2009. 303 – 306.
- Skoczowski, Stanislaw, Stefan Domek and Krzysztof Pietruszewicz. “Model following PID control system.” Kebernetes: The international journal of systems, cybernetics and management science. Emerald Group Publishing Limited, 2003. 818 – 828.
- Travis, Jeffrey and Jim Kring. LabVIEW for Everyone: Graphical Programming Made Easy and Fun. New Jersey: Pearson Education, 2007.
- Tunyasirirut, Satean and Santi Wangnipparnto. “Level Control in Horizontal Tank by Fuzzy-PID Cascade Control.” World Academy of Science, Engineering and Technology. November 2006.
- Velmex Inc. User Manual - VP9000 Programmable Stepping Motor Controller.
- Vlachogiannis, John G. and Ranjit K. Roy. “Robust PID controllers by Taguchi’s method.” The TQM Magazine. Emerald Group Publishing Limited: 2005. 456 – 466.
- Volk, Michael. Pump Characteristics and Applications. Ed. 2. Florida: CRC Press, 2005. 1-5, 16-18, 26-27.
- Wahlstrom, Ben. “Multiple Vat Leveling System.” United States Patent Application. US 2006/0192312 A1. Oregon: August 2006.

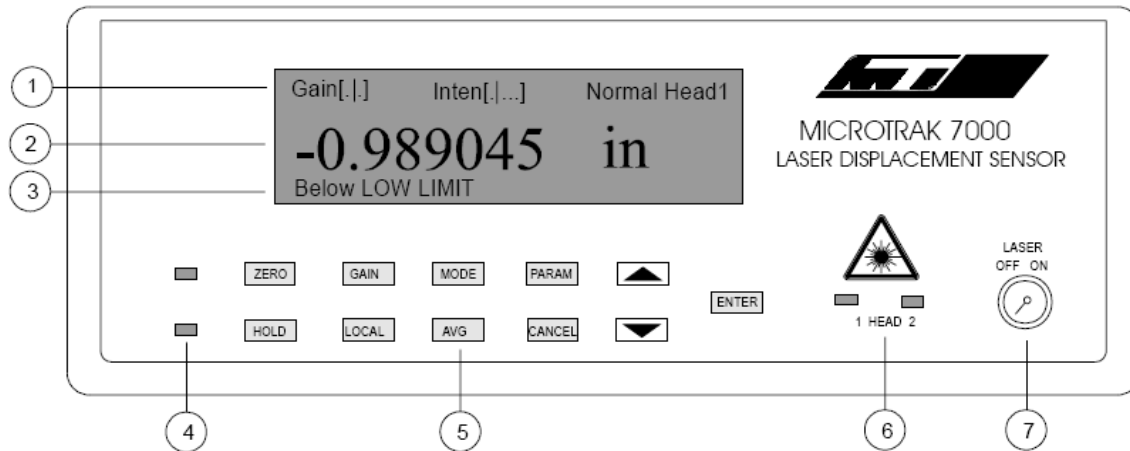
- Wicker, Ryan, Atul Ranade, Francisco Medina and Jeremy Palmer. “Practical Considerations for Micro-Stereolithography of Embedded Micro-Channels.” Rapid Prototyping Association of the Society of Manufacturing Engineers. Dearborn MI, May 2004. TP04PUB210
- Wicker, Ryan, Francisco Medina and Chris Elkins. “Multiple Material Micro-Fabrication: Extending Stereolithography to Tissue Engineering and Other Novel Applications.” Proceedings of the 15<sup>th</sup> annual Solid Freeform Fabrication Symposium. Austin TX, August 2004. 754-764.
- Wicker, Ryan, Francisco Medina and Chris Elkins. “Multi-Material Stereolithography.” United States Patent. US 7,556,490 B2. El Paso TX, July 2009.
- Wilkins, Larry C. “Laser Measurement of Liquid Level in a Holder.” United States Patent. US 7,082,828 B1. Indiana: August 2006.
- Wu, Jih-Huah, Cheng-Chung Pen and Joe-Air Jiang. “Applications of the Integrated High-Performance CMOS Image Sensor to Range Finders – from Optical Triangulation to the Automotive Field.” Sensors. March 2008. 1719-1739.
- Zhong, Quing-Chang. Robust Control of Time-delay Systems. Springer-Verlag London Limited, 2006. 17-30.
- Zollikofer, Christoph P. E. and Marcia S. Ponce de Leon. Virtual Reconstruction – A Primer in Computed-Assisted Paleontology and Biomedicine. New Jersey: John Wiley and Sons, 2005. 209-223.
- 3D Systems®. 250/50 Stereolithography Buildstation User Guide. California, 3D Systems, 1995.

## APENDIX A – DSM SOMOS® NANOFORM™ DATA SHEET

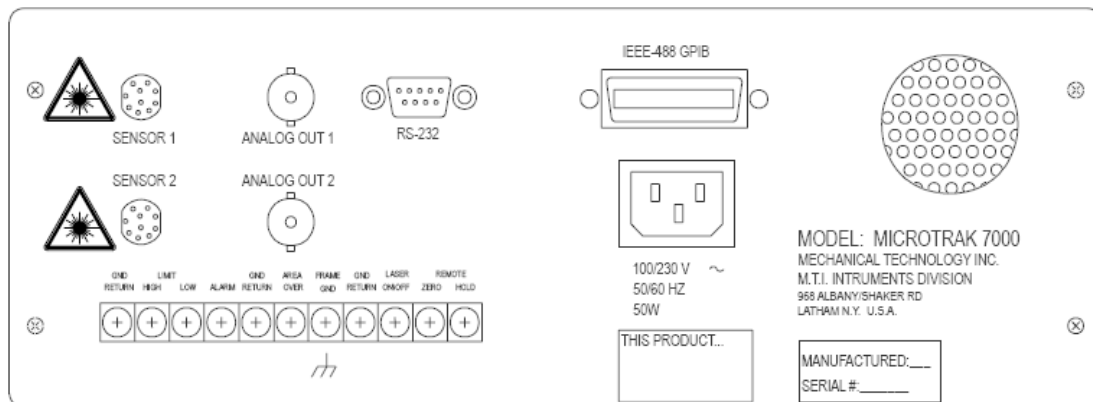
DSM Somos® NanoForm™ 15120 Data Sheet.

<b>Physical Properties - Liquid</b>	
<b>Appearance</b>	<b>Opaque gray</b>
<b>Viscosity</b>	<b>~570 cps at 30° C</b>
<b>Density</b>	<b>~1.33 g/cm<sup>3</sup> at 25° C (liquid) ~1.38 g/cm<sup>3</sup> (solid)</b>
<b>Optical Properties at 355 nm</b>	
<b>E<sub>C</sub></b>	<b>~16.3 mJ/cm<sup>2</sup></b>
<b>D<sub>P</sub></b>	<b>~0.0052 inch</b>
<b>E<sub>10</sub></b>	<b>112 mJ/cm<sup>2</sup></b>
<b>Mechanical Properties (UV Post cure)</b>	
<b>Tensile Strength</b>	<b>48 MPa</b>
<b>Elongation at Break</b>	<b>2.1 – 3.0 %</b>
<b>Modulus of Elasticity</b>	<b>5000 MPa</b>
<b>Thermal Properties</b>	
<b>Glass Transition Temperature</b>	<b>39° C (UV Post cure)</b>

## APENDIX B – MICROTRAK 7000™ LASER DISPLACEMENT SENSOR SPECIFICATIONS



Laser Sensor Processing Unit Display Panel by Microtrak.



Laser Sensor Processing Unit Rear Panel by Microtrak.

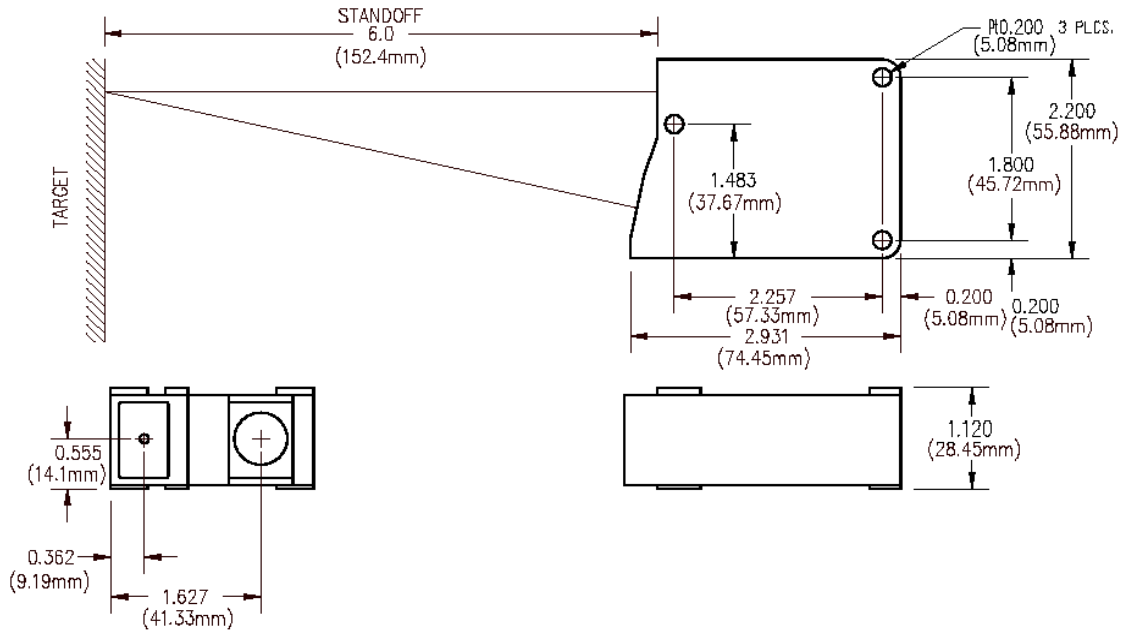


MTI Instruments. Microtrak 7000TM Laser Displacement Sensor Specifications.

MT-600 Diffuse Sensor Head	
Resolution	50.0 $\mu$ in. (1.27 $\mu$ m)
Standoff	6.0 in. (152.4 mm)
Measuring range	0.80 in. (20.3 mm)
Linearity	$\pm 0.1\%$ of range
Accuracy	$\pm 0.1\%$ of range
Dynamic range	96 dB
Reflectance range	100:1
Sampling freq	100 kHz
Freq response	20 kHz
Averaging	Low Pass Selectable Filter From 0.03 Hz to 20 kHz
Response time	95 $\mu$ s
Zero set	Equal to range of the head
Offset range	$\pm 99.999$ of units selected
Temp stability	0.03% FSR/ $^{\circ}$ F (.06% FSR/ $^{\circ}$ C)
Laser type	Semiconductor, visible red (Class II) 1 mW nominal, 3mW max. (Class IIb available)
Laser wavelength	670 nm
Ambient illumination	3500 lux maximum

MTI Instruments. Microtrak 7000TM Laser Displacement Sensor Specifications. Continued

Analog output	-10V to+10 VDC
Digital output	Open collector, HV protected 100 mA maximum current sinking
Digital input	Optically isolated, dry contact to ground activated
Data interfaces	RS-232C; 300-19,200 baud (selectable) IEEE-488: Externally controlled; 16 Bit parallel Digital Output
Remote inputs	Remote zero input, Remote hold input Remote laser interlock
Laser activation	Remotely connecting rear activation terminal to ground activates laser
External alarm output	High limit, Low limit, Bright or dark limit exceeded Linear range exceeded
Power	90-260 VAC, auto switching, 47-63 Hz, 50 W max.
Weight	Controller: 8.8 lb (4.0 kg) Head: 0.33 lb (0.15 kg)
Size	Controller: 12.0 in. (304.8 mm) W x 4.5 in. (114.3 mm) H x 10.0 in. (254 mm) D
	Head: 2.2 in. (55.9 mm) W x 1.0 in. (25.4 mm) H x 3.0 in. (76.2 mm) D
	32°F - 125°F (0°C 50°C)
Environnemental	30% - 90% RH, non-condensing



### MT 600 Laser Head

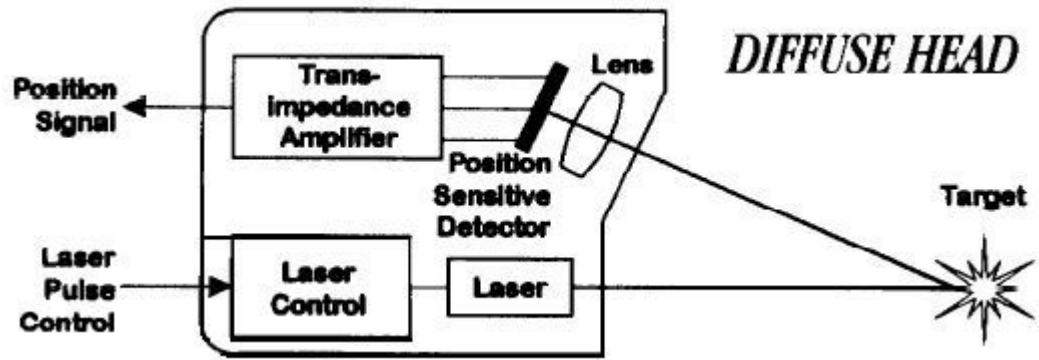
MT 600 Laser Head Dimensional Details.

MODEL	STANDOFF	RANGE	RESOLUTION	SPOT SIZE**	HEAD TYPE*
MT-100-5	1.0 in. (25.4 mm)	0.005 in. (0.127 mm)	0.1 $\mu$ in. (0.0025 $\mu$ m)	0.0012 x 0.0036 in. (30 x 90 $\mu$ m)	Specular
MT-100-20	1.0 in. (25.4 mm)	0.02 in. (0.51 mm)	0.5 $\mu$ in. (0.0127 $\mu$ m)	0.0012 x 0.0036 in. (30 x 90 $\mu$ m)	Specular
MT-250-200	2.5 in. (63.5 mm)	0.20 in. (5.1 mm)	5.0 $\mu$ in. (0.127 $\mu$ m)	0.0024 x 0.0072 in. (60 x 180 $\mu$ m)	Diffuse
MT-250-400	2.5 in. (63.5 mm)	0.40 in. (10.2 mm)	10.0 $\mu$ in. (0.254 $\mu$ m)	0.0024 x 0.0072 in. (60 x 180 $\mu$ m)	Diffuse
MT-600-800	6.0 in. (152.4 mm)	0.80 in. (20.3 mm)	50.0 $\mu$ in. (1.27 $\mu$ m)	0.006 x 0.010 in. (150 x 250 $\mu$ m)	Diffuse
MT-600-1600	6.0 in. (152.4 mm)	1.60 in. (40.6 mm)	100.0 $\mu$ in. (2.54 $\mu$ m)	0.006 x 0.010 in. (150 x 250 $\mu$ m)	Diffuse
MT-600-3000	6.0 in. (152.4 mm)	3.0 in. (76.2 mm)	200 $\mu$ in. (5.08 $\mu$ m)	0.006 x 0.010 in. (150 x 250 $\mu$ m)	Diffuse

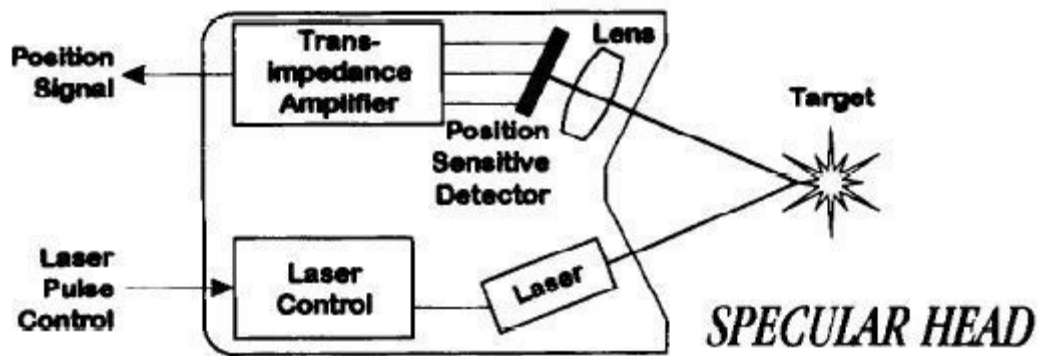
\*Diffuse sensors can be used for most surfaces. Highly reflective, mirrored surfaces require a specular sensor.

\*\* Note: For specialized applications, larger spot sizes are available, consult factory.

### Seven Standard MT Laser Head Models Details.



MT 600 Laser Head Diffuse Configuration.



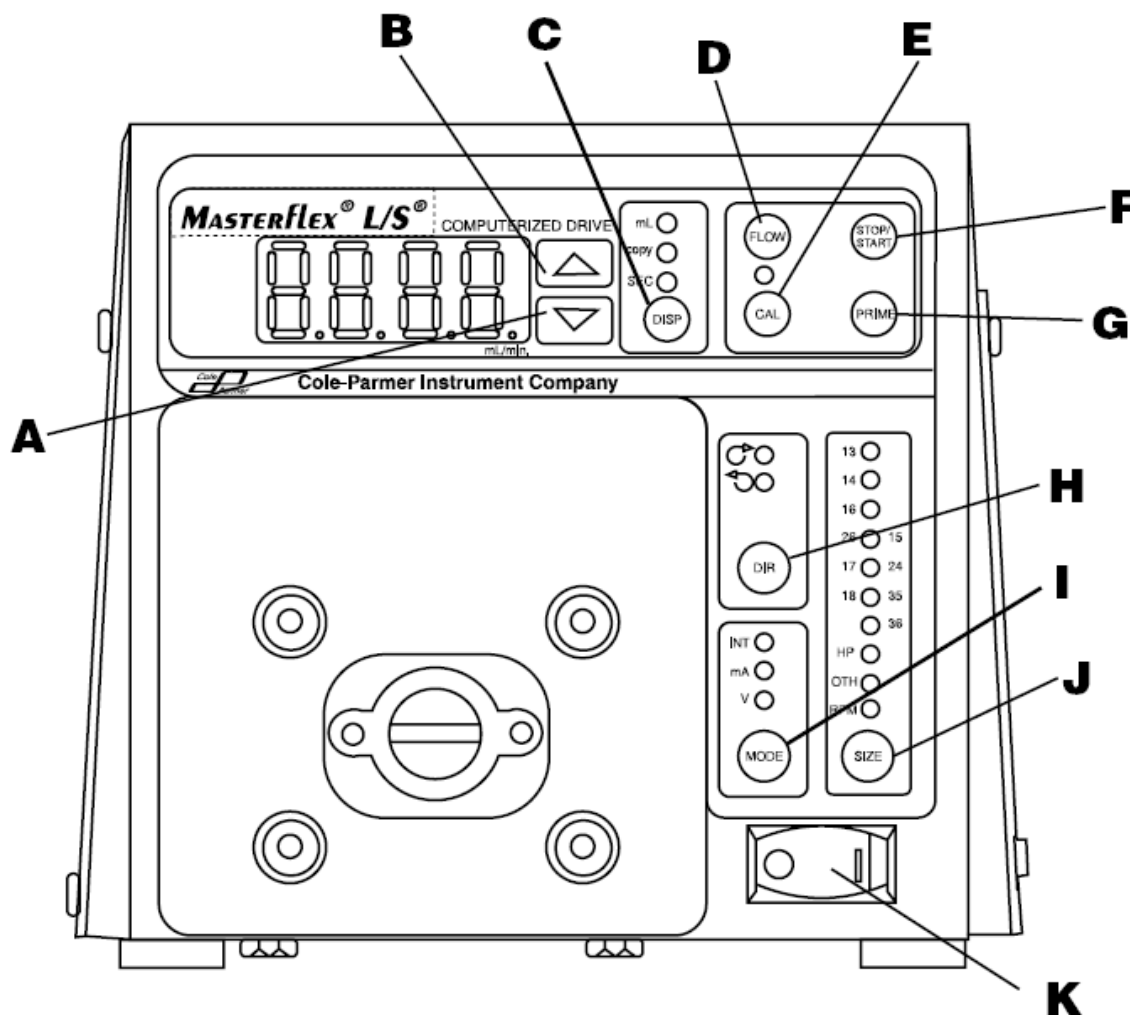
MT 600 Laser Head Specular Configuration.

## APENDIX C – MASTERFLEX® L/S® 7550-50 PERISTALTIC PUMP SPECIFICATIONS

### PUMP DRIVE MODEL 7550-50

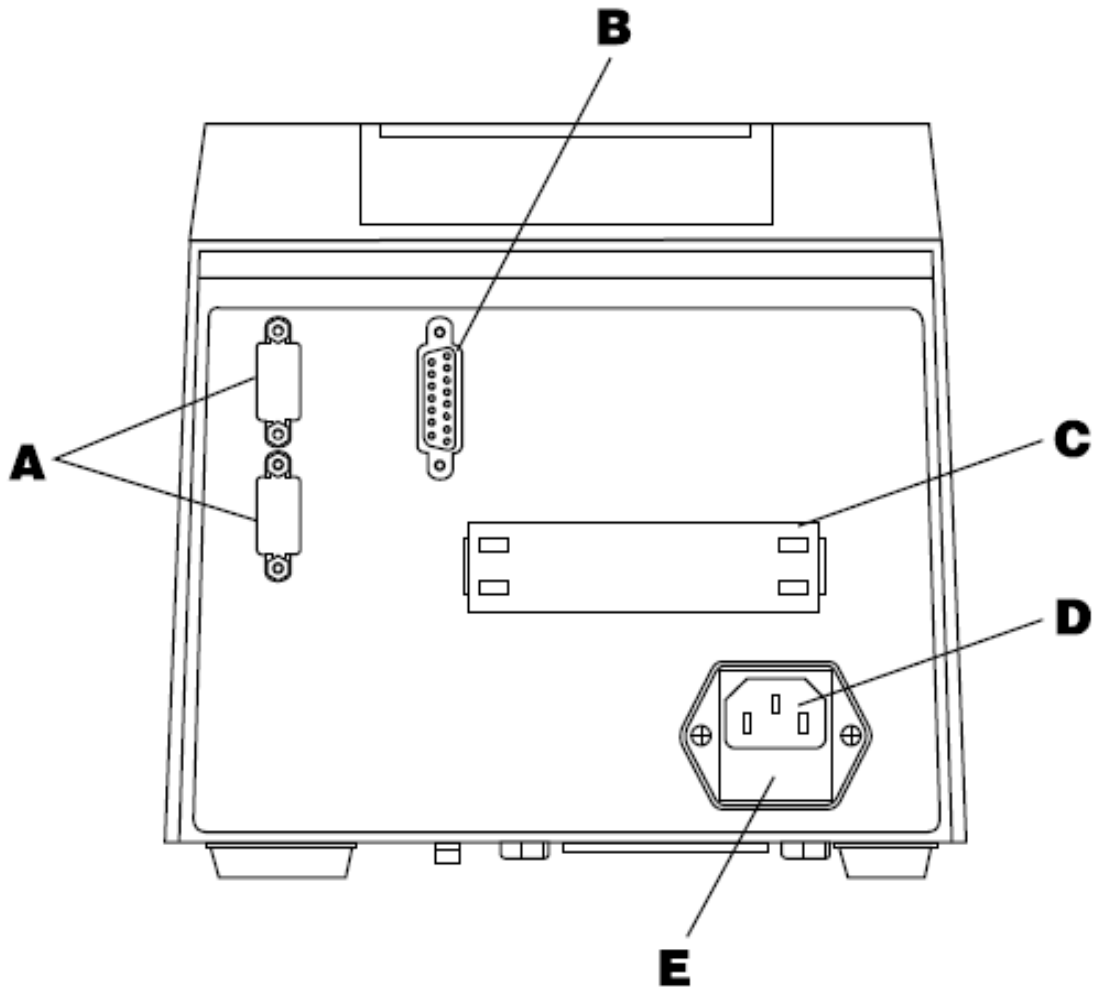
The Digital PWM BLDC Drive controls the speed of MASTERFLEX® L/S® Pump Heads to provide flow rates from 0.10 to 3400 mL/min. Mount up to 2 (600 rpm) or 4 (100 rpm) MASTERFLEX® L/S® Pump Heads and all MASTERFLEX-compatible pump heads.

### CONTROL/DISPLAY FUNCTIONS



Laser Sensor Processing Unit and Head by Microtrak.

- A. DOWN ARROW (DECREMENT)—Decrease value of a flashing display.
- B. UP ARROW (INCREMENT)—Increase value of a flashing display.
- C. DISPENSE/COPY—Select dispensed volume, number of copies of a dispensed volume, or the interval between dispenses.
- D. FLOW CONTROL—Set flow rate for selected tubing size. To change flow rate, press or arrow keys. (If pump is running, its speed will change with new settings.)
- E. CAL CONTROL—Refine built-in calibration, using a measured volume.
- F. STOP/START—Stop/Start motor.
- G. PRIME—Run pump at full speed to fill or clear lines.
- H. DIRECTION—To change motor direction.
- I. MODE SELECT—INT for internal control; mA for remote current control; V for remote voltage control.
- J. SIZE—Select tubing size.
- K. POWER SWITCH—All settings are retained in memory.



## SETUP AND DRIVE OPERATION

1. On 77301 connect Motor Cable plug to mating receptacle on the Controller.
2. Mount pump head and load tubing. (See pump head manual.)
3. Connect power cord to Controller and grounded power line outlet.
4. Turn pump on and select tubing size. NOTE: If CAL LED is lit, that tubing size has been previously field calibrated. If LED is not lit, the drive is operating with the built-in factory calibration. To clear a field calibration, press and hold the CAL switch until the

CAL light goes out. This will take about 3 seconds. To recalibrate for better accuracy, refer to Calibration section.

5. MODE selection (INT, mA, V).
6. Select motor Direction (CW or CCW).
7. PRIME and Calibrate the pump (if required).
8. Press FLOW key and watch display to set the flow rate with UP/DOWN arrow keys.
9. Press STOP/START key to begin pumping. NOTE: Normally, pump will not restart automatically after a brownout or power out condition.

Automatic Start Enable/Disable Press and hold STOP/START on power-up. After five (5) seconds, display will change to all dashes. Then, while holding STOP/START, press PRIME five (5) times. Display will flash "ON" or "OFF". Use UP/DOWN arrow keys to set automatic start option. Press any other key to exit. When "ON" is selected, pump will start automatically at power-up if it was "ON" when powered down.

## CALIBRATION

Use only MASTERFLEX precision tubing with MASTERFLEX pumps to ensure optimum performance.

1. Select correct tubing size and flow rate.
2. Press CAL, calibration volume appears.
3. Press STOP/START, the pump will use its stored memory to dispense the specified calibration sample quantity. The pump will stop automatically.



4. Weigh/measure the sample.
5. Use UP/DOWN arrow keys to correct the flashing display. NOTE: If the adjusted calibration is too great, "Err" will appear in the display. If this occurs, press the CAL control and repeat the calibration procedure. The microprocessor will retain one special calibration value per tubing size, even when power is turned off. The next calibration will replace the existing value.
6. Press SIZE to exit the calibration cycle.

#### DISPENSE/COPY

A first press of the DISP key results in the last entered dispense volume being displayed. The "mL" annunciator will illuminate and flash. The UP/DOWN keys are used to change the dispense volume, if desired. The STOP/START key then initiates delivery of the set volume. The amount remaining to be dispensed will be displayed during countdown. The dispense function is exited by pressing any key except UP, DOWN DISP, or STOP/START.

A second press of the DISP key causes the COPY annunciator to illuminate and flash. The STOP/START key is then used to deliver the desired volume without the need to know the volume in specific units. A third press of the DISP key enters the volume dispensed. The COPY annunciator stops flashing. The STOP/START key is then used to initiate delivery of the copied volume. The number of copies dispensed will be displayed after each dispense. The maximum number of copies is 9999. The STOP/START key is used to pause the copy dispense during dispensing; copy dispense can then be continued using the STOP/START key.

A fourth press of the DISP key results in the last entered interval between dispenses being displayed. The SEC annunciator will illuminate and flash. The UP/DOWN keys are used to change the time between dispenses, if desired, from 1 to 9999 seconds. The STOP/START key then initiates delivery of the set volume, with the drive automatically initiating a new dispense after each timeout. The remaining time will be displayed during countdown.

The STOP/START key is used to stop the dispense cycle. A time of 0 seconds (default) will require initiation of each dispense through the STOP/START key or the Remote STOP/START contact closure. Pressing the DISP key a fifth time exits this mode.

## SPECIFICATIONS

### Output:

Speed:	
7550-50	1.6 to 100 rev/min
Max Torque:	
7550-50	360 oz-in (26 kg•cm)
Speed regulation:	
Line	±0.25% F.S.
Load	±0.25% F.S.
Drift	±0.25% F.S.
Display:	Four-digit, seven-segment LED

### Remote outputs:

All units	Voltage speed output (0–10V DC @ 1 kΩ min)
All units	Current speed output (0–20 mA or 4–20 mA @ 0–600 Ω)
7550-50	RS-232C
7550-50	AUX 1 and 2 OUT (Contact closure 5A @ 115/230 Vrms)
7550-50	Tach output (TTL, 16 to 1000 Hz, 50% duty cycle, 10 Hz/rpm)
All units	Motor running output (N.O. & N.C. contact closure, 1A @ 28V AC/DC)

### Input:

Supply voltage limits:	Dual voltage—Automatically selected. 90 to 130 Vrms @ 50/60 Hz, or 200 to 260 Vrms @ 50/60 Hz
Max Current:	2.2A @ 115 Vrms, or 1.1A @ 230 Vrms
Installation Category:	Installation Category II per IEC 664 (Local level—appliances, portable equipment, etc.)

### Remote Inputs:

All units	STOP/START, CW/CCW, PRIME (Contact closure)
All units	Voltage input (0–10V DC @ 10 kΩ)
All units	Current input (0–20 mA or 4–20 mA @ 250 Ω)
7550-50	RS-232C
7550-50	AUX IN (Contact closure)

### Construction:

Dimensions (L x W x H):	
7550-50	11 1/2 in x 7 11/16 in x 7 3/16 in (292 x 196 x 182 mm)
Weight:	
7550-50	15 lb (6.8 kg)
Enclosure Rating:	
7550-50	IP 23 per IEC 529

### Environment:

Temperature, Operating:	0° to 40 °C (32° to 104 °F)
Temperature, Storage:	–25° to 65 °C (–13° to 149 °F)
Humidity (non-condensing):	10% to 90%
Altitude:	Less than 2000 m

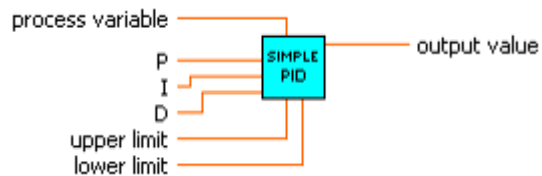
### Pollution Degree:

7550-50	Pollution Degree 2 per IEC 664 (Indoor use—lab, office)
Chemical Resistance:	Exposed material is aluminum, ABS plastic and vinyl
Compliance:	UL508C, CSA C22.2, No. 14-M91.
	(For CE Mark):
	EN61010-1/A2: 1995 (EU Low Voltage Directive) and
	EN61326-1/A1: 1998 (EU EMC Directive)

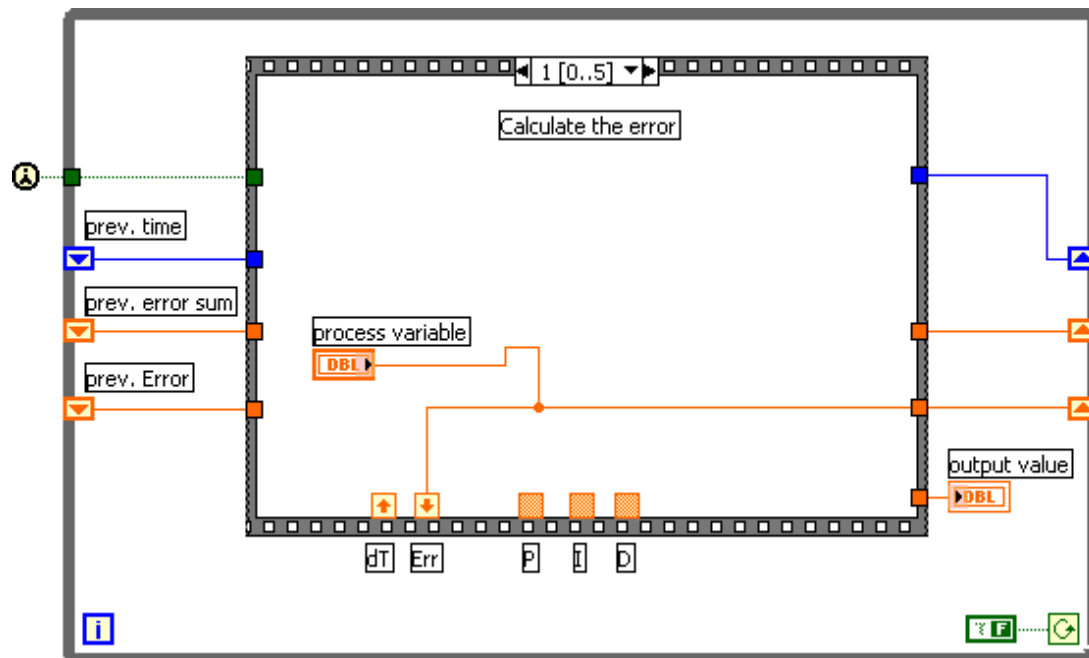
## APENDIX D LABVIEW CONTROL STRUCTURE

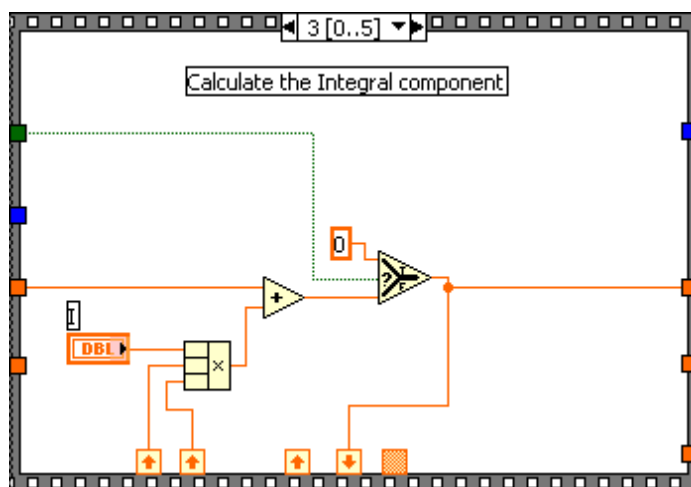
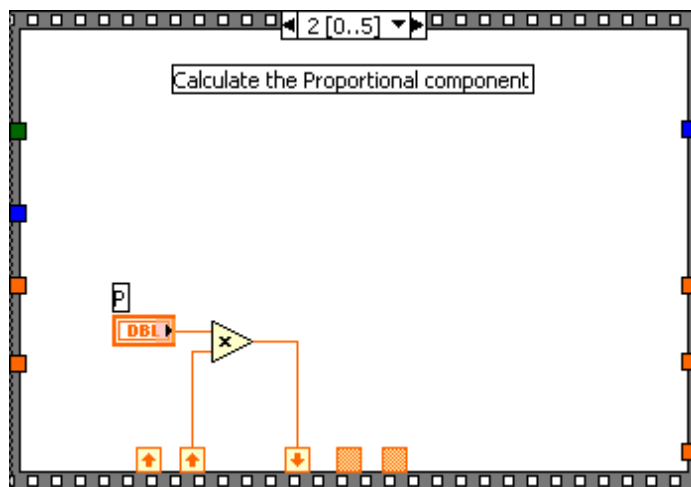
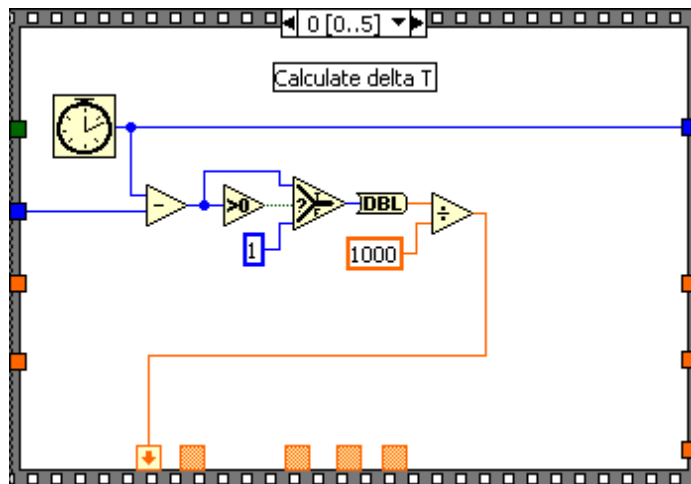
simple PID13jul05.vi

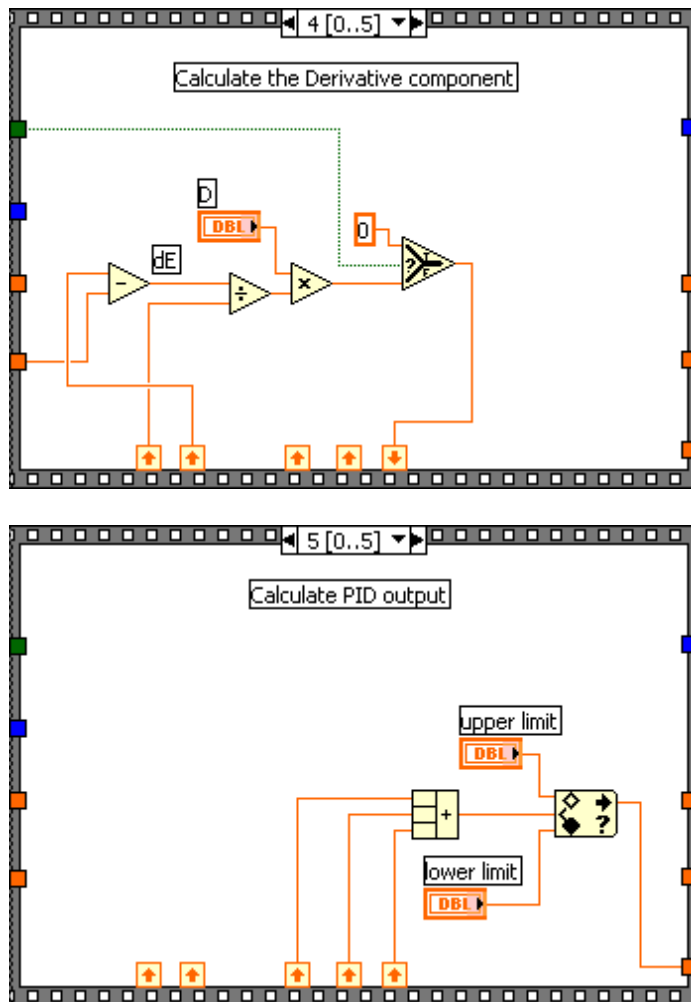
## Connector Pane



### Block Diagram





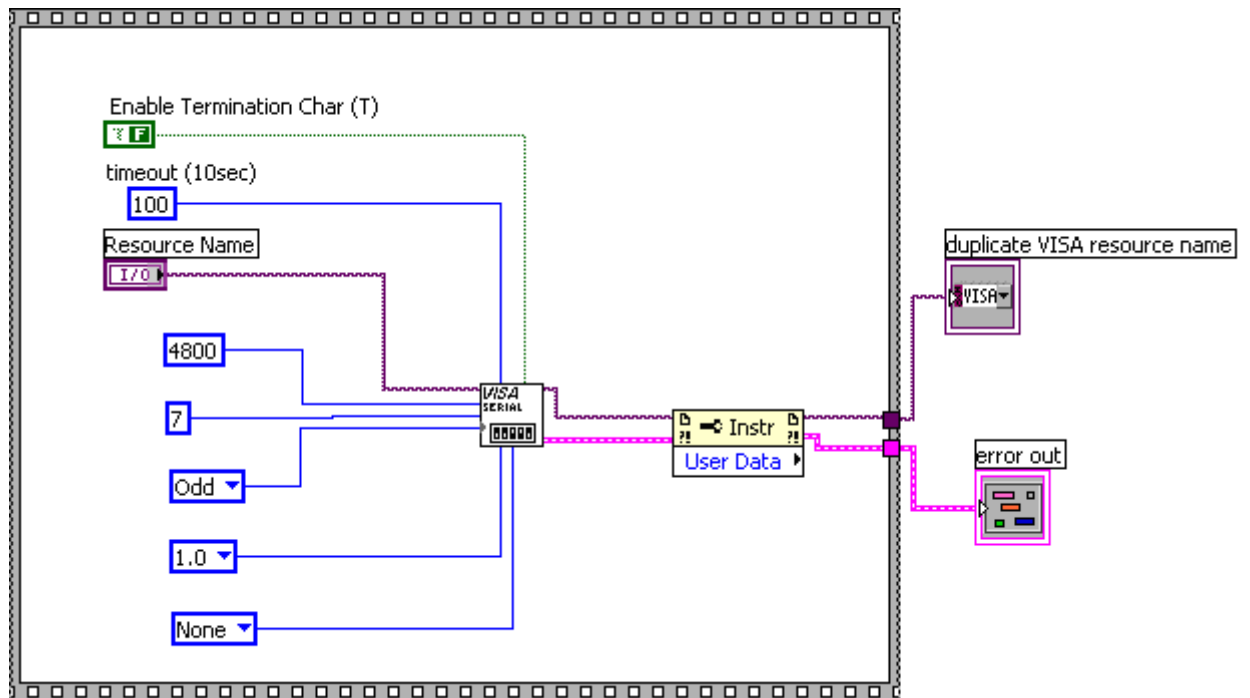


VisaConfig SubPump.vi

Connector Pane

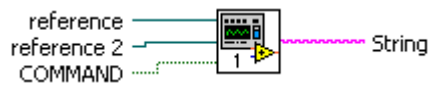


Block Diagram

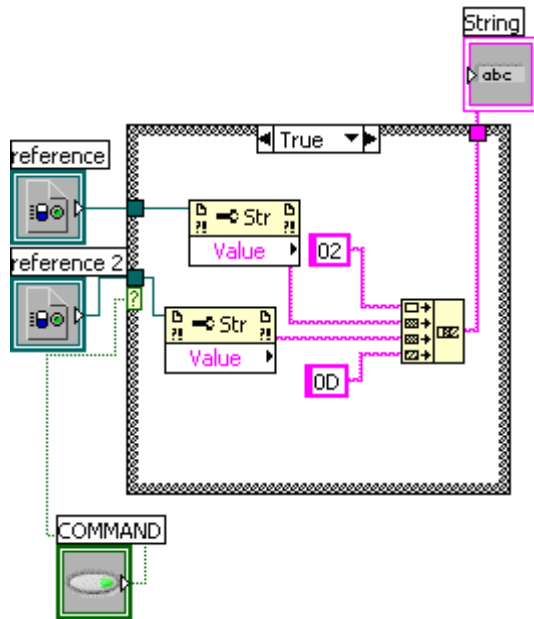


Device2 SubPump.vi

Connector Pane



Block Diagram

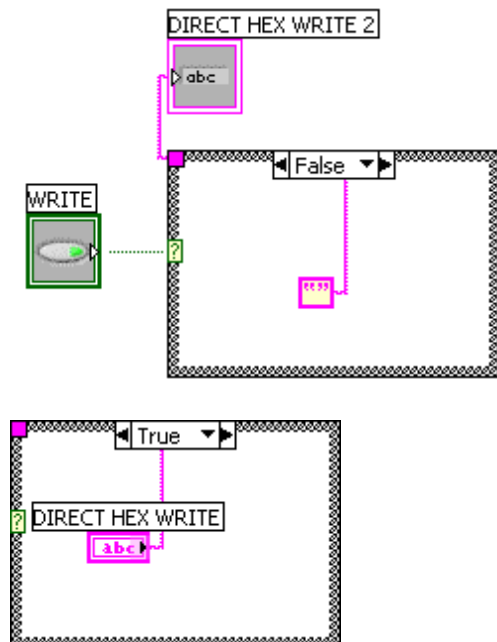


DirectWrite SubPump.vi

Connector Pane



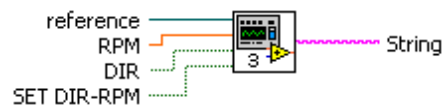
Block Diagram



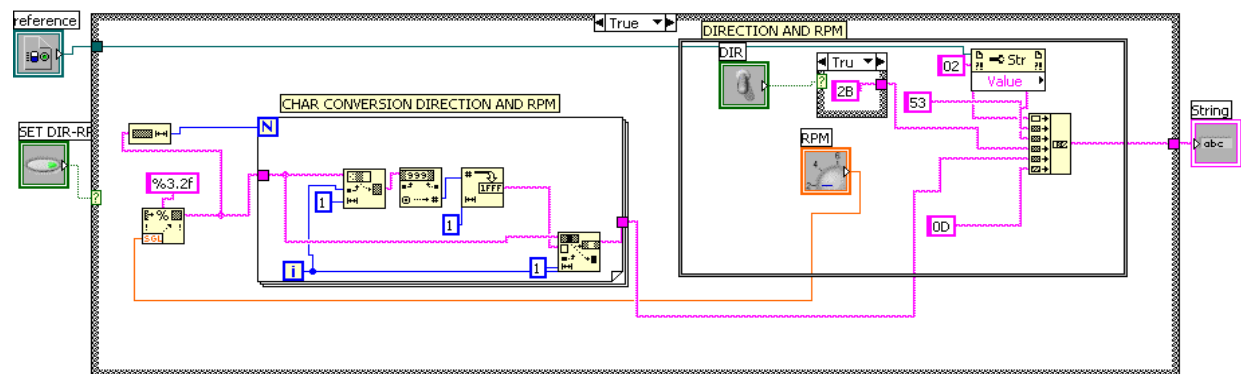


## DirRPMConv SubPump.vi

### Connector Pane

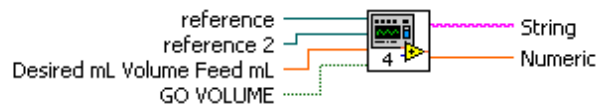


### Block Diagram



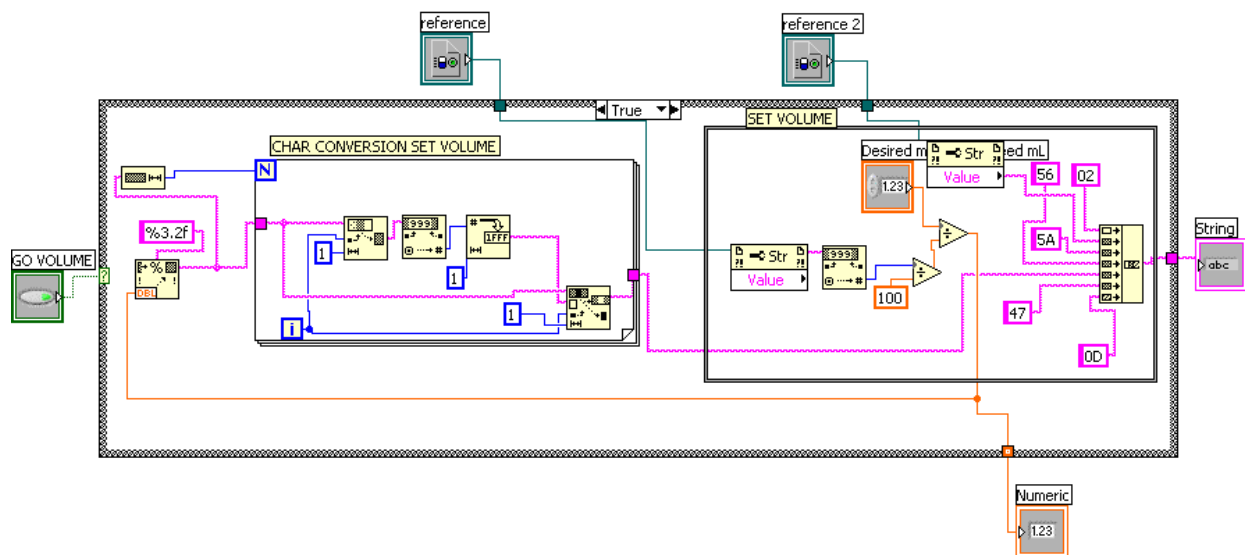
## VolConv SubPumpAuto.vi

### Connector Pane



### Block Diagram

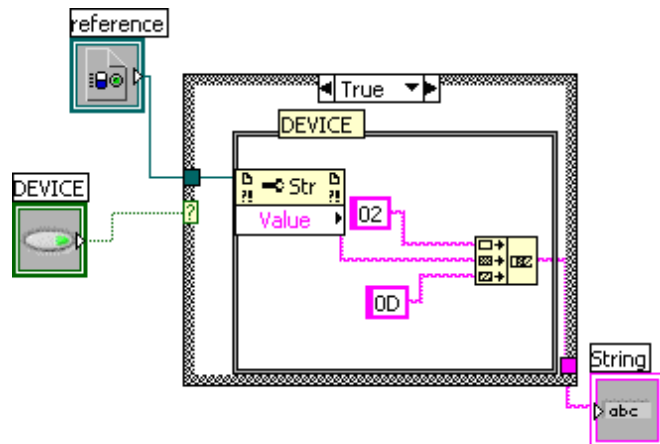
### Device SubPump.vi



### Connector Pane



### Block Diagram

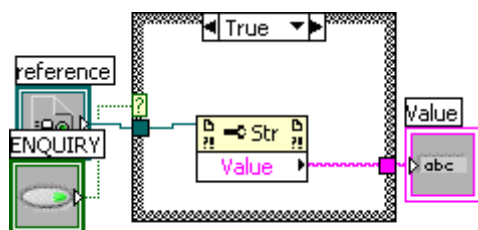


## Enquire SupPump.vi

### Connector Pane

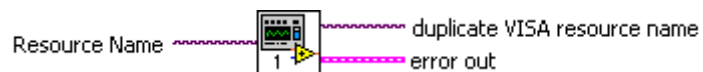


### Block Diagram

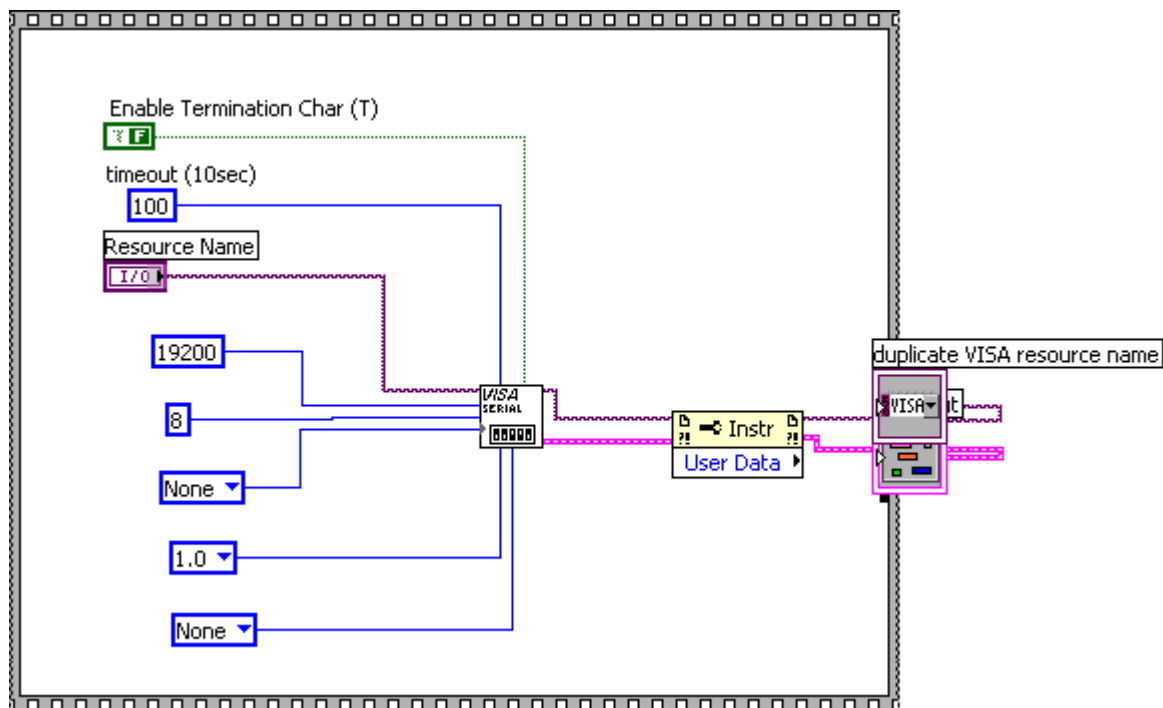


## VisaConfig SubSensor.vi

### Connector Pane

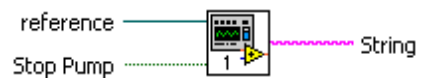


### Block Diagram

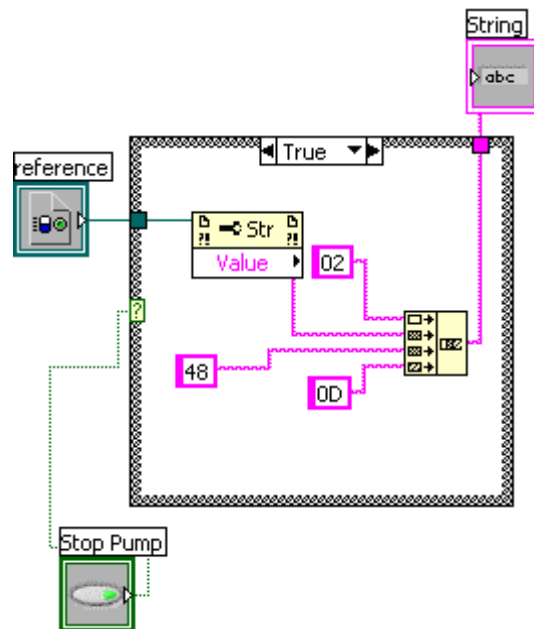


## Pump StopSubvi.vi

### Connector Pane

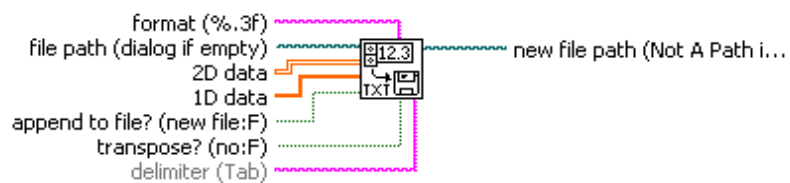


### Block Diagram

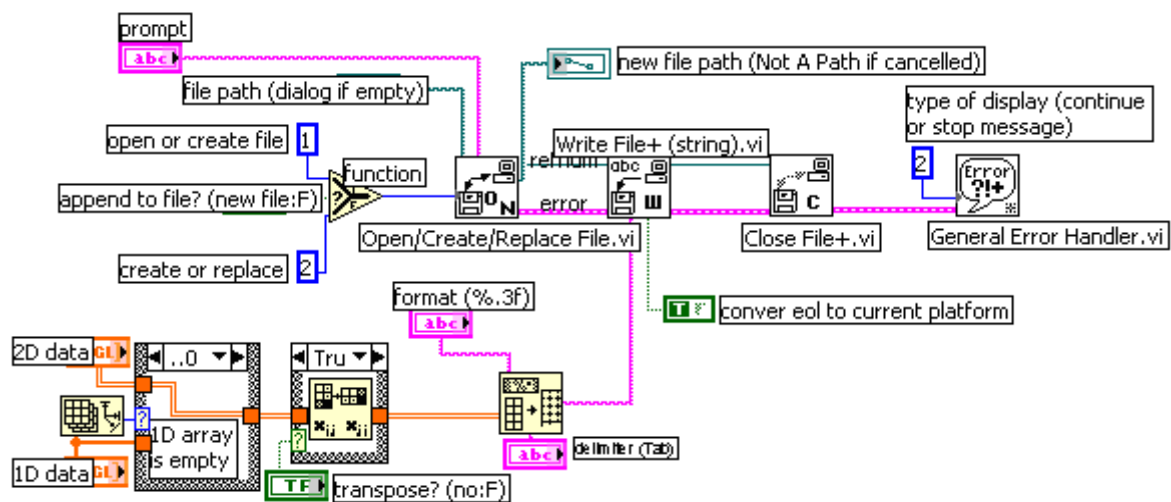


## Write To Spreadsheet File.vi

### Connector Pane



### Block Diagram



## APENDIX E - MICRO-EPSILON® OPTONCDT 1800® LASER DISPLACEMENT SENSOR SPECIFICATIONS

### Technical Data

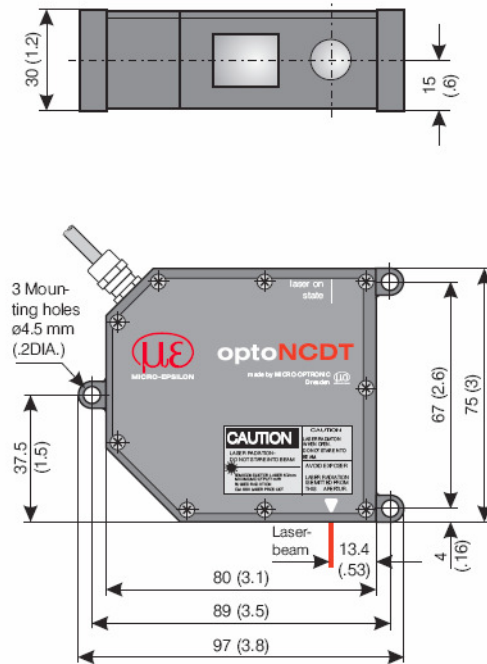
Model	ILD 1800-2	ILD 1800-10	ILD 1800-20	ILD 1800-50	ILD 1800-100	ILD 1800-200
Measuring range	2 mm (.08 ")	10 mm (.4 ")	20 mm (.8 ")	50 mm (2 ")	100 mm (4 ")	200 mm (8 ")
Start of measuring range	24 mm (.9 ")	30 mm (1.2 ")	40 mm (1.6 ")	45 mm (1.8 ")	70 mm (2.8 ")	70 mm (2.8 ")
Reference distance (midrange)	25 mm (1 ")	35 mm (1.4 ")	50 mm (2 ")	70 mm (2.7 ")	120 mm (4.7 ")	170 mm (6.69 ")
End of measuring range	26 mm (1 ")	40 mm (1.6 ")	60 mm (2.4 ")	95 mm (3.7 ")	170 mm (6.7 ")	270 mm (10.63 ")
Spot diameter (minimum)	35 $\mu$ m (at MMR)	50 $\mu$ m (at MMR)	45 $\mu$ m (at MMR)	55 $\mu$ m (at MMR)	60 $\mu$ m (at MMR)	1300 $\mu$ m (at SMR)
Linearity	2 $\mu$ m	8 $\mu$ m	16 $\mu$ m	40 $\mu$ m	80 $\mu$ m	200 $\mu$ m
	$\leq \pm 0.1$ % FSO	$\leq \pm 0.08$ % FSO				$\leq \pm 0.1$ % FSO
Resolution DC to 5 kHz	0.2 $\mu$ m	1 $\mu$ m	2 $\mu$ m	5 $\mu$ m	10 $\mu$ m	20 $\mu$ m
	0.01 % FSO					
Measuring rate	5 kHz					
Permissible ambient light	10,000 lx					
Light source	1 mW laser, wavelength: 670 nm (red)					
Laser safety class	Class 2 - DIN EN 60825-1 03.97 / IEC 825-1 11.93 / FDA					
Protection class	Sensor: IP 65 / Controller: IP 50					
Long term stability	0.05 % FSO/month					
Temperature stability	$\pm 0.01$ % FSO/ $^{\circ}$ C ( $\pm .005$ % FSO/ $^{\circ}$ F)					
Operating temperature	0 to 50 $^{\circ}$ C (32 to 122 $^{\circ}$ F)					
Storage temperature	-20 to 70 $^{\circ}$ C (-4 $^{\circ}$ to 158 $^{\circ}$ F)					
Output	Standard: $\pm 5$ V / Options: RS 232 or RS 485					
Supply voltage	24 VDC ( $\pm 15$ %), max. 500 mA					
Sensor cable standard extension	2 m (6.5 ') - integrated					
	5 (16.5 ') or 10 m (33 ') - without additional calibration					
Controller functions dimensions	auto zero / signal averaging					
	143 x 145 x 52 mm (5.6 " x 5.6 " x 2 ") - without mounting clips					
Weight	Sensor with cable: 0.6 kg / Controller: 1.1 kg					
Electromagnetic compatibility (EMC)	EN 50081-1 and EN 50082-2					
Vibration	2 g / 20 ... 500 Hz					
Shock	15 g / 6 ms					

FSO = Full Scale Output SMR = Start of Measuring Range MMR = Mid of Measuring Range

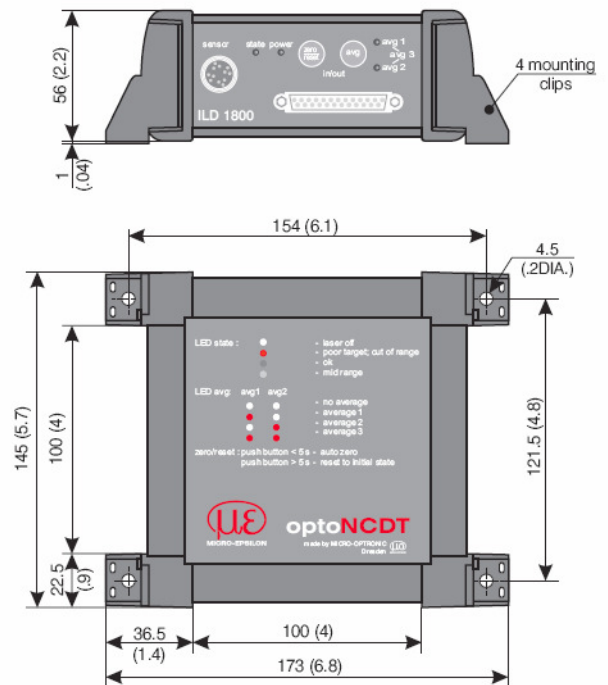
All specifications apply for a diffusely reflecting matt white ceramic target

**optoNCDT 1800** Dimensions in mm (inch), not to scale

Sensor



Controller



## **8.0 CURRICULUM VITAE**

Yinko Ibsain Grajeda Gamboa was born on April 27, 1978, in the city of Chihuahua, Chih., MX. Son of Jose Luís Grajeda and Mariana Gamboa. In 1996 graduated from Juarez Stake Academy a bilingual (English-Spanish) High School located in Colonia Juarez, Chih., Mexico. In 1997 graduated from Escuela Federal Francisco Villa Preparatory School located in Nuevo Casas Grandes, Chih., MX. In 2001 graduated with “Honors Student” recognition from the Instituto Tecnológico Superior de Nuevo Casas Grandes under the Bachelor’s Degree of Electro-Mechanical Engineering. During his Bachelor’s degree held an internship at the Comisión Federal de Electricidad (CFE). In 2001 joined the Comisión Federal de Electricidad serving in the position of “Agente Comercial” foreseeing the complete sale process of the low-to-mid tension electric energy services from 3 individual commercial agencies located in and nearby Nuevo Casas Grandes, Chih. MX. In the spring of 2004 was accepted into The University of Texas at El Paso (UTEP) Graduate School under the “Gobierno del Estado de Chihuahua Scholarship” in pursuit of the Degree of Master in Science of Mechanical Engineering and served as a Teacher and Research Assistant. In early 2005 joined Delphi Automotive Systems Mexico Technical Center (MTC) in Juarez, Chih. MX. to serve as “Product Development Engineer” working in the Sensors and Actuators advanced development group and particularly in the Controlled Brakes Group (DBC). In the summer of 2007 (under Delphi) received an Expatriate Assignment (ISP) to transfer product knowledge base to the Dayton, OH area. In late 2009 provided key support for the successful production launch of product line in a plant located in Shanghai, China.

This thesis was written by Yinko I. Grajeda.